UNIVERSITY OF MILANO-BICOCCA

DEPARTMENT OF STATISTICS AND QUANTITATIVE METHODS
DOCTORAL THESIS IN STATISTICS AND MATHEMATICS FOR FINANCE

Interest rate and credit risk models applied to finance and actuarial science

Author: Anna Maria Gambaro
Registration n. 787787

Supervisor: Gianluca Fusai

ACADEMIC YEAR 2016/2017

Abstract

The first part of the thesis proposes new bounds on the prices of European-style swaptions for affine and quadratic interest rate models. These bounds are computable whenever the joint characteristic function of the state variables is known. In particular, our lower bound involves the computation of a one-dimensional Fourier transform independently of the swap length. In addition, we control the error of our method by providing a new upper bound on swaption price that is applicable to all considered models. We test our bounds on different affine models and on a quadratic Gaussian model. In the second part of the work, we extended the lower and upper bounds to pricing swaption in a multiple-curve framework. In the third part, we propose a novel multiple-curve model, set in the Heath-Jarrow-Morton framework, with time-changed Lévy processes, in order to obtain a parsimonious but also flexible model, which is able to reproduce quoted volatility surface of interest rate options. The model is developed in a multiple-curve post crisis set-up and it allows for negative rates. First, we build arbitrage free term structures for zero coupon bonds and Libor Forward Rate Agreement (FRA) rates. Then, we price interest rate derivatives, as caps and swaptions, using the Fourier transform method. Two choices for the construction of the driving processes are calibrated to market data and results are examined and compared.
In the last part, we analyse common practice for determining the fair value of asset and liabilities of insurance funds and we propose an arbitrage free stochastic model for interest rate, credit and liquidity risks, that takes into account the dependences between different issuers. The impact of the common practice against our proposed model is tested for the evaluation of financial options written on with-profit policies issued by European insurance companies.

Acknowledgments

First and foremost, I would like to express my sincere gratitude to my supervisor Professor Gianluca Fusai, without his valuable advice and support this work could not be possible. Furthermore, his precious suggestions have been of great value for my professional and personal growth. I am also grateful to Professor Laura Ballota, she introduced me to the topic of Lévy and time-changed Lévy process and to the beautiful city of London. I would like to thank the PhD school in Statistics and Mathematical Finance and in particular the coordinator of the curriculum in Mathematical Finance, professor Fabio Bellini. A very special thank goes to my dear colleagues of PhD school, in particular Alberto Santangelo, who during three years shared with me the office and this experience. I would also like to express my thanks to Ruggero Caldana, he was of great support at the beginning of my doctoral thesis and to Riccardo Casalini for the valuable professional collaboration in the last part of my work. Last but not least, my special gratitude is due to my family and friends for their lovely support over all the years, especially my husband Nicholas.

Contents

Introduction

The largest portion of the global financial market is represented by fixed-income instruments, even larger than equities. According to the yearly statistics provided by the Bank for International Settlements, the notional amounts outstanding in 2016 for over-the-counter (OTC) interest rate derivatives is 418 trillion of dollars out of the total volume of 544 trillion of dollars (about the 76%). Furthermore, according to EMMI (European Money Markets Institute) the notional volume of outstanding financial contracts indexed to Euribor is estimated to be greater than 180 trillion of Euro.
Moreover, in the last decade the interest rate market has experienced great changes. The credit crunch in the summer of 2007 and the Eurozone sovereign debt crisis in 2009–2012 have particularly impacted fixed-income market. The principal rules in these crisis are played by counterparty risk, i.e. the risk of a counterparty default, and liquidity (or funding) risk, i.e. the risk of excessive costs of raising cash due to the lack of liquidity in the market. After the 2007 crisis significant spreads are observed between Libor/Euribor rates with different tenors and between Libor/Euribor rates and the overnight indexed swaps (OIS) rates. Due to the presence in the market of various interest rate curves linked to different tenors, practitioners and researchers developed a so-called multiple-curve approach. Finally, in last years, in order to provide a sufficient stimulus to the economy, central banks in Euro area have pushed interest rates into negative territory.
Swaptions (i.e. options written on interest rate swap contracts) are among the most liquid OTC derivatives and no exact swaption pricing formula is available for multi-factor interest rate models. Our **first contribution** is to develop accurate and efficient bounds to approximate the price of European-swaption in a single-curve pre-crisis framework. These bounds are computable for affine and quadratic models, whenever the joint characteristic function of the state variables is known. In particular, our lower bound involves the computation of a one-dimensional Fourier transform independently of the swap length. In addition, we control the error of our method by providing a new upper bound on swaption price that is applicable to all considered models. Then, our **second contribution** of our work is the extension of the swaption pricing bounds developed in the single-curve framework to an HJM (Heath Jarrow Morton) multiple-curve Gaussian model, which allows also for negative rates.
The **third contribution** of our work is the application of time-changed Lévy processes to the HJM multi-curve framework introduced previously. Our aim is to obtain a parsimonious but also flexible model, which is able to reproduce a quoted volatility surface of interest rate options. First, we build a term structure for zero

coupon bonds and Libor Forward Rate Agreement (FRA) rates and we derive sufficient conditions to ensure the absence of arbitrage. Then we price interest rate derivatives, as caps and swaptions, using the Fourier transform method. Finally two different choices for the construction of the driving processes are examined and compared.
Interest rate and credit/liquidity risks modelling are not only important for the financial sector but also for the insurance industry. In the last part of this thesis, we analyse common practice for determining the fair value of asset and liabilities of insurance funds. In the last years regulators introduced, with the Solvency II directive, a market consistent valuation framework for determining the fair value of asset and liabilities of insurance funds. A relevant aspect is how to deal with the estimation of sovereign credit and liquidity risk, that are important components in the valuation of the majority insurance funds, which are usually heavily invested in treasury bonds. The common practice is the adoption of the certainty equivalent approach (CEQ) for the risk neutral evaluation of insurance liabilities, which results in a deterministic risk adjustment of the securities cash flows. Hence, our **fourth contribution** is the application of an arbitrage free stochastic model for interest rate, credit and liquidity risks, which takes into account the dependences between different government bond issuers, to the valuation of financial options written on with-profit policies issued by European insurance companies. We test the impact of the common practice against our proposed model via Monte Carlo simulations. We conclude that in the estimation of options whose pay-off is determined by statutory accounting rules, which is often the case for traditional with-profit insurance products, the deterministic adjustment for risk of the securities cash flows is not appropriate, and that a more complete model such as the one described in this thesis is a viable and sensible alternative in the context of market consistent evaluations.
The work is organized as follows. First chapter presents a lower and upper bound to the price of European-swaption in (single-curve) affine and quadratic models. In the second chapter lower and upper bounds are extended to price swaption in a multiple-curve framework. Third chapter propose an HJM multiple-curve model with time-changed Lévy process, moreover interest rate option pricing formulae are presented and the model is calibrated to market data. In the fourth chapter we applied a complete stochastic model for interest rate, credit and liquidity risks to the valuation of embedded option in minimum guaranteed insurance funds.
The first two chapters refer to the following two papers [Gambaro et al., 2015], [Gambaro et al., 2017]. The third chapter consists in the second work produced for the doctoral thesis, [Gambaro et al., 2016a]. Finally, the paper [Gambaro et al., 2016b] is reported in the fourth chapter.

Chapter 1

Approximate pricing of swaptions in affine and quadratic models

The accurate pricing of swaption contracts is fundamental in interest rate markets. Swaptions are among the most liquid OTC derivatives and are largely used for hedging purposes. Many applications also require efficient computation of swaption prices, such as calibration, estimation of risk metrics and credit and debit value adjustment (CVA and DVA) valuation. In the calibration of interest rate models, a large number of swaptions with different maturities, swap lengths and strikes are priced using iterative procedures aimed at fitting market quotations. Similarly, in the estimation of risk metrics for a portfolio of swaptions, if a full revaluation setting is used and millions of possible scenarios are considered, a fast pricing algorithm is essential to obtain results in a reasonable time. In addition, the Basel III accords introduced the CVA and DVA charge for OTC contracts, and for the simplest and most popular kind of interest rate derivative, i.e. interest rate swap, the two adjustments can be estimated by pricing a portfolio of forward start European swaptions (see [Brigo and Masetti, 2005b]). Hence, the appeal of a fast and exact closed-form solution for the swaption pricing problem is explained.
The famous [Jamshidian, 1989] formula is applicable only when the short rate depends on a single stochastic factor while for multi-factor interest rate models, several approximate methods have been developed in the literature. [Munk, 1999] approximates the price of an option on a coupon bond by a multiple of the price of an option on a zero-coupon bond with time to maturity equal to the stochastic duration of the coupon bond. The method of [Schrager and Pelsser, 2006] is based on approximating the affine dynamics of the swap rate under the relevant swap measure. These methods are fast but not very accurate for out-of-the-money options. The method of [Collin-Dufresne and Goldstein, 2002] is based on an Edgeworth expansion of the density of the swap rate and requires a time-consuming calculation of the moments of the coupon bond and it provides reliable estimation only for a low volatility level. An estimation of the error of the [Collin-Dufresne and Goldstein, 2002] has been provided in [Zheng, 2013]. [Singleton and Umantsev, 2002] introduce the idea of approximating the exercise region in the space of the state variables. This method has the advantage of producing accurate results across a wide range of strikes, in particular for out-of-the-money swaptions. However, it does not allow a simple ex-

tension to general affine interest rate models because it requires the knowledge of the joint probability density function of the state variables in the closed form. [Kim, 2014] generalizes and simplifies the [Singleton and Umantsev, 2002] method. Up to now, Kim's method seems to be the most efficient proposed in the literature. Nevertheless, Kim's method requires the calculation of as many Fourier transforms as the number of cash flows in the underlying swap, which implies that the run time of the algorithm increases with the swap length. Moreover, none of these papers discusses the direction of the error, i.e. whether the price is overestimated or underestimated. Further, except for [Collin-Dufresne and Goldstein, 2002], none of the methods proposed in the literature is able to estimate or control the approximation error. Recently, a lower and an upper bound on swaption prices was proposed in [Nunes and Prazeres, 2014], but these are applicable only to Gaussian models.
Similar to [Singleton and Umantsev, 2002] and [Kim, 2014], we propose a lower bound that is based on an approximation of the exercise region via an event set defined through a function of the model factors. Our pricing formula consists of the valuation of an option on the approximate exercise region and requires a single Fourier transform. Our procedure gives a new perspective with respect to existing methods, such as those of [Singleton and Umantsev, 2002] and [Kim, 2014]. Indeed, we prove that their approximations are also lower bounds to the swaption price. To the best of our knowledge, this has not been reported previously. Moreover, we develop methods to control the approximation error by deriving a new upper bound on swaption prices.
The chapter is organized as follows. Section 2 introduces a general formula for the lower bound on swaption prices based on an approximation of the exercise region. In addition, the popular methods of [Singleton and Umantsev, 2002] and [Kim, 2014] are proved to be included in our setting. Then we apply the general lower bound formula to the case of affine models and Gaussian quadratic interest rate models and we find an efficient algorithm to calculate analytically the approximate swaption price. In Section 3, the new upper bound is presented for affine-quadratic models. Section 4 shows the results of numerical tests.

1.1 Lower bound on swaption prices

In this section, we discuss the general pricing formula for a receiver European-style swaption and the approximations presented in [Singleton and Umantsev, 2002] and [Kim, 2014]. In particular, we prove that these approximations are lower bounds.
A European swaption is a contract that gives the right to its owner to enter into an underlying interest rate swap, i.e. it is a European option on a swap rate. It can be equivalently interpreted as an option on a portfolio of zero-coupon bonds (or as an option on a coupon bond). Let t be the current date, T the option expiration date, $T_1, ..., T_n$ the underlying swap payment dates (by construction $t < T < T_1 < ... < T_n$) and R the fixed rate of the swap. The payoff of a receiver swaption is

$$\left(\sum_{h=1}^{n} w_h P(T, T_h) - 1 \right)^+ ,$$

where $w_h = R\,(T_h - T_{h-1})$ for $h = 1, .., n-1$, $w_n = R\,(T_n - T_{n-1}) + 1$, and $P(T, T_h)$ is the price at time T of a zero-coupon bond expiring at time T_h. The time t no-arbitrage price is the risk-neutral expected value of the discounted payoff,

$$C(t) = \mathbb{E}_t \left[e^{-\int_t^T r(\mathbf{X}(s))ds} \left(\sum_{h=1}^{n} w_h P(T, T_h) - 1 \right)^+ \right] \tag{1.1}$$

where $r(\mathbf{X}(s))$ is the short rate at time s, and $\mathbf{X}(s)$ denotes the state vector at time s of a multi-factor stochastic model. The price formula (1.1) after a change of measure to the T-forward measure becomes

$$C(t) \quad = \quad P(t,T)\, \mathbb{E}_t^T \left[\left(\sum_{h=1}^{n} w_h P(T, T_h) - 1 \right) I(\mathcal{A}) \right] \tag{1.2}$$

with I denoting the indicator function, and $\mathcal{A}$ is the exercise region, which is seen as a subset of the space events Ω,

$$\mathcal{A} = \{\omega \in \Omega : \sum_{h=1}^{n} w_h P(T, T_h) \geq 1\}.$$

By changing the measure of each expected value from the T forward measure to the T_h measure, the pricing formula in expression (1.2) can be written as

$$C(t) = \sum_{h=1}^{n} w_h P(t, T_h)\, \mathbb{P}_t^{T_h}[\mathcal{A}] - P(t,T)\, \mathbb{P}_t^T[\mathcal{A}]$$

where $\mathbb{P}_t^S[\mathcal{A}]$ denotes the time t probability of the exercise set $\mathcal{A}$ under the S-forward measure. [Singleton and Umantsev, 2002] and [Kim, 2014] replace the exercise set $\mathcal{A}$ in the above formula by a new set $\mathcal{G}$ that makes the computation of the swaption price much simpler, and then their approximate pricing formula reads as (see [Singleton and Umantsev, 2002] and [Kim, 2014] for further details)

$$C_{\mathcal{G}}(t) = \sum_{h=1}^{n} w_h P(t, T_h)\, \mathbb{P}_t^{T_h}[\mathcal{G}] - P(t,T)\, \mathbb{P}_t^T[\mathcal{G}]. \tag{1.3}$$

The choice of the approximate exercise region is made so that the above probabilities can be computed by performing $n+1$ Fourier inversions, where n is the number of payments in the underlying swap. We can now show that $C_{\mathcal{G}}(t)$ is a lower bound approximation to the true price. Indeed, we observe that for any event set $\mathcal{G} \subset \Omega$:

$$\begin{aligned}
&\mathbb{E}_t^T \left[\left(\sum_{h=1}^{n} w_h P(T, T_h) - 1 \right)^+ \right] \geq \mathbb{E}_t^T \left[\left(\sum_{h=1}^{n} w_h P(T, T_h) - 1 \right)^+ I(\mathcal{G}) \right] \\
&\geq \mathbb{E}_t^T \left[\left(\sum_{h=1}^{n} w_h P(T, T_h) - 1 \right) I(\mathcal{G}) \right]
\end{aligned}$$

Then by discounting we obtain:

$$C(t) \geq LB_{\mathcal{G}}(t) := P(t,T)\,\mathbb{E}_t^T\left[\left(\sum_{h=1}^{n} w_h P(T,T_h) - 1\right) I(\mathcal{G})\right], \tag{1.4}$$

i.e. $LB_{\mathcal{G}}(t)$ is a lower bound to the swaption price for all possible sets $\mathcal{G}$. Using the same change of measures as in [Singleton and Umantsev, 2002] and [Kim, 2014], it immediately follows that

$$LB_{\mathcal{G}}(t) = C_{\mathcal{G}}(t).$$

Therefore, the approximate pricing formula presented in [Singleton and Umantsev, 2002] and [Kim, 2014] are indeed lower bounds. This was not previously noted. In particular, our new framework allows us to control the approximation error by providing an upper bound. In addition, we show how to speed up the computation of the formula (1.4) by performing a single Fourier transform. This allows a reduction of the computational cost, mainly when we have to price swaptions written on long-maturity swaps.

1.1.1 Affine and Gaussian quadratic models

In affine and quadratic interest rate models, the price at T of a zero-coupon bond with expiration $T_h > T$ can be written as the exponential of a quadratic form of the state variables,

$$P(T,T_h) = e^{\mathbf{X}^\top(T)C_h\mathbf{X}(T)+\mathbf{b}_h^\top\mathbf{X}(T)+a_h} \tag{1.5}$$

for $\mathbf{X}(T)$ a d-dimensional state vector and $a_h = A(T-T_h)$, $\mathbf{b}_h = \mathbf{B}(T-T_h)$ and $C_h = C(T-T_h)$ functions of the payment date T_h, which are model specific. Fixing a date T_h, $\mathbf{b}_h$ is a d-dimensional vector and C_h is a $d \times d$ symmetric matrix.
From the literature ([Ahn et al., 2002], [Leippold and Wu, 2002] and [Kim, 2014]), we know that if the risk-neutral dynamics of the state variates are Gaussian, then the functions $A(\tau)$, $\mathbf{B}(\tau)$ and $C(\tau)$ are the solution of a system of ordinary differential equations with initial condition $A(0) = 0$, $\mathbf{B}(0) = \underline{0}$, $C(0) = 0_{d\times d}$. Affine models can be obtained by forcing C_h to be a null matrix. For affine models, under certain regularity conditions, the functions $A(\tau)$ and $\mathbf{B}(\tau)$ are the solution of a system of $d+1$ ordinary differential equations that are completely determined by the specification of the risk-neutral dynamics of the short rate (see [Duffie and Kan, 1996] and [Duffie et al., 2000] for further details). The solutions of these equations are known in closed form for most common affine models.
From [Duffie et al., 2000] and [Kim, 2014], we know that the quadratic T-forward joint characteristic function of the model factors $\mathbf{X}$ has the form

$$\begin{aligned} &\Phi(\boldsymbol{\lambda},\Lambda) = \mathbb{E}_t^T\left[e^{\boldsymbol{\lambda}^\top\mathbf{X}(T)+\mathbf{X}(T)^\top\Lambda\mathbf{X}(T)}\right] \qquad (1.6)\\ = \;& e^{\tilde{A}(T-t,\boldsymbol{\lambda},\Lambda)-A(T-t)+(\tilde{\mathbf{B}}(T-t,\boldsymbol{\lambda},\Lambda)-\mathbf{B}(T-t))^\top\mathbf{X}(t)+\mathbf{X}(t)^\top(\tilde{C}(T-t,\boldsymbol{\lambda},\Lambda)-C(T-t))\mathbf{X}(t)} \end{aligned}$$

where $\boldsymbol{\lambda} \in \mathbb{C}^d$ and Λ is a complex $d \times d$ symmetric matrix. If $\mathbf{X}(t)$ is a Gaussian quadratic process (or an affine process, i.e. Λ, $\tilde{C}$ and C are null matrices), the functions $\tilde{A}(\tau, \boldsymbol{\lambda}, \Lambda)$, $\tilde{\mathbf{B}}(\tau, \boldsymbol{\lambda}, \Lambda)$ and $\tilde{C}(\tau, \boldsymbol{\lambda}, \Lambda)$ are the solutions of the same ODE system of the zero-coupon bond functions, but with initial conditions $\tilde{A}(0, \boldsymbol{\lambda}, \Lambda) = 0$, $\tilde{\mathbf{B}}(0, \boldsymbol{\lambda}, \Lambda) = \boldsymbol{\lambda}$, and $\tilde{C}(0, \boldsymbol{\lambda}, \Lambda) = \Lambda$.
In the case of a quadratic model, it is convenient to define the approximate exercise region $\mathcal{G}$ using a quadratic form of the state vector,

$$\mathcal{G} = \{\omega \in \Omega : \mathbf{X}(T)^\top \Gamma \, \mathbf{X}(T) + \boldsymbol{\beta}^\top \mathbf{X}(T) \geq k\},$$

where Γ is a constant $d \times d$ symmetric matrix, $\boldsymbol{\beta} \in \mathbb{R}^d$ and $k \in \mathbb{R}$.

Proposition 1.1.1. *The lower bound to the European swaption price for quadratic interest rate models is given by the following formula:*

$$LB(t) = \max_{k \in \mathbb{R},\, \boldsymbol{\beta} \in \mathbb{R}^d,\, \Gamma \in Sym_d(\mathbb{R})} LB_{\boldsymbol{\beta},\Gamma}(k; t), \tag{1.7}$$

where

$$LB_{\beta,\Gamma}(k; t) \;=\; P(t,T)\, \frac{e^{-\delta k}}{\pi} \int_0^{+\infty} Re\left(e^{-i\gamma k} \psi(\delta + i\gamma)\right) d\gamma, \tag{1.8}$$

and

$$\psi(z) = \left(\sum_{h=1}^{n} w_h e^{a_h} \Phi\left(\mathbf{b}_h + z\boldsymbol{\beta}, C_h + z\Gamma\right) - \Phi\left(z\boldsymbol{\beta}, z\Gamma\right) \right) \frac{1}{z}, \tag{1.9}$$

with $\psi(z)$ defined for $Re(z) > 0$ for receiver swaptions and for $Re(z) < 0$ for payer swaptions. The integral in formula (1.8) must be interpreted as a Cauchy principal value integral and δ is a positive or negative constant for receiver or payer swaptions, respectively.

Proof: See Appendix A.1.

1.2 The approximate exercise region

1.2.1 The geometric average approximate exercise region

The approximate exercise set is defined through the logarithm of the geometric average of the portfolio of zero coupon bonds

$$\begin{aligned} \mathcal{G} &= \{\omega \in \Omega : g(\mathbf{X}(T)) \geq k\}, \\ G(\mathbf{X}(T)) &= \prod_{h=1}^{n} P(T, T_h)^{w_h}, \\ g(\mathbf{X}(T)) &= \ln\left(G(\mathbf{X}(T))\right) = \sum_{h=1}^{n} w_h \ln(P(T, T_h)). \end{aligned}$$

For linear-quadratic models, $\mathcal{G}$ and $g(\mathbf{X})$ are given by

$$\mathcal{G} = \{\omega \in \Omega : \mathbf{X}(T)^\top \Gamma \mathbf{X}(T) + \boldsymbol{\beta}^\top \mathbf{X}(T) + \alpha \geq k\},$$

where $\Gamma = \sum_{h=1}^n w_h\, C_h$, $\boldsymbol{\beta} = \sum_{h=1}^n w_h \mathbf{b}_h$ and $\alpha = \sum_{h=1}^n w_h a_h$.
Since we don't know the optimum value of the parameter k, then the pricing method requires the maximization of the lower bound, $LB(k; t, T, \{T_h\}_{h=1}^n, R)$, seen as a function of k. The optimization can be accelerated looking for a good starting point. We suggest the following

$$\tilde{k} = \log\left(\frac{1}{\sum_{h=1}^n w_h}\right) = -\log\left(\sum_{h=1}^n R(T_h - T_{h-1})\right).$$

According to this choice $\mathcal{G}_{\tilde{k}} = \{\omega \in \Omega : g(\mathbf{X}(T)) \geq \tilde{k}\}$ is the greatest possible subset of the true exercise region, $\mathcal{A}$. In fact normalizing the weights, the expression of the true exercise region can be rewritten as

$$\mathcal{A} = \{\omega \in \Omega : \sum_{h=1}^n w_h P(T, T_h) \geq 1\} = \{\omega \in \Omega : \sum_{h=1}^n \tilde{w}_h P(T, T_h) \geq e^{\tilde{k}}\} =$$
$$= \{\omega \in \Omega : A(\mathbf{X}) \geq e^{\tilde{k}}\},$$

where $A(\mathbf{X})$ is the arithmetic mean of the ZCBs portfolio, $\tilde{w}_h = \frac{w_h}{\sum_{h=1}^n w_h}$ and so $\sum_{h=1}^n \tilde{w}_h = 1$.
By the arithmetic-geometric inequality we know that $A(\mathbf{X}) \geq G(\mathbf{X})\ \forall \mathbf{X}$, then $\forall k > \tilde{k}$

$$\mathcal{A} \supseteq \mathcal{G}_{\tilde{k}} \supseteq \mathcal{G}_k.$$

Instead if $k < \tilde{k}$ then it is no more guaranteed that $\mathcal{G}_k$ is a subset of the true exercise region.

1.2.2 The Taylor (or tangent hyperplane) approximation

For two-factor affine interest rate models, [Singleton and Umantsev, 2002] propose to approximate the exercise boundary of an option on a coupon bond with a straight line that closely matches the exercise boundary where the conditional density of the model factors is concentrated. [Kim, 2014] improves on the [Singleton and Umantsev, 2002] idea and considers three different types of approximation for the exercise region. We choose its approximation "A" because it appears to be the most accurate.[1] In the approximation "A", the approximate exercise region is obtained by a first-order Taylor expansion of the coupon bond price, which is defined as

$$B(\mathbf{X}(T)) = \sum_{h=1}^n w_h P(T, T_h), \tag{1.10}$$

[1] The three approximations presented in [Kim, 2014] are lower bounds, as proved in Section 1.1. Therefore, the most precise is the one that produces the highest price, which was not discussed in the Kim paper.

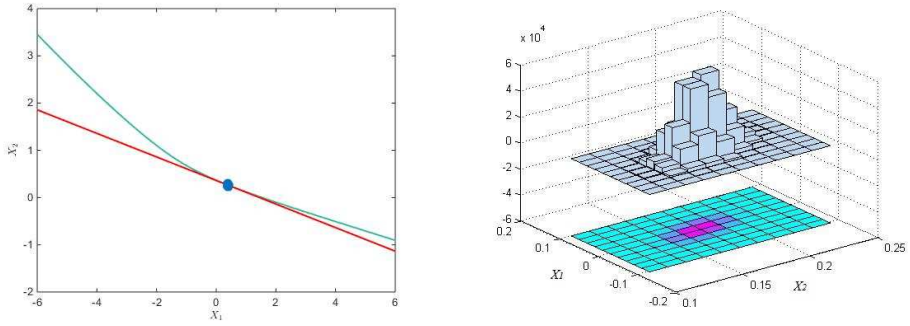

(a) Exercise regions (b) Histogram of the density

Figure 1.1: The first figure shows the true and the approximate exercise boundary for a 2×10 years swaption with the two-factor CIR model. Light blue and red lines are the boundary of the true region and of the approximate set, respectively. The region represented by a blue circle is where the joint probability density function of the two factors is highest at the maturity of the option. The second figure is the histogram of the joint probability density function of the two factors at maturity.

around the point on the true exercise boundary where the density function of the model factors is largest. Moreover, [Kim, 2014] extends his approximation "A" to Gaussian quadratic interest rate models using a second-order Taylor expansion of the coupon bond. In this way, the optimization of the lower bound (formula (1.7)), which can be very expensive, is not performed. It is instead replaced by a preliminary search of the parameters Γ, $\boldsymbol{\beta}$ and k, which are chosen via the Taylor expansion of the coupon bond price.
In particular, for affine models, the first-order Taylor expansion of the coupon bond is a tangent hyperplane approximation. In fact, the approximate exercise boundary is defined as

$$\boldsymbol{\beta}^\top \mathbf{X}(T) + \alpha = 0,$$

with

$$\alpha = -\nabla B(\mathbf{X}^*)^\top \mathbf{X}^*, \quad \boldsymbol{\beta} = \nabla B(\mathbf{X}^*) \quad \text{and} \quad k = -\alpha. \tag{1.11}$$

Hence, it is a tangent hyperplane to the true exercise boundary at the point, $\mathbf{X}(T) = \mathbf{X}^*$, where the density function of the model factors is the largest. In order to calculate the point $\mathbf{X}^*$, we use the equation (2.20) of [Kim, 2014]. A two-dimensional visualization of the approximate exercise region is shown in Figure 1.1. Once Γ, $\boldsymbol{\beta}$ and k are found, the Kim approximation requires the computation of $n+1$ forward probability $\mathbb{P}_t^{T_h}[\mathcal{G}]$, as in formula (1.3). This is done by performing $n+1$ one-dimensional Fourier inversions. In contrast, our lower bound is calculated as in formula (1.8), i.e. performing a single one-dimensional Fourier transform with respect to the parameter k.

1.3 Upper bound on swaption price

In this section, we define a new upper bound to swaption prices that is applicable to all affine and quadratic interest rate models. First of all, it is straightforward to see that for a lower bound defined by a generic approximate exercise set $\mathcal{G}$, the (undiscounted) approximation error is

$$\begin{aligned} & \frac{1}{P(t,T)}\left(C(t)-\widehat{LB}(t)\right) \\ = \;& \mathbb{E}_t^T[(B(\mathbf{X}(T))-1)^+]-\mathbb{E}_t^T[(B(\mathbf{X}(T))-1)I(\mathcal{G})] \\ = \;& \mathbb{E}_t^T[(B(\mathbf{X}(T))-1)^+I(\mathcal{G}^c)]+\mathbb{E}_t^T[(1-B(\mathbf{X}(T)))^+I(\mathcal{G})] \\ = \;& \Delta_1+\Delta_2, \end{aligned}$$

where $B(\mathbf{X}(T))$ is the coupon bond price defined as in formula (1.10). The previous formula for the approximation error is valid also for payer swaptions. In general, Δ_1 and Δ_2 are not explicitly computable. However, we can provide upper bounds ϵ_1 and ϵ_2 to them. Hence, an upper bound to the swaption price easily follows:

$$UB(t)=\widehat{LB}(t)+P(t,T)\,(\epsilon_1+\epsilon_2), \tag{1.12}$$

for $\epsilon_1 \geq \Delta_1$ and $\epsilon_2 \geq \Delta_2$.
For every set of strikes $(K_1,...,K_n)$ such that $\sum_{h=1}^n K_h = 1$, upper bounds to the errors are

$$\Delta_1 \leq \epsilon_1 = \sum_{h=1}^{n} \mathbb{E}_t^T[(w_h P(T,T_h)-K_h)^+\, I(\mathcal{G}^c)], \tag{1.13}$$

$$\Delta_2 \leq \epsilon_2 = \sum_{h=1}^{n} \mathbb{E}_t^T[(K_h-w_h P(T,T_h))^+\, I(\mathcal{G})], \tag{1.14}$$

where $P(T,T_h)$ is the price at time T of the zero-coupon bond with maturity T_h. However, without a proper choice of the strikes $(K_1,...,K_n)$, the approximations can be very rough and so we want to find the values of $(K_1,...,K_n)$ that reduce the error without performing a time-consuming multidimensional numerical minimization. Given that

$$\begin{aligned} (B(\mathbf{X}(T))-1)^+ &= B(\mathbf{X}(T))\,\left(1-\frac{1}{B(\mathbf{X}(T))}\right)^+ \\ &= \sum_{h=1}^{n} w_h P(T,T_h)\,\left(1-\frac{1}{B(\mathbf{X}(T))}\right)^+ \\ &= \sum_{h=1}^{n}\left(w_h P(T,T_h)-\frac{w_h P(T,T_h)}{B(\mathbf{X}(T))}\right)^+ \end{aligned} \tag{1.15}$$

as $B(\mathbf{X}(T)) > 0$ and $w_h P(T,T_h) > 0\ \forall \mathbf{X}(T)$, we note that the following equality holds:

$$\mathbb{E}_t^T[(B(\mathbf{X}(T))-1)^+\, I(\mathcal{G}^c)] = \sum_{h=1}^{n} \mathbb{E}_t^T[(w_h P(T,T_h)-K_h(\mathbf{X}(T)))^+\; I(\mathcal{G}^c)],$$

for

$$K_h(\mathbf{X}(T)) = \frac{w_h P(T,T_h)}{B(\mathbf{X}(T))}.$$

By similar reasoning, we also have:

$$\mathbb{E}_t^T[(1 - B(\mathbf{X}(T)))^+ \, I(\mathcal{G})] = \sum_{h=1}^{n} \mathbb{E}_t^T[(K_h(\mathbf{X}(T)) - w_h P(T,T_h))^+ \, I(\mathcal{G})].$$

Hence, if in formula (1.13) and (1.14), we choose the strikes $(K_1, ..., K_n)$ in the following way:

$$K_h = K_h(\mathbf{X}^*) = w_h \, P(T,T_h)|_{\mathbf{X}(T)=\mathbf{X}^*}, \tag{1.16}$$

then the equalities $\epsilon_1 = \Delta_1$ and $\epsilon_2 = \Delta_2$ hold in $\mathbf{X}(T) = \mathbf{X}^*$, the point on the true exercise boundary where the density function of the model factors is largest. The computation of $\mathbf{X}^*$ is explained in Section 1.1.1.
This allows us to avoid a multidimensional optimization with respect to $(K_1, ...K_n)$.

1.3.1 Affine and Gaussian quadratic models

The following proposition explains how to compute the quantities ϵ_1 and ϵ_2 defined in expressions (1.13) and (1.14), and hence the upper bound in formula (1.12), using the Fourier Transform method.

Proposition 1.3.1. *The upper bound to the European swaption price for quadratic interest rate models is given by the following formula:*

$$UB(t) = \widehat{LB}(t) + P(t,T) \, (\epsilon_1(-\alpha) + \epsilon_2(-\alpha)) \tag{1.17}$$

where

$$\begin{aligned}
\epsilon_1(k) &= \frac{1}{2\pi^2} \int_0^{+\infty} d\gamma \, Re \left(\int_{-\infty}^{+\infty} d\omega \sum_{h=1}^{n} w_h e^{a_h} \, e^{-(\delta+i\gamma)k} e^{-(\eta+i\omega)k_h} \, \psi_h(\delta+i\gamma, \eta+i\omega) \right), \\
\epsilon_2(k) &= -\frac{1}{2\,\pi^2} \int_0^{+\infty} d\gamma \, Re \left(\int_{-\infty}^{+\infty} d\omega \sum_{h=1}^{n} w_h e^{a_h} \, e^{(\delta-i\gamma)k} e^{(\eta-i\omega)k_h} \, \psi_h(-\delta+i\gamma, -\eta+i\omega) \right),
\end{aligned}$$

and

$$\psi_h(z,y) = -\frac{\Phi\left(z\boldsymbol{\beta} + (y+1)\mathbf{b}_h, z\Gamma + (y+1)C_h\right)}{zy(y+1)}, \tag{1.18}$$

where $\widehat{LB}(t)$ is given in Proposition 1.1.1, $k_h = log(K_h) - log(w_h) - a_h$, K_h are defined in equation (1.16) and $\Phi(\boldsymbol{\lambda}, \Lambda)$ is defined in equation (1.6). The upper bound formula is valid for both receiver and payer swaptions. If $Re(z) < 0$ and $Re(y) > 0$, $\psi_h(z,y)$ is the double Fourier transform of

$$\mathbb{E}_t^T[(e^{\mathbf{b}_h{}^\top \mathbf{X} + \mathbf{X}^\top C_h \mathbf{X}} - e^{k_h})^+ \, I(\mathbf{X}^\top \Gamma \mathbf{X} + \boldsymbol{\beta}^\top \mathbf{X} < k)],$$

and if $Re(z) > 0$ and $Re(y) < -1$, $\psi_h(z,y)$ is the transform of

$$\mathbb{E}_t^T[(e^{k_h} - e^{\mathbf{b}_h{}^\top \mathbf{X} + \mathbf{X}^\top C_h \mathbf{X}})^+ \, I(\mathbf{X}^\top \Gamma \mathbf{X} + \boldsymbol{\beta}^\top \mathbf{X} > k)],$$

with $\delta > 0$, $\eta > 1$ constants.

Proof: See Appendix A.2.
We note some important mathematical features of the swaption pricing problem in the affine interest rate model case. In this set up, C_h and Γ are null matrices, which simplifies the upper bound formula. The coupon bond $B(\mathbf{X}(T))$ seen as a function of the model factors $\mathbf{X}(T)$ is convex as it is a positive linear combination of convex functions, the ZCBs. In fact, the zero-coupon price seen as a function of the state vector, i.e. $P(T, T_h) = e^{\mathbf{b}_h^\top \mathbf{X}(T) + a_h}$, is a convex function because it is composed of convex monotone functions, the exponential, and a linear function of $\mathbf{X}$. Thus, the convexity of the sub-level $\{B(\mathbf{X}(T)) \leq 1\}$ ensues from the previous argument.
Choosing the tangent hyperplane approximation as the lower bound and resorting to the hyperplane separation theorem, it follows immediately that the approximate exercise region is included in the true region, as graphically illustrated in Figure 2 for a two-factor case,

$$\mathcal{G} = \{\boldsymbol{\beta}^\top \mathbf{X} + \alpha \geq 0\} \subseteq \{B(\mathbf{X}(T)) \geq 1\},$$

provided that α and $\boldsymbol{\beta}$ are defined as in formula (1.11).

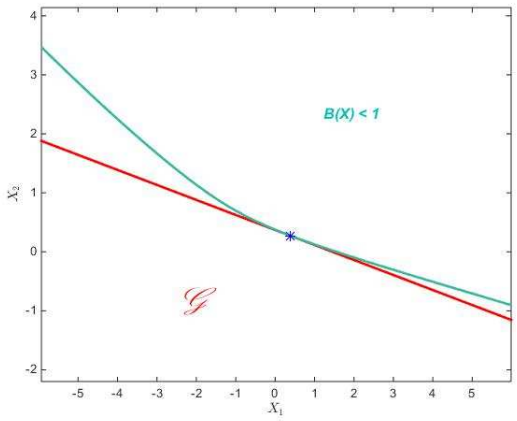

Figure 1.2: The light blue line represents the true exercise boundary for a 2×10-year swaption with a two-factor CIR model. The blue star indicates the point $\mathbf{X}^*$. The approximate exercise region $\mathcal{G}$ is the half-space below the red line. Since the sub-level $\{B(\mathbf{X}(T)) \leq 1\}$ is convex, then $\mathcal{G} \cap \{B(\mathbf{X}(T)) \leq 1\} = \emptyset$ by the hyperplane separation theorem.

Hence, the separation theorem guarantees that Δ_2 is zero, which allows us to compute only the term ϵ_1 in Proposition 1.3.1.
It is possible to show that for one-factor affine interest rate models, the upper bound coincides with the [Jamshidian, 1989] formula.

1.4 Bounds for affine Gaussian specification

For the affine Gaussian model, the lower bound can be calculated analytically as follows:

$$LB_{\boldsymbol{\beta}}(k;t) = P(t,T)\,\omega\,\left(\sum_{h=1}^{n} w_h\, e^{a_h+\mathbf{b}_h^\top\boldsymbol{\mu}+\frac{1}{2}V_h+\frac{1}{2}d_h^2}\, N(\omega\,(d_h-d)) - N(-\omega\,d)\right),$$

where $\omega = 1$ for receiver swaptions and $\omega = -1$ for payer swaptions. The upper bound formula can be simplified to

$$\epsilon_1(k) = \int_{-\infty}^{d} dz\,\frac{1}{\sqrt{2\pi}}e^{-\frac{z^2}{2}}\,\sum_{h=1}^{n} w_h e^{a_h}\left(e^{M_h+\frac{V_h}{2}}\,N\left(\frac{M_h-\log Y_h+V_h}{\sqrt{V_h}}\right) - Y_h N\left(\frac{M_h-\log Y_h}{\sqrt{V_h}}\right)\right),$$

where $d = \frac{k-\boldsymbol{\beta}^\top\boldsymbol{\mu}}{\sqrt{\boldsymbol{\beta}^\top V\boldsymbol{\beta}}}$, $d_h = \mathbf{b}_h^\top\mathbf{v}$, $V_h = \mathbf{b}_h^\top(V-\mathbf{v}\mathbf{v}^\top)\mathbf{b}_h$, $\mathbf{v} = \frac{V\boldsymbol{\beta}}{\sqrt{\boldsymbol{\beta}^\top V\boldsymbol{\beta}}}$, $M_h = \mathbf{b}_h^\top\boldsymbol{\mu}+z\mathbf{b}_h^\top\mathbf{v}$, $Y_h = \frac{K_h}{w_h e^{a_h}}$ and $\mu = \mathbb{E}_t^T[\mathbf{X}(T)]$ and $V = Var_t(\mathbf{X}(T))$ are the mean and covariance matrix of the variable $\mathbf{X}(T)$ that is multivariate normal under the T-forward measure. $N(x)$ represents the standard Gaussian cumulative distribution function. Proofs of the simplified bounds are in Appendix A.3 and A.4.

1.5 Numerical results

For each model, we fix a set of parameters and we calculate a matrix of swaption prices with different maturities, swap lengths and three different strikes, i.e. ATMF (at-the-money forward), ITMF (0.85 $\times$ ATMF for affine models and ATMF - 0.75% for the quadratic model) and OTMF (1.15 $\times$ ATMF for affine models and ATMF + 0.75% for the quadratic model). This is a common choice in the literature (see, for instance, [Schrager and Pelsser, 2006], [Singleton and Umantsev, 2002] and [Kim, 2014]). The description and values of the parameters for each model are reported, respectively, in Appendix B and D. The tested models are a three-factor affine Gaussian model, a two-factor affine Cox, Ingersoll and Ross (CIR) model, a two-factor affine Gaussian model with double exponential jumps and a two-factor Gaussian quadratic model. Monte Carlo is used as a benchmark for the computation of the true swaption price. The 97.5% mean-centred Monte Carlo confidence interval is used as a measure of the accuracy. For the affine three-factor Gaussian model, we add as a benchmark the lower bound proposed in [Nunes and Prazeres, 2014], which is extremely accurate. For the affine three-factor Gaussian model, lower bounds are obtained via the closed formula described in Section 1.4. Kim's prices are calculated using the closed price formula for the T-forward probabilities (formula (3.9) and (3.16), [Kim, 2014]). For the two-factor CIR model, the Gaussian model with jumps and the Gaussian quadratic model, the integrals involved in the lower bounds and in Kim's method are evaluated by a Gauss-Kronrod quadrature rule using Matlab's built-in function **quadgk**. The Matlab function **quadgk** is also used for the integral appearing in the upper bound formula for the three-factor Gaussian model (see Section 1.4). For the two-factor CIR model, the Gaussian model with jumps and the Gaussian quadratic model, the upper bound formula requires the calculus of double integrals that are evaluated using Matlab's function **quad2d**, an iterative algorithm that divides the integration

region into quadrants and approximates the integral over each quadrant by a two-dimensional Gauss quadrature rule.
Another important fact is that our lower bound formula is suitable for use as a control variate to reduce the Monte Carlo simulation error. The approximate formula is easily implemented in a Monte Carlo scheme and turns out to be very effective. In this way, the simulation error is considerably reduced.
Numerical results obtained with parameters reported in Appendix D are shown in Tables 1.1-1.12. Computational time for each pricing method is also given in Table 1.14.

1.5.1 Test with random parameters

In this section, we test the robustness of the bounds' approximation to parameter changes. We use 100 randomly simulated parameters for the two-factor CIR model. The model parameters are independent and uniformly distributed within a reasonable range, which is shown in Appendix D.
For each set of simulated parameters, we calculate a matrix of swaption prices with different maturities and swap lengths and three different strikes, i.e. ATM, ITMF (0.85 $\times$ ATMF) and OTMF (1.15 $\times$ ATMF).
For each swaption, we calculate the root mean square deviation (RMSD) of the lower and upper bounds with respect to the Monte Carlo estimation, which is used as the benchmark:

$$RMSD = \frac{1}{\sqrt{N}} \sqrt{\frac{\sum_{i=1}^{N} (B_i - MC_i)^2}{(MC_{avg})^2}}, \quad MC_{avg} = \frac{\sum_{i=1}^{N} MC_i}{N},$$

where N is the number of random trials, $B_i = LB_i$ or $B_i = UB_i$ (lower or upper bound) and MC_i is the Monte Carlo estimation of the swaption price with the i^{th} set of random parameters and MC_{avg} is the average of Monte Carlo prices over all random trials. Monte Carlo values are estimated using 10^7 simulations. Numerical results of this test are shown in Table 1.13.

1.5.2 Comments on numerical results

Numerical results are presented across a wide class of affine models and for the Gaussian quadratic model. The tangent hyperplane lower bound and the approximation "A" of [Kim, 2014] produce the same prices because they are two different implementations of the same approximation. However, the new algorithm, which requires the computation of a single Fourier inversion, is faster across all models for which the characteristic function is known in its closed form. In fact, in Table 1.14, our implementation of the lower bound is faster than Kim's method except for the Gaussian quadratic model for which the characteristic function is available in a semi-analytical form (see Appendix B). The improvement in computational performance is more evident for swaptions with a large number of cash flows, as illustrated in Table 1.15. For the three factor Gaussian affine model, [Nunes and Prazeres, 2014] conditioning approach is more efficient than our bounds, however our aim is to find approximations that are applicable to a wider class of models and not

only to Gaussian affine models. Comparing the speed of different methods is not simple because each algorithm should be optimized. However, our considerations about the efficiency of an algorithm are also justified by theoretical reasoning and confirmed by our estimations of the computational time. The lower bound with the (log-)geometric approximate exercise region is slightly less accurate and less efficient than the tangent hyperplane lower bound. Moreover, for the Gaussian quadratic model, it fails to reproduce OTMF swaption prices with a long swap length. However, it can be useful when it is difficult to find the correct point of tangency (i.e. the point $\mathbf{X}^*$ on the true exercise boundary, where the density of the model factor is highest, see Section 1.2.2).

Our upper bound is applicable to all affine-quadratic models and it is particularly efficient for affine models. In the literature, upper bounds are available only for Gaussian affine models. In particular, for the three-factor affine Gaussian model, we compare our bounds with the ones proposed by [Nunes and Prazeres, 2014]. Lower bound proposed by [Nunes and Prazeres, 2014] is comparable to our lower bound for all maturities and strikes. We find that our upper bound is less accurate for ATMF options but it seems to be more accurate for OTMF options (see Tables 1.1-1.3). We observe that for the given set of parameters, price estimated using our bounds and the conditioning approach are very close. On the other hand, with reference to computational time (see Table 1.14), [Nunes and Prazeres, 2014] approach is more efficient than our bounds. However, our aim is to find approximations that are applicable to a wider class of models and not only to Gaussian affine models.

The computation of the upper bound is slower than the lower bound calculation, but it is still faster than Monte Carlo simulations for a comparable accuracy (see Table 1.14). In addition, the range between the lower and upper bound is always narrow so, in practice, the combined use of the two bounds provides an accurate estimate of the true price.

In each table we compute the mean absolute percentage error (MAPE) of bounds with respect to Monte Carlo prices, taken as a benchmark, for fixed maturity and strike.

The RMSD computation performed for the two-factor CIR model and reported in Table 1.13 is an important validation for the stability of the accuracy of the bounds to changes in the parameter set. The RMSD of the lower bound for at-the-money and in-the-money options is less than 0.1% of the Monte Carlo average price, which is a good result. The relative error is larger for out-of-the-money options, in particular for the swaptions with a long swap length. Indeed, the maximum error is around 0.3% of the Monte Carlo price. The RMSDs of the upper bound are greater than the RMSDs of the lower bound, in particular for swaptions with longer swap lengths. However, the maximum RMSD of the upper bound is about 0.8% of the Monte Carlo price, which is also confirmation of the good performance of the upper bound.

In conclusion, numerical results confirm our hypothesis about the performance of the new algorithm in terms of computational times for the calculus of the lower bound, except for quadratic models in which the characteristic function is not analytic. Moreover, numerical tests show a very good accuracy of the new upper bound for different models across tenors, maturities and strikes.

Opt. Mat.	**1**					
Swap length	**MC**	**LB (G)**	**LB (HP)**	**UB (HP)**	**LB (CA)**	**UB (CA)**
1	20.817	20.817	20.817	20.818	20.817	20.817
	0.001			0.001		0.000
2	33.119	33.119	33.119	33.129	33.119	33.120
	0.002			0.010		0.001
5	53.312	53.312	53.312	53.396	53.312	53.323
	0.002			0.084		0.011
10	65.583	65.579	65.584	65.758	65.584	65.613
	0.003			0.174		0.029
MAPE		0.002%	0.0005%	0.115%	0.0005%	0.018%
Opt. Mat.	**2**					
Swap length	**MC**	**LB (G)**	**LB (HP)**	**UB (HP)**	**LB (CA)**	**UB (CA)**
1	23.555	23.554	23.554	23.555	23.554	23.555
	0.001			0.001		0.0001
2	38.434	38.434	38.434	38.444	38.434	38.435
	0.002			0.010		0.002
5	63.688	63.686	63.686	63.764	63.686	63.702
	0.003			0.078		0.015
10	79.068	79.062	79.067	79.224	79.067	79.106
	0.004			0.157		0.039
MAPE		0.004%	0.002%	0.086%	0.002%	0.018%
Opt. Mat.	**5**					
Swap length	**MC**	**LB (G)**	**LB (HP)**	**UB (HP)**	**LB (CA)**	**UB (CA)**
1	23.207	23.207	23.207	23.208	23.207	23.207
	0.001			0.001		0.0001
2	38.723	38.722	38.722	38.730	38.722	38.724
	0.002			0.008		0.002
5	65.684	65.683	65.683	65.741	65.683	65.700
	0.003			0.058		0.017
10	82.161	82.156	82.159	82.273	82.159	82.201
	0.004			0.114		0.042
MAPE		0.003%	0.001%	0.061%	0.001%	0.019%

Table 1.1: The table shows **ATMF payer swaption** prices for the **three-factor Gaussian model** at three different maturities (1Y, 2Y and 5Y). For each swaption, we report the price in basis points estimated with the Monte Carlo method, MC, the geometric lower bound, LB (G), the hyperplane approximation lower bound, LB (HP), the upper bound, UB (HP), and the lower and upper bounds obtained with the conditional approach of [Nunes and Prazeres, 2014], LB (CA) and UB(CA). Monte Carlo prices are estimated using 10^9 simulations, the antithetic variates method and the exact probability distribution. Below each Monte Carlo price, the size of the confidence interval at 97.5% is reported in basis points. The distance between the lower and the upper bounds is provided below each upper bound value.

Opt. Mat.	**1**					
Swap length	**MC**	**LB (G)**	**LB (HP)**	**UB (HP)**	**LB (CA)**	**UB (CA)**
1	79.4449 0.0003	79.4449	79.4449	79.4451 0.0002	79.4449	79.4449 0.0001
2	154.5632 0.0003	154.5632	154.5632	154.5646 0.0014	154.5632	154.5642 0.0010
5	361.4695 0.0001	361.4695	361.4695	361.4713 0.0018	361.4695	361.4793 0.0098
10	636.9818 0.0001	636.9816	636.9818	636.9819 0.0001	636.9818	637.0074 0.0256
MAPE		0.00002%	0.00002%	0.0004%	0.00002%	0.0019%
Opt. Mat.	**2**					
Swap length	**MC**	**LB (G)**	**LB (HP)**	**UB (HP)**	**LB (CA)**	**UB (CA)**
1	78.4043 0.0005	78.4039	78.4039	78.4042 0.0003	78.4039	78.4040 0.0001
2	150.9113 0.0005	150.9108	150.9108	150.9131 0.0023	150.9108	150.9121 0.0013
5	346.2753 0.0003	346.2753	346.2753	346.2813 0.0061	346.2753	346.2884 0.0132
10	604.8099 0.0002	604.8098	604.8101	604.8113 0.0013	604.8101	604.8443 0.0342
MAPE		0.0002%	0.0002%	0.0008%	0.0002%	0.0026%
Opt. Mat.	**5**					
Swap length	**MC**	**LB (G)**	**LB (HP)**	**UB (HP)**	**LB (CA)**	**UB (CA)**
1	69.4421 0.0005	69.4420	69.4420	69.4423 0.0003	69.4420	69.4421 0.0001
2	131.9486 0.0007	131.9485	131.9485	131.9511 0.0026	131.9485	131.9500 0.0015
5	295.1619 0.0006	295.1618	295.1619	295.1717 0.0098	295.1619	295.1762 0.0143
10	508.8398 0.0003	508.8397	508.8398	508.8444 0.0046	508.8398	508.8766 0.0368
MAPE		0.0001%	0.0001%	0.0016%	0.0001%	0.0033%

Table 1.2: The table shows **ITMF (0.85 $\times$ ATMF) payer swaption** prices for the **three-factor Gaussian model** at three different maturities (1Y, 2Y and 5Y). For each swaption, we report the price in basis points estimated with the Monte Carlo method, MC, the geometric lower bound, LB (G), the hyperplane approximation lower bound, LB (HP), the upper bound, UB (HP), and the lower and upper bounds obtained with the conditional approach of [Nunes and Prazeres, 2014], LB (CA) and UB(CA). Monte Carlo prices are estimated using 10^9 simulations, the antithetic variates method and the exact probability distribution. Below each Monte Carlo price, the size of the confidence interval at 97.5% is reported in basis points. The distance between the lower and the upper bounds is provided below each upper bound value.

Opt. Mat.	1					
Swap length	**MC**	**LB (G)**	**LB (HP)**	**UB (HP)**	**LB (CA)**	**UB (CA)**
1	1.5700	1.5700	1.5700	1.5703	1.5700	1.5701
	0.0003			0.0003		0.0001
2	1.0649	1.0648	1.0648	1.0671	1.0648	1.0661
	0.0003			0.0022		0.0013
5	0.1496	0.1495	0.1495	0.1523	0.1495	0.1624
	0.0001			0.0027		0.0129
10	0.00268	0.00268	0.00268	0.00281	0.00268	-
	0.00002			0.0001		-
MAPE		0.0327%	0.0327%	1.788%	0.032%	2.914%
Opt. Mat.	**2**					
Swap length	**MC**	**LB (G)**	**LB (HP)**	**UB (HP)**	**LB (CA)**	**UB (CA)**
1	2.8242	2.8238	2.8238	2.8242	2.8238	2.8239
	0.0005			0.0005		0.0002
2	2.6128	2.6123	2.6123	2.6162	2.6123	2.6141
	0.0006			0.0039		0.0018
5	0.9049	0.9048	0.9048	0.9141	0.9048	0.9222
	0.0004			0.0093		0.0174
10	0.0756	0.0756	0.0756	0.0776	0.0756	0.1199
	0.0001			0.0019		0.0443
MAPE		0.017%	0.017%	0.928%	0.017%	15.146%
Opt. Mat.	**5**					
Swap length	**MC**	**LB (G)**	**LB (HP)**	**UB (HP)**	**LB (CA)**	**UB (CA)**
1	3.7940	3.7938	3.7938	3.7943	3.7938	3.7940
	0.0006			0.0005		0.0002
2	4.3224	4.3223	4.3223	4.3265	4.3223	4.3242
	0.0008			0.0043		0.0020
5	2.5697	2.5693	2.5696	2.5839	2.5696	2.5884
	0.0007			0.0144		0.0189
10	0.5166	0.5164	0.5166	0.5231	0.5166	0.5643
	0.0003			0.0065		0.0477
MAPE		0.015%	0.003%	0.481%	0.003%	2.503%

Table 1.3: The table shows **OTMF (1.15 $\times$ ATMF) payer swaption** prices for the **three-factor Gaussian model** at three different maturities (1Y, 2Y and 5Y). For each swaption, we report the price in basis points estimated with the Monte Carlo method, MC, the geometric lower bound, LB (G), the hyperplane approximation lower bound, LB (HP), the upper bound, UB (HP), and the lower and upper bounds obtained with the conditional approach of [Nunes and Prazeres, 2014], LB (CA) and UB(CA). Monte Carlo prices are estimated using 10^9 simulations, the antithetic variates method and the exact probability distribution. Below each Monte Carlo price, the size of the confidence interval at 97.5% is reported in basis points. The distance between the lower and the upper bounds is provided below each upper bound value.

Opt. Mat.	1					
Swap length	**MC**	**LB (G)**	**LB (HP)**	**UB (HP)**	**MC (CV)**	**Kim**
1	48.469 0.004	48.466	48.466	48.467 0.001	48.466 10^{-4}	48.466
2	85.876 0.008	85.871	85.871	85.883 0.012	85.871 10^{-4}	85.871
5	169.437 0.016	169.427	169.428	169.639 0.211	169.428 10^{-4}	169.428
10	265.834 0.025	265.779	265.820	266.634 0.814	265.818 0.004	265.820
MAPE		0.010%	0.005%	0.108%		

Opt. Mat.	2					
Swap length	**MC**	**LB (G)**	**LB (HP)**	**UB (HP)**	**MC (CV)**	**Kim**
1	59.359 0.005	59.361	59.361	59.362 0.001	59.361 10^{-4}	59.361
2	106.885 0.010	106.890	106.890	106.904 0.014	106.890 10^{-4}	106.890
5	216.868 0.020	216.879	216.880	217.103 0.222	216.881 10^{-4}	216.880
10	344.969 0.033	344.949	344.990	345.795 0.805	344.992 0.005	344.990
MAPE		0.005%	0.005%	0.093%		

Opt. Mat.	5					
Swap length	**MC**	**LB (G)**	**LB (HP)**	**UB (HP)**	**MC (CV)**	**Kim**
1	66.979 0.006	66.970	66.970	66.971 0.001	66.970 10^{-4}	66.970
2	123.847 0.011	123.830	123.830	123.842 0.012	123.830 10^{-4}	123.830
5	261.403 0.025	261.366	261.368	261.525 0.157	261.368 10^{-4}	261.368
10	422.939 0.042	422.857	422.883	423.408 0.525	422.887 0.004	422.883
MAPE		0.015%	0.013%	0.044%		

Table 1.4: The table shows **ATMF payer swaption** prices for the **two-factor CIR model** at three different maturities (1Y, 2Y and 5Y). For each swaption, we report the price in basis points estimated with the Monte Carlo method, MC, the geometric lower bound, LB (G), the hyperplane approximation lower bound, LB (HP), the upper bound, UB, the Monte Carlo with control variable technique, MC (CV), and the approximation "A" of [Kim, 2014]. Monte Carlo without and with control variable are estimated using 10^9 and 10^5 simulations, respectively, and the exact probability distribution. Below each Monte Carlo price, the size of the confidence interval at 97.5% is reported in basis points. The distance between the lower and the upper bounds is provided below each upper bound value.

Opt. Mat.	1					
Swap length	**MC**	**LB (G)**	**LB (HP)**	**UB**	**MC (CV)**	**Kim**
1	107.578 0.002	107.577	107.577	107.578 0.001	107.577 10^{-4}	107.577
2	208.039 0.004	208.037	208.037	208.045 0.008	208.037 10^{-4}	208.037
5	475.672 0.007	475.668	475.669	475.782 0.113	475.669 10^{-4}	475.669
10	812.488 0.009	812.470	812.482	812.917 0.435	812.482 0.002	812.482
MAPE		0.001%	0.001%	0.020%		

Opt. Mat.	2					
Swap length	**MC**	**LB (G)**	**LB (HP)**	**UB**	**MC (CV)**	**Kim**
1	116.838 0.003	116.839	116.839	116.840 0.001	116.839 10^{-4}	116.839
2	222.361 0.006	222.363	222.363	222.373 0.010	222.363 10^{-4}	222.363
5	493.297 0.011	493.301	493.301	493.454 0.152	493.301 10^{-4}	493.301
10	825.213 0.017	825.202	825.218	825.772 0.554	825.219 0.003	825.218
MAPE		0.001%	0.001%	0.027%		

Opt. Mat.	5					
Swap length	**MC**	**LB (G)**	**LB (HP)**	**UB**	**MC (CV)**	**Kim**
1	114.936 0.004	114.930	114.930	114.931 0.001	114.930 10^{-4}	114.930
2	217.219 0.008	217.208	217.208	217.217 0.009	217.208 10^{-4}	217.208
5	473.353 0.016	473.330	473.331	473.455 0.124	473.331 10^{-4}	473.331
10	778.608 0.028	778.559	778.572	778.993 0.420	778.573 0.002	778.572
MAPE		0.005%	0.005%	0.019%		

Table 1.5: The table shows **ITMF (0.85 $\times$ ATMF) payer swaption** prices for the **two-factor CIR model** at three different maturities (1Y, 2Y and 5Y). For each swaption, we report the price in basis points estimated with the Monte Carlo method, MC, the geometric lower bound, LB (G), the hyperplane approximation lower bound, LB (HP), the upper bound, UB, the Monte Carlo with control variable technique, MC (CV), and the approximation "A" of [Kim, 2014]. Monte Carlo without and with control variable are estimated using 10^9 and 10^5 simulations, respectively, and the exact probability distribution. Below each Monte Carlo price, the size of the confidence interval at 97.5% is reported in basis points. The distance between the lower and the upper bounds is provided below each upper bound value.

Opt. Mat.	1					
Swap length	**MC**	**LB (G)**	**LB (HP)**	**UB**	**MC (CV)**	**Kim**
1	15.977 0.006	15.973	15.973	15.973 0.001	15.973 10^{-4}	15.973
2	23.73 0.011	23.724	23.724	23.733 0.009	23.724 10^{-4}	23.724
5	33.576 0.024	33.565	33.567	33.698 0.132	33.567 10^{-4}	33.567
10	42.469 0.039	42.425	42.458	42.873 0.414	42.459 0.005	42.458
MAPE		0.047%	0.026%	0.337%		

Opt. Mat.	2					
Swap length	**MC**	**LB (G)**	**LB (HP)**	**UB**	**MC (CV)**	**Kim**
1	24.445 0.007	24.446	24.446	24.447 0.001	24.446 10^{-4}	24.446
2	39.961 0.013	39.964	39.964	39.977 0.013	39.964 10^{-4}	39.964
5	68.731 0.029	68.740	68.742	68.918 0.176	68.742 0.001	68.742
10	99.027 0.048	99.004	99.049	99.626 0.577	99.045 0.005	99.049
MAPE		0.012%	0.013%	0.232%		

Opt. Mat.	5					
Swap length	**MC**	**LB (G)**	**LB (HP)**	**UB**	**MC (CV)**	**Kim**
1	34.558 0.008	34.546	34.546	34.547 0.001	34.546 10^{-4}	34.546
2	61.86 0.015	61.838	61.838	61.849 0.011	61.838 10^{-4}	61.838
5	124.445 0.032	124.396	124.398	124.546 0.148	124.399 0.001	124.398
10	196.344 0.056	196.230	196.265	196.742 0.476	196.266 0.005	196.265
MAPE		0.042%	0.037%	0.083%		

Table 1.6: The table shows **OTMF (1.15 $\times$ ATMF) payer swaption** prices for the **two-factor CIR model** at three different maturities (1Y, 2Y and 5Y). For each swaption, we report the price in basis points estimated with the Monte Carlo method, MC, the geometric lower bound, LB (G), the hyperplane approximation lower bound, LB (HP), the upper bound, UB, the Monte Carlo with control variable technique, MC (CV), and the approximation "A" of [Kim, 2014]. Monte Carlo without and with control variable are estimated using 10^9 and 10^5 simulations, respectively, and the exact probability distribution. Below each Monte Carlo price, the size of the confidence interval at 97.5% is reported in basis points. The distance between the lower and the upper bounds is provided below each upper bound value.

Opt. Mat.	**1**					
Swap length	MC	LB (G)	LB (HP)	UB (HP)	MC (CV)	Kim
1	403.88 0.37	403.77	403.77	403.77 0.00	403.77 0.00001	403.77
2	546.54 0.61	546.17	546.17	546.39 0.22	546.17 0.00001	546.17
5	857.58 1.02	856.73	856.93	859.96 3.03	856.93 0.0006	856.93
10	963.67 1.13	962.77	962.96	964.51 1.55	962.96 0.00012	962.96
MAPE		0.071%	0.061%	0.105%		

Opt. Mat.	**2**					
Swap length	MC	LB (G)	LB (HP)	UB (HP)	MC (CV)	Kim
1	434.32 0.39	434.24	434.24	434.24 0.00	434.24 0.00001	434.24
2	678.54 0.73	677.82	677.82	678.33 0.50	677.82 0.00004	677.82
5	1238.63 1.28	1236.76	1236.99	1240.84 3.86	1236.99 0.001	1236.99
10	1426.94 1.42	1425.00	1425.19	1426.95 1.77	1425.19 0.0003	1425.19
MAPE		0.103%	0.095%	0.057%		

Opt. Mat.	**5**					
Swap length	MC	LB (G)	LB (HP)	UB (HP)	MC (CV)	Kim
1	473.22 0.44	473.45	473.45	473.48 0.03	473.45 0.00001	473.45
2	926.64 0.91	925.17	925.17	926.28 1.11	925.17 0.0001	925.17
5	1986.48 1.64	1983.64	1983.83	1987.31 3.48	1983.84 0.002	1983.83
10	2341.44 1.83	2339.38	2339.51	2340.84 1.33	2339.51 0.0003	2339.51
MAPE		0.110%	0.106%	0.041%		

Table 1.7: The table shows **ATMF payer swaption** prices for the **two-factor Gaussian model with exponential jump sizes** at three different maturities (1Y, 2Y and 5Y). Parameter values are calibrated to the Euribor six-month curve from January 4th, 2015. For each swaption, we report the price in basis points estimated with the Monte Carlo method, MC, the geometric lower bound, LB (G), the hyperplane approximation lower bound, LB (HP), the upper bound, UB, the Monte Carlo with control variable technique, MC (CV), and the approximation "A" of [Kim, 2014]. Monte Carlo without and with control variable are estimated using 8×10^6 and 10^5 simulations, respectively, an Euler scheme with a time step equal to 0.0005 and the antithetic variates technique. Below each Monte Carlo price, the size of the confidence interval at 97.5% is reported in basis points. The distance between the lower and the upper bounds is provided below each upper bound value.

Opt. Mat.	**1**					
Swap length	MC	LB (G)	LB (HP)	UB (HP)	MC (CV)	Kim
1	428.39 0.38	428.16	428.16	428.52 0.36	428.16 0.00001	428.16
2	640.68 0.64	640.35	640.35	640.45 0.10	640.35 0.00002	640.35
5	1360.17 1.08	1359.32	1359.44	1360.83 1.39	1359.44 0.0005	1359.44
10	2500.03 1.12	2499.21	2499.24	2501.74 2.51	2499.24 0.00018	2499.24
MAPE		0.050%	0.047%	0.046%		

Opt. Mat.	**2**					
Swap length	MC	LB (G)	LB (HP)	UB (HP)	MC (CV)	Kim
1	458.34 0.40	458.37	458.37	458.37 0.00	458.37 0.00001	458.37
2	768.02 1.07	768.01	768.01	768.30 0.29	768.01 0.00007	768.01
5	1700.29 1.34	1698.58	1698.72	1700.66 1.94	1698.72 0.001	1698.72
10	2792.62 1.42	2790.86	2790.91	2793.15 2.24	2790.91 0.0004	2790.91
MAPE		0.043%	0.040%	0.021%		

Opt. Mat.	**5**					
Swap length	MC	LB (G)	LB (HP)	UB (HP)	MC (CV)	Kim
1	496.72 0.45	496.84	496.84	496.96 0.12	496.84 0.00001	496.84
2	1011.09 0.94	1010.49	1010.49	1011.31 0.81	1010.49 0.00004	1010.49
5	2399.67 1.71	2396.76	2396.88	2399.13 2.24	2396.88 0.001	2396.88
10	3459.41 1.34	3457.41	3457.46	3458.80 1.35	3457.46 0.0002	3457.46
MAPE		0.066%	0.064%	0.028%		

Table 1.8: The table shows **ITMF (0.85 $\times$ ATMF) payer swaption** prices for the **two-factor Gaussian model with exponential jump sizes** at three different maturities (1Y, 2Y and 5Y). Parameter values are calibrated to the Euribor six-month curve from January 4th, 2015. For each swaption, we report the price in basis points estimated with the Monte Carlo method, MC, the geometric lower bound, LB (G), the hyperplane approximation lower bound, LB (HP), the upper bound, UB, the Monte Carlo with control variable technique, MC (CV), and the approximation "A" of [Kim, 2014]. Monte Carlo without and with control variable are estimated using 8×10^6 and 10^5 simulations, respectively, an Euler scheme with a time step equal to 0.0005 and the antithetic variates technique. Below each Monte Carlo price, the size of the confidence interval at 97.5% is reported in basis points. The distance between the lower and the upper bounds is provided below each upper bound value.

Opt. Mat.	**1**					
Swap length	MC	LB (G)	LB (HP)	UB (HP)	MC (CV)	Kim
1	243.47 0.30	243.35	243.35	243.38 0.02	243.35 0.00001	243.35
2	159.23 0.40	158.92	158.92	159.82 0.89	158.92 0.0001	158.92
5	136.63 0.50	136.17	136.28	137.77 1.49	136.28 0.0007	136.28
10	79.13 0.41	78.96	78.99	79.09 0.10	78.99 0.00002	78.99
MAPE		0.20%	0.17%	0.32%		

Opt. Mat.	**2**					
Swap length	MC	LB (G)	LB (HP)	UB (HP)	MC (CV)	Kim
1	273.48 0.32	273.41	273.41	273.43 0.02	273.41 0.00001	273.41
2	261.82 0.51	261.00	261.00	262.25 1.25	261.00 0.0004	261.00
5	265.11 0.68	263.92	264.13	267.07 2.94	264.13 0.001	264.13
10	161.29 0.58	160.82	160.89	161.17 0.28	160.89 0.001	160.89
MAPE		0.27%	0.24%	0.25%		

Opt. Mat.	**5**					
Swap length	MC	LB (G)	LB (HP)	UB (HP)	MC (CV)	Kim
1	314.50 0.36	314.82	314.82	314.91 0.09	314.82 0.00001	314.82
2	460.58 0.68	459.26	459.27	461.01 1.74	459.27 0.0005	459.27
5	591.07 0.99	588.97	589.36	591.92 2.56	589.36 0.002	589.36
10	397.28 0.88	395.91	396.04	396.79 0.75	396.04 0.0004	396.04
MAPE		0.27%	0.25%	0.12%		

Table 1.9: The table shows **OTMF (1.15 $\times$ ATMF) payer swaption** prices for the **two-factor Gaussian model with exponential jump sizes** at three different maturities (1Y, 2Y and 5Y). Parameter values are calibrated to the Euribor six-month curve from January 4th, 2015. For each swaption, we report the price in basis points estimated with the Monte Carlo method, MC, the geometric lower bound, LB (G), the hyperplane approximation lower bound, LB (HP), the upper bound, UB, the Monte Carlo with control variable technique, MC (CV), and the approximation "A" of [Kim, 2014]. Monte Carlo without and with control variable are estimated using 8×10^6 and 10^5 simulations, respectively, an Euler scheme with a time step equal to 0.0005 and the antithetic variates technique. Below each Monte Carlo price, the size of the confidence interval at 97.5% is reported in basis points. The distance between the lower and the upper bounds is provided below each upper bound value.

Opt. Mat.	1					
Swap length	**MC**	**LB (G)**	**LB (T)**	**UB**	**MC (CV)**	**Kim**
2	52.35 0.03	52.32	52.32	52.33 0.02	52.32	52.32 0.00001
5	106.44 0.05	106.39	106.39	106.5 0.11	106.39	106.39 0.00001
10	148.35 0.06	148.31	148.32	148.54 0.22	148.31	148.32 0.00001
MAPE		0.05%	0.04%	0.07%		

Opt. Mat.	2					
Swap length	**MC**	**LB (G)**	**LB (T)**	**UB**	**MC (CV)**	**Kim**
2	65.68 0.03	65.69	65.69	65.69 0.01	65.69	65.69 0.00001
5	129.98 0.06	130.00	130.00	130.05 0.06	130.00	130.00 0.00001
10	182.14 0.06	182.17	182.17	182.25 0.08	182.17	182.17 0.00001
MAPE		0.01%	0.01%	0.05%		

Opt. Mat.	5					
Swap length	**MC**	**LB (G)**	**LB (T)**	**UB**	**MC (CV)**	**Kim**
2	65.87 0.03	65.87	65.87	65.87 0	65.87	65.87 0.00001
5	130.10 0.04	130.10	130.10	130.12 0.02	130.1	130.1 0.0001
10	190.54 0.04	190.54	190.53	190.64 0.11	190.53	190.54 0.0004
MAPE		0.001%	0.002%	0.02%		

Table 1.10: The table shows **ATMF payer swaption** prices for the **two-factor Gaussian quadratic model** at three different maturities (1Y, 2Y and 5Y). For each swaption, we report the price in basis points estimated with the Monte Carlo method, MC, the geometric lower bound, LB (G), the (second order) Taylor approximation lower bound, LB (T), the upper bound, UB, the Monte Carlo with control variable technique, MC (CV), and the approximation "A" of [Kim, 2014]. Monte Carlo without and with control variable are estimated using 8×10^6 and 10^5 simulations, respectively, an Euler scheme with a time step equal to 0.0005 and the antithetic variates technique. Below each Monte Carlo price, the size of the confidence interval at 97.5% is reported in basis points. The distance between the lower and the upper bounds is provided below each upper bound value.

Opt. Mat.	1					
Swap length	**MC**	**LB (G)**	**LB (T)**	**UB**	**MC (CV)**	**Kim**
2	138.51	138.47	138.47	138.49	138.47	138.47
	0.02			0.01		0.00001
5	304.44	304.39	304.39	304.43	304.39	304.39
	0.02			0.05		0.00001
10	494.61	494.59	494.59	494.73	494.58	494.59
	0.02			0.14		0.00001
MAPE		0.02%	0.02%	0.02%		

Opt. Mat.	2					
Swap length	**MC**	**LB (G)**	**LB (T)**	**UB**	**MC (CV)**	**Kim**
2	140.42	140.42	140.42	140.42	140.42	140.42
	0.02			0.01		0.00001
5	304.26	304.26	304.26	304.31	304.26	304.26
	0.03			0.05		0.00001
10	488.15	488.14	488.14	488.26	488.14	488.14
	0.02			0.12		0.00001
MAPE		0.001%	0.001%	0.01%		

Opt. Mat.	5					
Swap length	**MC**	**LB (G)**	**LB (T)**	**UB**	**MC (CV)**	**Kim**
2	124.36	124.37	124.37	124.37	124.37	124.37
	0.02			0.01		0.00001
5	268.66	268.66	268.67	268.69	268.66	268.66
	0.03			0.02		0.00003
10	432.70	432.71	432.70	432.78	432.70	432.70
	0.04			0.08		0.0001
MAPE		0.004%	0.002%	0.01%		

Table 1.11: The table shows **ITMF (ATMF - 0.75%) payer swaption** prices for the **two-factor Gaussian quadratic model** at three different maturities (1Y, 2Y and 5Y). For each swaption, we report the price in basis points estimated with the Monte Carlo method, MC, the geometric lower bound, LB (G), the (second order) Taylor approximation lower bound, LB (T), the upper bound, UB, the Monte Carlo with control variable technique, MC (CV), and the approximation "A" of [Kim, 2014]. Monte Carlo without and with control variable are estimated using 8×10^6 and 10^5 simulations, respectively, an Euler scheme with a time step equal to 0.0005 and the antithetic variates technique. Below each Monte Carlo price, the size of the confidence interval at 97.5% is reported in basis points. The distance between the lower and the upper bounds is provided below each upper bound value.

Opt. Mat.	1					
Swap length	**MC**	**LB (G)**	**LB (T)**	**UB**	**MC (CV)**	**Kim**
2	11.87	11.86	11.86	11.87	11.86	11.86
	0.02			0.01		0.00001
5	17.90	17.90	17.89	17.95	17.89	17.89
	0.03			0.06		0.00001
10	12.21	-	12.23	12.31	12.22	12.23
	0.02			0.08		0.00001
MAPE		-	0.11%	0.37%		

Opt. Mat.	2					
Swap length	**MC**	**LB (G)**	**LB (T)**	**UB**	**MC (CV)**	**Kim**
2	23.04	23.04	23.04	23.05	23.04	23.04
	0.03			0		0.00001
5	34.52	34.40	34.54	34.56	34.54	34.54
	0.04			0.03		0.00001
10	27.95	-	27.97	28.01	27.97	27.97
	0.03			0.04		0.00001
MAPE		-	0.05%	0.13%		

Opt. Mat.	5					
Swap length	**MC**	**LB (G)**	**LB (T)**	**UB**	**MC (CV)**	**Kim**
2	27.55	27.55	27.55	27.55	27.55	27.55
	0.02			0		0.00004
5	39.84	39.82	39.82	39.86	39.82	39.84
	0.03			0.04		0.0004
10	36.10	-	36.05	36.52	36.05	36.11
	0.03			0.47		0.0008
MAPE		-	0.06%	0.41%		

Table 1.12: The table shows **OTMF (ATMF + 0.75%) payer swaption** prices for the **two-factor Gaussian quadratic model** at three different maturities (1Y, 2Y and 5Y). For each swaption, we report the price in basis points estimated with the Monte Carlo method, MC, the geometric lower bound, LB (G), the (second order) Taylor approximation lower bound, LB (T), the upper bound, UB, the Monte Carlo with control variable technique, MC (CV), and the approximation "A" of [Kim, 2014]. Monte Carlo without and with control variable are estimated using 8×10^6 and 10^5 simulations, respectively, an Euler scheme with a time step equal to 0.0005 and the antithetic variates technique. Below each Monte Carlo price, the size of the confidence interval at 97.5% is reported in basis points. The distance between the lower and the upper bounds is provided below each upper bound value.

RMSD - LB (HP)											
ATM	1	2	5	ITM	1	2	5	OTM	1	2	5
1	0.05%	0.07%	0.08%	1	0.01%	0.02%	0.02%	1	0.2%	0.2%	0.2%
2	0.05%	0.07%	0.08%	2	0.01%	0.01%	0.01%	2	0.2%	0.2%	0.2%
5	0.05%	0.07%	0.09%	5	0.004%	0.01%	0.01%	5	0.2%	0.3%	0.3%
10	0.05%	0.07%	0.09%	10	0.004%	0.01%	0.01%	10	0.2%	0.3%	0.3%

RMSD - UB (HP)											
ATM	1	2	5	ITM	1	2	5	OTM	1	2	5
1	0.05%	0.07%	0.08%	1	0.01%	0.02%	0.01%	1	0.2%	0.2%	0.2%
2	0.06%	0.09%	0.11%	2	0.01%	0.02%	0.02%	2	0.2%	0.3%	0.3%
5	0.14%	0.20%	0.28%	5	0.03%	0.05%	0.08%	5	0.3%	0.5%	0.6%
10	0.15%	0.22%	0.32%	10	0.04%	0.06%	0.09%	10	0.3%	0.5%	0.7%

Table 1.13: These tables report for each swaption the RMSD value of the bounds with respect to the Monte Carlo value obtained by randomly sampling 100 parameter sets.

3 factor Gaussian model

Overall time (sec)	MC	LB (G)	LB (HP)	UB (HP)	Kim	LB (CA)	UB (CA)
ATMF	32×10^2	0.122	0.084	0.140	0.141	0.024	0.024
ITMF	32×10^2	0.117	0.170	0.223	0.219	0.035	0.035
OTMF	32×10^2	0.113	0.169	0.223	0.219	0.037	0.037

2 factor CIR model

Overall time (sec)	MC	LB (G)	LB (HP)	UB (HP)	Kim
ATMF	23×10^2	1.456	0.146	17.054	0.391
ITMF	23×10^2	1.199	0.150	17.015	0.341
OTMF	23×10^2	1.314	0.152	17.018	0.395

2 factor Gaussian model with exponential jumps

Overall time (sec)	MC	LB (G)	LB (HP)	UB (HP)	Kim
ATMF	35×10^3	2.643	1.957	132.229	1.968
ITMF	35×10^3	2.643	0.868	129.218	0.977
OTMF	35×10^3	2.643	0.845	149.071	0.966

2 factor Gaussian quadratic model

Overall time (sec)	MC	LB (HP)	UB (HP)	Kim
ATMF	1.472×10^3	0.861	587.403	0.665
ITMF	1.472×10^3	1.124	635.807	0.717
OTMF	1.472×10^3	1.019	509.202	0.633

Table 1.14: Computational times shown in the table are the overall time needed for calculating the matrices of swaption prices reported in Tables 1.1-1.12.

Swap length (y)	LB (HP) (sec)	Kim (sec)	LB (HP) (%)	Kim (%)
1	0.024	0.022	-	-
2	0.023	0.026	0%	20%
5	0.023	0.034	0%	55%
10	0.032	0.051	34%	132%
15	0.040	0.071	69%	225%
20	0.048	0.089	102%	305%

Table 1.15: For each swaption, we report in the first two columns the run time in seconds and in the last two columns the percentage variation between the run times and the first row. The maturity of the swaptions is two years and the frequency of payments is six months.

Chapter 2

Approximate pricing of swaption in a multiple-curve framework

In this chapter, we extend the lower and upper bounds to multiple-curve models that reflect the presence of various interest curves in the market after the 2007 crisis. Multiple-curve interest rate models are widely discussed in the literature (see, among others [Ametrano and Bianchetti, 2009], [Morini, 2009] and recently [Moreni and Pallavicini, 2014] and [Fanelli, 2016]). In particular, we concentrate on the affine multiple-curve model developed in [Moreni and Pallavicini, 2014]. To the best of our knowledge, none of the approximate methods previously described for pricing swaptions has been developed for a multiple-curve interest rate framework. The extension of the previous discussed bounds to a multiple curve framework is not trivial, because, as we see in the next section, in a multiple curve market, the pricing formula of swaption changes substantially. In particular, a swaption is no more a plain vanilla option written on a basket of ZCB (or on a coupon bound).
The chapter is organised as follows. In Section 2 we introduce the weighted Gaussian multiple curve model of [Moreni and Pallavicini, 2014]. In Sections 3 and 4, we extend the lower and upper bound formulas developed in the previous chapter to the multiple-curve model. Section 5 presents numerical results.

2.1 Multiple-curve model

The (payer) swaption formula in the multi-curve framework becomes

$$C(t) = P(t,T)\,\mathbb{E}_t^T\left[\left(\sum_{j=1}^{n} P(T,T_j)\,x\,(F^x(T,T_j,x)-K)\right)^+\right] \tag{2.1}$$

where $x = T_j - T_{j-1}$ is the tenor $\forall j = 1, ..., n$ and $T_0 = T$. $F^x(t,T,x)$ is the fair rate of a FRA contract written on the Libor rate between $T-x$ and T and tenor x (usually x = 1M, 3M, 6M or 12M). $P(t,T)$ is the price at time t of a risk-free zero-coupon bond with maturity T. We test the lower and upper bounds to the multiple-curve weighted Gaussian model presented in [Moreni and Pallavicini, 2014]. In this model,

the zero-coupon bond price process has the following dynamic

$$P(t,T) = \frac{P(0,T)}{P(0,t)}\, e^{\int_0^t (\Sigma(s,t)-\Sigma(s,T))^\top\, dW(s) + \int_0^t (A(s,t)-A(s,T))\, ds}, \tag{2.2}$$

where

$\Sigma(t,T) = \int_t^T \sigma(t,u)\, du$ is a d-dimensional vector volatility function,

$W(t)$ is a d-dimensional standard Brownian motion,

$A(t,T) = \frac{1}{2}\Sigma(t,T)^\top \Sigma(t,T)$.

[Moreni and Pallavicini, 2014] define the risk-free forward rate F^0, which can be identified in the market using the overnight rate. It is built as the simple compounded forward rate in a classical single-curve framework. The risk-free forward rate at time t for the interval $[T-x, T]$ is

$$F^0(t,T,x) = \frac{1}{x}\left(\frac{P(t,T-x)}{P(t,T)} - 1\right). \tag{2.3}$$

Substituting equation (2.2) into (2.3), the following dynamic under the risk-neutral measure is obtained

$$F^0(t,T,x) = \frac{1}{x}\left[(1 + x\, F^0(0,T,x)) e^{\int_0^t \Sigma^0(s,T,x)^\top\, dW(s) + \int_0^t A^0(s,T,x)\, ds} - 1\right], \tag{2.4}$$

where

$\Sigma^0(s,T,x) = \Sigma(s,T) - \Sigma(s,T-x) = \int_{T-x}^T \sigma(s,u)\, du$,

$A^0(s,T,x) = A(s,T) - A(s,T-x) = \frac{1}{2}\Sigma(s,T)^\top\, \Sigma(s,T) - \frac{1}{2}\Sigma(s,T-x)^\top\, \Sigma(s,T-x)$.

The Libor FRA rate $F^x(t,T,x)$ is the fair rate of a FRA contract written on the Libor rate with tenor x (usually x = 1M, 3M, 6M or 12M). It is defined as

$$F^x(t,T,x) = \mathbb{E}_t^T\left[L(T-x,T)\right], \tag{2.5}$$

where

$L(T-x,T)$ is the spot Libor rate, fixed at time $T-x$ for the time interval $[T-x,T]$,

$\mathbb{E}_t^T[\,]$ denotes the expectation under T-forward measure, $\mathbb{P}^T$.

To model the FRA rate, these constraints have to be respected

(i) $F^x(t,T,x)$ has to be a martingale under the T-forward measure,

(ii) $\lim_{x\to 0} F^x(t,T,x) = \lim_{x\to 0} F^0(t,T,x)$ and $F^x(t,T,x) \sim F^0(t,T,x)$ if $x \sim 0$.

Hence, under the risk-neutral $\mathbb{P}$ measure, the FRA rate is in the form

$$F^x(t,T,x) = \frac{1}{x}\left[(1 + x\, F^x(0,T,x)) e^{\int_0^t \Sigma^x(s,T,x)^\top\, dW(s) + \int_0^t A^x(s,T,x)\, ds} - 1\right], \tag{2.6}$$

where

- $\Sigma^x(s,T,x) = \int_{T-x}^T \sigma(s,u;T,x)\, du$ is a d-dimensional volatility function,
- in order to satisfy condition (ii) $\sigma(s,T;T,0) = \sigma(s,T)$,
- to satisfy condition (i)

$$A^x(s,T,x) \;=\; -\frac{1}{2}\Sigma^x(s,T,x)^\top\, \Sigma^x(s,T,x) + \Sigma^x(s,T,x)^\top\, \Sigma(s,T). \tag{2.7}$$

2.1.1 Volatility specification

The weighted Gaussian specification of the multiple-curve model assumes a deterministic volatility in the form

$$\begin{aligned} \sigma(t,u;T,x) &= h(t)\, q(u;T,x)\, g(t,u), \\ g(t,u) &= \exp\left(-\lambda(u-t)\right), \\ h(t) &= \epsilon(t)\, h\, R, \end{aligned}$$

where λ is a deterministic array function, h is a diagonal matrix, and R is an upper triangular matrix such that $\rho = R^\top R$ is a correlation matrix. The model allows for a time-varying common volatility shape $\epsilon(t)$ of the form

$$\epsilon(t) = 1 + (\beta_0 - 1 + \beta_1\, t)e^{\beta_2\, t},$$

where β_0, β_1 and β_2 are three positive constants. Furthermore, the matrix q is given by

$$q_{i,j}(u;T,x) = e^{-\eta_i\, x}\, \mathrm{I}(i=j) \quad \text{for } i,j = 1,...,d$$

where η is a deterministic constant vector.

2.1.2 Markovian specification for the weighted Gaussian model

By plugging the expression for the volatility into formula (2.6), it is possible to work out the expression leading to the following Markovian representation of the FRA rate:

$$\log\left(\frac{1+x\,F^x(t,T,x)}{1+x\,F^x(0,T,x)}\right) = G(t,T,x)^\top\, \mathbf{X}(t) + a(t,T,x), \tag{2.8}$$

where $a(t,T,x)$ is a deterministic coefficient and it has the following form:

$$\begin{aligned} a(t,T,x) &= G(t,T,x)^\top\, Y(t) \left(G(t,T) - \frac{1}{2}G(t,T,x)\right) \\ (Y(t))_{ik} &= \int_0^t g_i(s,t)(h^\top(s)\, h(s))_{ik} g_k(s,t) ds \quad i,k = 1,...,d, \end{aligned}$$

$G(t,T,x)$ is a deterministic vector with components

$$G_i(t,T,x) = \int_{T-x}^{T} q_{ii}(u;T,x)\, g_i(t,u)\, du,$$

$G(t,T)$ is a deterministic vector with components

$$G_i(t,T) = \int_t^T g_i(t,u)\, du,$$

and $\mathbf{X}(t)$ is a vector Markovian process with components, under the risk-neutral measure, in the form

$$X_i(t) = \sum_{j=1}^{d} \int_0^t g_i(s,t) \left(h_{i,j}^\top(s) dW_j(s) + (h^\top(s)\, h(s))_{i,j} \left(\int_s^t g_i(s,y) dy\right) ds\right).$$

A similar Markovian representation can be obtained for the ZCB price,

$$\log\left(P(t,T)\frac{P(0,t)}{P(0,T)}\right) = -G(t,T)^\top\,\mathbf{X}(t) + a(t,T), \tag{2.9}$$

where $a(t,T)$ is a deterministic coefficient and it has the following form:

$$a(t,T) \;=\; -\frac{1}{2}G(t,T)^\top Y(t) G(t,T).$$

2.2 Extension of the lower bound formula to a multi-curve weighted Gaussian model

Using the Markovian representation of the FRA rate and of the risk-free ZCBs in the swaption pricing formula (see Section 2.1), we obtain

$$C(t) = P(t,T)\,\mathbb{E}_t^T\left[\left(\sum_{j=1}^{n} w_{1j}\,e^{(G_{1j})^\top\mathbf{X}(T)+a_{1j}} - w_{2j}\,e^{(G_{2j})^\top\mathbf{X}(T)+a_{2j}}\right)\mathrm{I}(\mathcal{A})\right],$$

where

$\mathcal{A}$ is the exercise region and is in the form

$$\mathcal{A} = \{\omega\in\Omega : \sum_{j=1}^{n} w_{1j}\,e^{(G_{1j})^\top\mathbf{X}(T)+a_{1j}} - w_{2j}\,e^{(G_{2j})^\top\mathbf{X}(T)+a_{2j}} > 0\},$$

$w_{1j} = \frac{P(t,T_j)}{P(t,T)}(1 + x\,F^x(t,T_j,x))$ and $w_{2j} = \frac{P(t,T_j)}{P(t,T)}(1+xK)$,

$G_{1j} = G(T,T_j,x) - G(T,T_j)$ and $G_{2j} = -G(T,T_j)$,

$a_{1j} = a(T,T_j,x) + a(T,T_j)$ and $a_{2j} = a(T,T_j)$.

If we substitute the set $\mathcal{A}$ with any other event set $\mathcal{G}\in\Omega$, we obtain a lower bound of the true price. In the affine class models, it is convenient to define the set $\mathcal{G}$ using a linear function of the state variates,

$$\mathcal{G} = \{\omega\in\Omega : \boldsymbol{\beta}^\top\mathbf{X}(T) \geq k\},$$

with $\boldsymbol{\beta}$ and α defined in formula (1.11). The lower bound is provided in the following proposition.

Proposition 2.2.1. *The lower bound to the European swaption price, for the multiple-curve weighted Gaussian model, is given by the following formula*

$$\widehat{LB}(t) = \max_{k\in\mathbb{R},\,\beta\in\mathbb{R}^d} LB_\beta(k;t). \tag{2.10}$$

For fixed parameters k and β, the lower bound is

$$\begin{aligned} LB_\beta(k;t) \;&=\; P(t,T)\,\omega\sum_{j=1}^{n}\left(w_{1j}\,\exp\left((G_{1j})^\top\mu + a_{1j} + \frac{1}{2}V_{1j}^G + \frac{1}{2}(d_{1j})^2\right)\mathcal{N}(\omega\,(d_{1j}-d))\right.\\ &-\; \left. w_{2j}\,\exp\left((G_{2j})^\top\mu + a_{2j} + \frac{1}{2}V_{2j}^G + \frac{1}{2}(d_{2j})^2\right)\mathcal{N}(\omega\,(d_{2j}-d))\right), \end{aligned} \tag{2.11}$$

where $\omega = -1$ *for receiver swaption and* $\omega = 1$ *for payer swaption,* $d = \frac{k-\boldsymbol{\beta}^\top \boldsymbol{\mu}}{\sqrt{\boldsymbol{\beta}^\top V \boldsymbol{\beta}}}$, $d_{ij} = (G_{ij})^\top v$ *for* $i = 1, 2$ *and* $j = 1, ..., d$, $v = \frac{V\beta}{\sqrt{\beta^\top V \beta}}$, $V_{ij}^G = (G_{ij})^\top (V - v\, v^\top)\, G_{ij}$ *for* $i = 1, 2$ *and* $j = 1, ..., d$ *and* $\mu = \mathbb{E}_t^T[\mathbf{X}(T)]$ *and* $V = Var_t(\mathbf{X}(T))$ *are the mean and covariance matrix of the variable* $\mathbf{X}(T)$*, which is multivariate normal under the* T*-forward measure.*

Proof: See Appendix C.1.

2.3 Extension of the upper bound formula to a multi-curve weighted Gaussian model

In a multiple-curve framework, the swaption price can also be written as

$$C(t) = P(t,T)\, \mathbb{E}_t^T \left[(B_1(\mathbf{X}(T)) - B_2(\mathbf{X}(T)))^+ \right] \tag{2.12}$$

where

$$\begin{aligned} B_1(\mathbf{X}(T)) &= \sum_{j=1}^{n} P(T,T_j)\, (1 + x\, F^x(T,T_j,x)) = \sum_{j=1}^{n} w_{1j}\, e^{(G_{1j})^\top \mathbf{X}(T) + a_{1j}}, \\ B_2(\mathbf{X}(T)) &= (1 + x\, K) \sum_{j=1}^{n} P(T,T_j) = \sum_{j=1}^{n} w_{2j}\, e^{(G_{2j})^\top \mathbf{X}(T) + a_{2j}}. \end{aligned}$$

Hence, the (undiscounted) approximation error of the lower bound defined in Proposition 2.2.1 is

$$\begin{aligned} & \frac{1}{P(t,T)} \left(C(t) - \widehat{LB}(t) \right) \\ = \;& \mathbb{E}_t^T[(B_1(\mathbf{X}(T)) - B_2(\mathbf{X}(T)))^+ I(\mathcal{G}^c)] + \mathbb{E}_t^T[(B_2(\mathbf{X}(T)) - B_1(\mathbf{X}(T)))^+ I(\mathcal{G})] \\ = \;& \Delta_1 + \Delta_2. \end{aligned}$$

The previous equality holds for both receiver and payer swaptions. Applying the same reasoning as in the single-curve case, we find that the upper bound is

$$UB(t) = \hat{LB}(t) + P(t,T)(\epsilon_1 + \epsilon_2), \tag{2.13}$$

where ϵ_1 and ϵ_2 are the upper bounds for Δ_1 and Δ_2 and their expressions are as follows:

$$\begin{aligned} \epsilon_1 &= \sum_{j=1}^{n} \mathbb{E}_t^T[P(T,T_j)\, (1 + x\, F^x(T,T_j,x) - K_j)^+\, I(\mathcal{G}^c)] \\ &= \sum_{j=1}^{n} \mathbb{E}^T \left[\left(w_{1j}\, e^{G_{1j}^\top \mathbf{X}(T) + a_{1j}} - \tilde{w}_{2j}\, e^{G_{2j}^\top \mathbf{X}(T) + a_{2j}} \right)^+ I(\mathcal{G}^c) \right], \qquad (2.14) \\ \epsilon_2 &= \sum_{j=1}^{n} \mathbb{E}_t^T[P(T,T_j)\, (K_j - 1 - x\, F^x(T,T_j,x))^+\, I(\mathcal{G})] \\ &= \sum_{j=1}^{n} \mathbb{E}^T \left[\left(\tilde{w}_{2j}\, e^{G_{2j}^\top \mathbf{X}(T) + a_{2j}} - w_{1j}\, e^{G_{1j}^\top \mathbf{X}(T) + a_{1j}} \right)^+ I(\mathcal{G}) \right], \qquad (2.15) \end{aligned}$$

where $\tilde{w}_{2j} = \frac{P(t,T_j)}{P(t,T)} K_j$ and

$$K_j = 1 + x\, F(T, T_j, x)|_{\mathbf{X}(T)=\mathbf{X}^*}, \tag{2.16}$$

where $\mathbf{X}^*$ is the point on the true exercise boundary (i.e. $B_1(\mathbf{X}(T)) - B_2(\mathbf{X}(T) = 0)$) where the density function of the model factors is largest.

Proposition 2.3.1. *The upper bound to the European swaption price for the multiple-curve weighted Gaussian model is given by the following formula:*

$$UB(t) = \widehat{LB}(t) + P(t,T)\,(\epsilon_1(-\alpha) + \epsilon_2(-\alpha)), \tag{2.17}$$

where

$$\begin{aligned}
\epsilon_1(k) &= \int_{-\infty}^{d} dz\, \frac{1}{\sqrt{2\pi}} e^{-\frac{z^2}{2}} \sum_{j=1}^{n} w_{1j}\, e^{a_{1j}+M_{1j}+\frac{1}{2}V_{1j}^G}\, N\left(d_{1j}\right) - \tilde{w}_{2j}\, e^{a_{2,j}+M_{2j}+\frac{1}{2}V_{2j}^G}\, N\left(d_{2j}\right), \\
d_{1j} &= \frac{\log\left(\frac{w_{1j}}{\tilde{w}_{2j}}\right) + M_{1j} + a_{1j} - M_{2j} - a_{2j} + V_{1j}^G - Cov_j}{\sqrt{V_{1j}^G + V_{2j}^G - 2Cov_j}}, \\
d_{2j} &= d_{1j} - \sqrt{V_{1j}^G + V_{2j}^G - 2Cov_j}, \\
\epsilon_2(k) &= \int_{d}^{+\infty} dz\, \frac{1}{\sqrt{2\pi}} e^{-\frac{z^2}{2}} \sum_{j=1}^{n} \tilde{w}_{2j}\, e^{a_{2j}+M_{2j}+\frac{1}{2}V_{2j}^G}\, N\left(\delta_{1j}\right) - w_{1j}\, e^{a_{1j}+M_{1j}+\frac{1}{2}V_{1j}^G}\, N\left(\delta_{2j}\right), \\
\delta_{1j} &= \frac{-\log\left(\frac{w_{1j}}{\tilde{w}_{2j}}\right) - M_{1j} - a_{1j} + M_{2j} + a_{2j} + V_{2j}^G - Cov_j}{\sqrt{V_{1j}^G + V_{2j}^G - 2Cov_j}}, \\
\delta_{2j} &= \delta_{1j} - \sqrt{V_{1j}^G + V_{2j}^G - 2Cov_j},
\end{aligned}$$

and $\widehat{LB}(t)$ is given in Proposition 2.2.1, $d = \frac{k-\beta^\top \mu}{\sqrt{\beta^\top V \beta}}$, $V_{ij}^G = G_{ij}^\top (V - vv^\top) G_{ij}$ and $Cov_j = G_{1j}^\top (V - vv^\top) G_{2j}$ for $i = 1, 2$ and $j = 1, ..., d$, $M_{ij} = G_{ij}^\top \mu + z G_{ij}^\top v$ for $i = 1, 2$ and $j = 1, ..., d$ $v = \frac{V\beta}{\sqrt{\beta^\top V \beta}}$, and $\mu = \mathbb{E}_t^T[\mathbf{X}(T)]$ and $V = Var_t(\mathbf{X}(T))$ are the mean and covariance matrix of the variable $\mathbf{X}(T)$, which is multivariate normal under the T-forward measure and $N(x)$ is the standard Gaussian cumulative distribution function. The upper bound formula holds for both receiver and payer swaption.

Proof: See Appendix C.2.

2.4 Numerical results

As in the single curve case, we fix a set of parameters and we calculate a matrix of swaption prices with different maturities, swap lengths and three different strikes, i.e. ATMF (at-the-money forward), ITMF (0.85 × ATMF) and OTMF (1.15 × ATMF). The values of the parameters are reported in Appendix D. The tested model is the two-factor affine multiple-curve Gaussian model. Monte Carlo is used as a benchmark for the computation of the true swaption price. The 97.5% mean-centred Monte

Carlo confidence interval is used as a measure of the accuracy. The lower bounds is obtained via the closed formula described in Section 2.2. The Matlab function **quadgk** is used for the integral appearing in the upper bound formula (see Section 2.3). Numerical results obtained with parameters reported in Appendix D are shown in Tables 2.2-2.4. Computational time is also given in Table 2.1.
The tangent hyperplane lower bound and the approximation "A" of [Kim, 2014] produce the same prices because they are two different implementations of the same approximation. However, the new algorithm, which requires the computation of a single Fourier inversion, is faster for the Gaussian multiple-curve model of which we know an analytical pricing formula for the lower bound. In fact, in Table 2.1, our implementation of the lower bound is faster than Kim's method. The improvement in computational performance is more evident for swaptions with a large number of cash flows. As in the single curve case, comparing the speed of different methods is not simple because each algorithm should be optimized. However, our considerations about the efficiency of an algorithm are also justified by theoretical reasoning and confirmed by our estimations of the computational time. Our bounds are applicable to all affine-quadratic models, both in single- and multiple-curve frameworks, and they are particularly efficient for affine models. The computation of the upper bound is slower than the lower bound calculation, but it is still faster than Monte Carlo simulations for a comparable accuracy (see Table 2.1). In addition, the range between the lower and upper bound is always narrow so, in practice, the combined use of the two bounds provides an accurate estimate of the true price. For the multiple-curve model, we compare our bounds with an approximate method that is widely used in the market, i.e. the freezing drift approximation (see [Moreni and Pallavicini, 2014]) and we find that the lower and upper bounds perform better for swaptions with long maturities (2Y and 5Y in Tables 2.2-2.4) with comparable computational times. Moreover, the freezing technique is a generic approximation, i.e. we cannot know a priori if the approximated price underestimates or overestimates the true price. In each table we compute the mean absolute percentage error (MAPE) of bounds with respect to Monte Carlo prices, taken as a benchmark, for fixed maturity and strike.

Conclusions

In this first two chapters, we propose a general lower bound formula of the swaption price based on an approximation of the exercise region. We note that previous approximations, such as the [Kim, 2014] and [Singleton and Umantsev, 2002] methods, represent a particular case of our general formula and so they can also be interpreted as lower bounds. Moreover, we provide a new algorithm to implement the lower bound that is found to be more efficient for interest rate models in which the joint characteristic function of state variables is known in analytical form. Further, we provide a new upper bound to swaption prices that is applicable to all affine-quadratic models and that is accurate and computable in a reasonable time. Therefore, the lower bound approximation error is controlled. Finally, we extend lower and upper bounds to multiple-curve models. Numerical results confirm our hypothesis about the performance of the new algorithm in terms of computational

times for the calculus of the lower bound, except for quadratic models in which the characteristic function is not analytic. Moreover, numerical tests show a very good accuracy of the new upper bound for different models across tenors, maturities and strikes.

2 factor multiple-curve Gaussian model

Overall time (sec)	MC	LB (HP)	UB	Kim
ATMF	43.280	0.094	0.416	0.346
ITMF	43.3603	0.114	0.403	0.309
OTMF	42.040	0.116	0.409	0.315

Table 2.1: Computational times shown in the table are the overall time needed for calculating the matrices of swaption prices reported in Tables 2.2-2.4.

Opt. Mat.	1			
Swap length	**MC**	**LB (HP)**	**UB**	**Freezing**
1	37.396 0.002	37.397	38.54 1.143	37.286 0.11
2	71.233 0.003	71.235	72.045 0.811	71.245 0.011
5	172.64 0.008	172.644	173.66 1.016	172.748 0.108
10	318.57 0.015	318.576	319.658 1.083	319.361 0.792
MAPE		0.002%	1.283%	0.155%

Opt. Mat.	2			
Swap length	**MC**	**LB (HP)**	**UB**	**Freezing**
1	56.128 0.003	56.131	56.932 0.801	55.542 0.586
2	106.625 0.005	106.63	107.183 0.553	106.015 0.61
5	255.82 0.012	255.832	256.526 0.694	254.594 1.225
10	467.734 0.022	467.756	468.496 0.74	467.056 0.678
MAPE		0.005%	0.599%	0.560%

Opt. Mat.	5			
Swap length	**MC**	**LB (HP)**	**UB**	**Freezing**
1	77.727 0.004	77.725	77.993 0.267	72.826 4.900
2	146.539 0.007	146.536	146.718 0.181	138.249 8.290
5	345.864 0.016	345.859	346.086 0.228	326.836 19.028
10	622.779 0.029	622.769	623.012 0.243	591.763 31.016
MAPE		0.002%	0.141%	5.611%

Table 2.2: The table shows **ATMF payer swaption** prices for the **two-factor multiple-curve Gaussian model** at three different maturities (1Y, 2Y and 5Y). For each swaption, we report the price in basis point as estimated with the Monte Carlo method (MC), the hyperplane approximation lower bound (LB), the upper bound (UB) and the freezing technique. Monte Carlo values are estimated using 10^9 simulations, the antithetic variates method and the exact probability distribution. Below each Monte Carlo price, the size of the confidence interval at 97.5% is reported in basis points. The distance between the lower and the upper bounds is provided below each upper bound value. The error of the freezing techniques is estimated as the difference between the approximated price and the Monte Carlo price.

Opt. Mat.	1			
Swap length	**MC**	**LB (HP)**	**UB**	**Freezing**
1	47.814 0.002	47.814	48.935 1.121	47.659 0.155
2	100.76 0.003	100.762	101.539 0.777	100.693 0.068
5	273.07 0.007	273.073	274.015 0.942	272.934 0.135
10	557.826 0.013	557.83	558.793 0.963	558.364 0.538
MAPE		0.001%	0.909%	0.134%

Opt. Mat.	2			
Swap length	**MC**	**LB (HP)**	**UB**	**Freezing**
1	70.136 0.003	70.139	70.927 0.788	69.376 0.76
2	142.769 0.005	142.774	143.312 0.537	141.805 0.965
5	365.386 0.011	365.397	366.061 0.664	363.166 2.22
10	706.939 0.02	706.96	707.656 0.696	704.774 2.165
MAPE		0.003%	0.448%	0.668%

Opt. Mat.	5			
Swap length	**MC**	**LB (HP)**	**UB**	**Freezing**
1	100.195 0.004	100.193	100.454 0.261	93.816 6.378
2	195.296 0.007	195.293	195.47 0.176	183.977 11.318
5	469.529 0.015	469.523	469.744 0.221	443.005 26.524
10	861.93 0.028	861.92	862.154 0.235	817.64 44.291
MAPE		0.001%	0.105%	5.737%

Table 2.3: The table shows **ITMF (0.85 $\times$ ATMF) payer swaption** prices for the **two-factor multiple-curve Gaussian model** at three different maturities (1Y, 2Y and 5Y). For each swaption, we report the price in basis point as estimated with the Monte Carlo method (MC), the hyperplane approximation lower bound (LB), the upper bound (UB) and the freezing technique. Monte Carlo values are estimated using 10^9 simulations, the antithetic variates method and the exact probability distribution. Below each Monte Carlo price, the size of the confidence interval at 97.5% is reported in basis points. The distance between the lower and the upper bounds is provided below each upper bound value. The error of the freezing techniques is estimated as the difference between the approximated price and the Monte Carlo price.

Opt. Mat.	1			
Swap length	**MC**	**LB (HP)**	**UB**	**Freezing**
1	28.556 0.002	28.556	29.677 1.12	28.481 0.075
2	47.929 0.003	47.93	48.706 0.776	47.98 0.051
5	99.692 0.007	99.695	100.636 0.94	99.881 0.189
10	157.949 0.013	157.953	158.913 0.96	158.619 0.67
MAPE		0.002%	1.776%	0.245%

Opt. Mat.	2			
Swap length	**MC**	**LB (HP)**	**UB**	**Freezing**
1	44.051 0.003	44.054	44.841 0.787	43.61 0.441
2	76.962 0.005	76.968	77.504 0.536	76.608 0.354
5	170.002 0.011	170.014	170.677 0.662	169.429 0.573
10	288.059 0.02	288.081	288.775 0.694	288.16 0.1
MAPE		0.007%	0.786%	0.458%

Opt. Mat.	3			
Swap length	**MC**	**LB (HP)**	**UB**	**Freezing**
1	58.779 0.004	58.778	59.039 0.261	55.111 3.668
2	106.418 0.007	106.416	106.592 0.176	100.557 5.862
5	245.442 0.015	245.436	245.656 0.22	232.329 13.113
10	431.263 0.028	431.253	431.486 0.234	410.522 20.741
MAPE		0.002%	0.186%	5.475%

Table 2.4: The table shows **OTMF (1.15 $\times$ ATMF) payer swaption** prices for the **two-factor multiple-curve Gaussian model** at three different maturities (1Y, 2Y and 5Y). For each swaption, we report the price in basis point as estimated with the Monte Carlo method (MC), the hyperplane approximation lower bound (LB), the upper bound (UB) and the freezing technique. Monte Carlo values are estimated using 10^9 simulations, the antithetic variates method and the exact probability distribution. Below each Monte Carlo price, the size of the confidence interval at 97.5% is reported in basis points. The distance between the lower and the upper bounds is provided below each upper bound value. The error of the freezing techniques is estimated as the difference between the approximated price and the Monte Carlo price.

Chapter 3

HJM multiple-curve model with time-changed Lévy processes

In this chapter we propose a parsimonious model for the term structure of interest rate in a multi-curve framework, which is capable of reproducing volatility surfaces of interest rate options quoted in the market. Our multi-curve framework is inspired by the HJM multi-curve scheme presented in [Moreni and Pallavicini, 2014] due to its parsimony and analytically tractability. In particular, this multiple curve framework does not introduce different underlying assets for each forward rate tenor (e.g. 1M, 3M, 6M) and hence, it avoids an over-parametrization issues in calibration procedure. In fact, the market quotes interest rate options only on few yield curves. For instance, actively traded swaptions and cap/floor are only those indexed to the three-month Libor curve (maturity one-year for swaption and maturities from one to two years for cap/floor) and the six-month Libor curve (maturities from 2 or 3 to 30 years). Moreover in [Moreni and Pallavicini, 2014] work, Libor FRA rate is modelled, which is a real traded asset, instead of Libor bond rate, as suggested also in [Mercurio, 2010]. Furthermore, their multi-curve scheme allows for negatives rates, which recently appear in Euro market. [Moreni and Pallavicini, 2014] use a multi-factor diffusion process as driving process of the HJM multi-curve model. However, Gaussian models are not rich enough to reproduce the term structure of the volatility smile of interest rate options, unless a large number of factors is used. In order to improve the flexibility of interest rate models, [Eberlein and Raible, 1999] introduce Lévy process in an HJM setting. [Eberlein and Raible, 1999] work is extended by [Crépey et al., 2015] to a multi-curve framework. The model in [Crépey et al., 2015] reproduces very well the swaption volatility smile at fixed maturity (and swap tenor), but it requires time-dependent parameters in order to fit the term structure of the volatility. Instead, we propose a model that is able to reproduce the quoted volatility term structure of cap/floor (or swaptions), across maturities and strikes, without introducing time-dependent parameters. In this way we maintain the parsimony of the model.

Hence, in order to obtain a parsimonious but also flexible model, we extend [Moreni and Pallavicini, 2014] multi-curve model using time-changed Lévy as driving processes for the ZCB and the FRA rate dynamics. Time-changed Lévy processes are introduced in finance by [Carr and Wu, 2004] for pricing equity derivatives. How-

ever, recent, empirical studies, such as [Leippold and Strømberg, 2014], suggest the application of time-changed Lévy process to interest rate financial products. In particular, Lévy processes generate very flexible return innovation distribution and take into account potential discontinuities in Libor dynamics. Moreover, our model exhibit through the the random time a stochastic behaviour of the Libor volatility and a dependence between the base Lévy process and the volatility. These features enable the model to reproduce not only the volatility smile but also the volatility term structure of interest rate options.
The chapter outline is as follows. In Section 1 we present the time-changed Lévy process. In Section 2 we build the HJM multiple-curve model and we study the martingale property of integrated time-changed Lévy process in order to show that the model is theoretically well posed. In particular, we derive drift conditions on the zero coupon bond price and Libor FRA rate processes that ensure the no-arbitrage requirement Section 3 develops the pricing of interest rate derivatives. In Section 4 two different driving process constructions are presented. Numerical results are shown in Section 5 .

3.1 Time-changed Lévy process

Let $(\Omega, \mathcal{F}, \mathbb{P})$ be a probability space, endowed with a standard complete filtration $\mathcal{F} = (\mathcal{F}_t)_{t\geq 0}$. We define on the probability space a Lévy process $X = (X(t))_{t\geq 0}$, a stochastic process with stationary and independent increments. The law of the increments is infinitely divisible and hence by the Lévy–Khintchine formula

$$\begin{aligned} &\mathbb{E}\left[e^{iu\,X(t)}\right] = e^{\psi(u)\ t}, \\ &\psi(u) = iu\,b - \frac{1}{2}u^2 c + \int_{\mathbb{R}} (e^{iu\,x} - 1 - iu\,h(x))\nu(dx), \end{aligned} \tag{3.1}$$

where $h(x)$ is a suitable truncation function, $b \in \mathbb{R}$ is the drift, $c > 0$ is the coefficient of the diffusive part and ν is the Lévy measure of X, i.e. a positive measure on $\mathbb{R}\backslash\{0\}$ such that $\int_{\mathbb{R}}(1\wedge x^2)\nu(dx) < \infty$. The triplet (b, c, ν) is called the characteristic triplet of X, the drift b depends on the choice of the truncation function h. As in [Eberlein and Raible, 1999] we assume the following regularity condition, in order to guarantee the existence of an interval, on which the moment generating function of the Lévy process is well defined.

Assumption 3.1.1. There exist constants M_1, M_2 and $\epsilon > 0$ such that

$$\int_{|x|>1} e^{u\,x}\nu(dx) < \infty \tag{3.2}$$

for all $u \in [-(1+\epsilon)M_1, (1+\epsilon)M_2]$.

The Assumption 3.1.1 holds if and only if the moment generating function is finite in the interval $[-(1+\epsilon)M_1, (1+\epsilon)M_2]$, i.e.

$$\mathbb{E}\left[e^{uX(t)}\right] < \infty$$

for all $u \in [-(1+\epsilon)M_1, (1+\epsilon)M_2]$. Furthermore, Assumption 3.1.1 implies that $h(x) = x$ can be used as truncation function (see [Eberlein and Kluge, 2006]); this is equivalent to say that

i) X is a special semimartingale with the canonical representation

$$X(t) = bt + \sqrt{c}W_t + \int_0^t \int_{\mathbb{R}} x(\mu^X(ds, dx) - \nu(dx)ds),$$

where $\mu^X(ds, dx)$ is the counting measure of the jumps of X and $\nu(dx)$ is the Lévy measure of X.

ii) the cumulant generating function of X, κ, is defined for any $z \in \mathbb{C}$ such that $Re(z) \in [-(1+\epsilon)M_1, (1+\epsilon)M_2]$ as

$$\kappa(z) = zb + \frac{1}{2}z^2\, c + \int_{\mathbb{R}} (e^{z\,x} - 1 - z\,x)\nu(dx)$$

and if ψ is defined as in the Lévy–Khintchine formula, then we have the relation $\kappa(z) = \psi(-iz)$.

Definition 3.1.2. Let $(\Omega, \mathcal{F}, \mathbb{P})$ be a probability space, endowed with a standard complete filtration $\mathcal{F} = (\mathcal{F}_t)_{t\geq 0}$; a process $\tau = (\tau(t))_{t\geq 0}$ is called a time change if

i) τ is a real positive and increasing right continuous process with left limits (RCLL);

ii) for every $t \geq 0$, $\tau(t)$ is a stopping time respect to the filtration $\mathcal{F}$ and is finite $\mathbb{P}$-almost surely;

iii) $\tau(0) = 0$ and $\lim_{t\to\infty} \tau(t) = \infty$.

We denote by $\mathcal{F}_\tau$ the collection of all sets $A \in \mathcal{F}$, such that $A \cap \{\tau \leq t\} \in \mathcal{F}_t$ for all $t \in \mathbb{R}^+$. Consequently, we can define a time-changed filtration,

$$\mathcal{G} = (\mathcal{G}_t)_{t\geq 0},\ \ \mathcal{G}_t = \mathcal{F}_{\tau(t)}.$$

The time change is said to be continuous if τ is a continuous process. In particular, as in [Carr and Wu, 2004], the time change τ is modelled as an increasing semimartingale characterized in terms of its positive intensity $v(t)$ as

$$\tau(t) = \int_0^t v(s_-)ds, \tag{3.3}$$

hence τ is absolutely continuous.
Let X be a Lévy process with the properties previously described and τ an absolutely continuous time change defined as in equation 3.3. Then a time-changed Lévy process is defined as $Y = X(\tau)$, i.e. for any $t \geq 0$ $Y(t) = X(\tau(t))$. From proposition E.3.1, the Laplace cumulant process of the process Y is defined as

$$\kappa(u)\, \tau(t),$$

for any $u \in [-(1+\epsilon)M_1, (1+\epsilon)M_2]$, i.e. the process

$$M_u(t) = e^{uY(t) - \kappa(u)\,\tau(t)}$$

is a local martingale.
Moreover, Y has the canonical representation

$$\begin{aligned} Y(t) &= b\tau(t) + \sqrt{c}\, W_{\tau(t)} + \int_0^{\tau(t)} \int_{\mathbb{R}} x(\mu^X(ds,dx) - \nu(dx)ds) \\ &= b\int_0^t v(s_-)ds + \sqrt{c}\int_0^t \sqrt{v(s_-)}\, dW(s) + \int_0^t \int_{\mathbb{R}} x(\mu^Y(ds,dx) - \nu(dx)v(s_-)ds), \end{aligned} \tag{3.4}$$

where (b, c, ν) is the characteristic triplet of the Lévy process X, $\mu^Y(ds,dx)$ is the random measure of the jumps of Y with $\mathbb{P}$-compensator $\nu^Y(ds,dx) = \nu(dx)\, v(s_-)\, ds$. If $\nu(dx)$ is expressed in term of its Lévy density, i.e. $\nu(dx) = \pi(x)dx$, then $\pi(x)v(t_-)$ is the arrival rate of the jumps of the semimartingale Y.

3.2 Multiple-curve HJM model with T.C. Lévy

In this section we build an arbitrage free HJM multiple-curve framework with time-changed Lévy as driving process.

3.2.1 Risk free bond prices

Let $X(t)$ and $\tau(t)$ be a Lévy process and a continuous time change with properties previously described and $Y(t) = X(\tau(t))$ a time-changed Lévy process. We model the zero coupon bond price process as,

$$P(t,T) = \frac{P(0,T)}{P(0,t)}\, e^{\int_0^t (\Sigma(s,t) - \Sigma(s,T))\, dY(s) + \int_0^t (A(s,t) - A(s,T))\, v(s_-)\, ds}, \tag{3.5}$$

where $\Sigma(t,T) = \int_t^T \sigma(t,u)\, du$ is the volatility function, $\tau(t) = \int_0^t v(s_-)ds$ is a random time change, $Y(t) = X(\tau(t))$ is a time-changed Lévy process, $A(t,T) = \psi(i\,\Sigma(t,T))$ and $\psi(u)$ is the characteristic exponent of the Lévy process X defined in equation 3.1. In order to define the bond price process in a HJM framework, we make the following standard assumptions as reported in [Eberlein and Raible, 1999]

Assumption 3.2.1. The initial bond prices are given by a deterministic, positive, and twice continuously differentiable function $T \to P(0,T)$ on the interval $[0, \bar{T}]$.

Assumption 3.2.2. $P(T,T)$= 1 on the interval $\forall T \in [0, \bar{T}]$.

We slightly modify the assumption related to the volatility function.

Assumption 3.2.3. The volatility is a continuous bounded function $\Sigma : \mathbb{R}_+ \times [0, \bar{T}] \to [0, \bar{\Sigma}]$ that is null outside $\Delta = \{(t,T) : 0 \le t \le T \le \bar{T}\}$. Moreover $\bar{\Sigma} \le \min\{M_1, M_2\}$ and Σ is twice differentiable in Δ.

The last one assures that the volatility is bounded and that the volatility of a just-maturing bond is zero because its value is known for sure.

3.2.2 Libor FRA rate

As in [Moreni and Pallavicini, 2014], we define the risk free forward rate F^0, which can be identified in the market with the overnight rate. F^0 is built as the linear compounded forward rate in a classical single curve framework.
The risk free forward rate at time t for the interval $[T-x, T]$ is

$$F^0(t,T,x) = \frac{1}{x}\left(\frac{P(t,T-x)}{P(t,T)} - 1\right). \tag{3.6}$$

Substituting the dynamic of the risk free ZCB, equation 3.5, in the previous formula, we obtain the following dynamics for the risk free forward rate under the risk neutral $\mathbb{P}$ measure

$$F^0(t,T,x) = \frac{1}{x}\left[(1 + x\, F^0(0,T,x))e^{\int_0^t \Sigma^0(s,T,x)\, dY(s) + \int_0^t A^0(s,T,x)\, v(s_-)\, ds} - 1\right]. \tag{3.7}$$

for

$$\Sigma^0(s,T,x) = \Sigma(s,T) - \Sigma(s,T-x) = \int_{T-x}^T \sigma(s,u)\, du,$$

$$A^0(s,T,x) = A(s,T) - A(s,T-x) = \int_{T-x}^T \alpha(s,u)\, du.$$

The Libor FRA rate $F^x(t,T,x)$ is the fair rate of a FRA contract written on the Libor rate with tenor x (usually x = 1M, 3M, 6M or 12M) and it is defined as

$$F^x(t,T,x) = \mathbb{E}_t^T\left[L(T-x,T)\right], \tag{3.8}$$

where $L(T-x,T)$ is the spot Libor rate, fixed at time $T-x$ for the time interval $[T-x,T]$, $\mathbb{E}_t^T[\ ]$ denotes the expectation under the T-forward measure, $\mathbb{P}^T$, defined by a density process, which is the discounted risk free ZCB bond price

$$\left.\frac{d\mathbb{P}^T}{d\mathbb{P}}\right|_{\mathcal{F}_t} = \frac{P(t,T)}{\beta(t)\, P(0,T)} = e^{-\int_0^t \Sigma(s,T)\, dY(s) - \int_0^t \psi(i\,\Sigma(s,T))\, v(s_-)\, ds}, \tag{3.9}$$

and $\beta(t) = e^{\int_0^t r(s)ds}$ is the money market account.
We model the FRA rate using time-changed Lévy processes under the risk neutral $\mathbb{P}$ measure, as

$$F^x(t,T,x) = \frac{1}{x}\left[(1 + x\, F^x(0,T,x))e^{\int_0^t \Sigma^x(s,T,x)\, dY(s) + \int_0^t A^x(s,T,x)\, v(s_-)\, ds} - 1\right], \tag{3.10}$$

with $\Sigma^x(s,T,x) = \int_{T-x}^T \sigma(s,u;T,x)\, du$. The FRA rate dynamic has to respect the following constraints

(i) $F^x(t,T,x)$ has to be a martingale under the T-forward measure,

(ii) $\lim_{x\to 0} F^x(t,T,x) = \lim_{x\to 0} F^0(t,T,x) = f(t,T)$

(iii) $F^x(t,T,x) \sim F^0(t,T,x)$ if $x \sim 0$, i.e. for a tenor that goes to zero the FRA rate is similar to the risk free forward rate.

In order to satisfy the martingale condition (i) previously stated, we impose in formula 3.10 that

$$A^x(s,T,x) \quad = \quad \psi(i\Sigma(s,T)) - \psi(i\,\Sigma(s,T) - i\,\Sigma^x(s,T,x)),$$

while in order to fulfil conditions (ii) and (iii), we require that

$$\sigma(s,T;T,0) \quad = \quad \sigma(s,T). \tag{3.11}$$

Similarly to the HJM zero coupon bond volatility function, the HJM forward volatility function has to satisfy the following assumption, which ensures the boundedness of the volatility and consequently the existence of the log-FRA rate moment generating function (see Assumption 3.2).

Assumption 3.2.4. The forward volatility is a continuous bounded function,

$$\Sigma^x : \mathbb{R}_+ \times \{(T,x) : 0 \le x \le T\} \to [0, \bar{\Sigma}^x],$$

that is null outside $\Delta_2 = \{(t,T,x) : 0 \le t \le T,\ 0 \le x \le T \le \bar{T}\}$. Moreover $\bar{\Sigma}^x \le \min\{M_1, M_2\}$ and Σ^x is twice differentiable if $t \le T$.

Finally, to ensure the tractability and a Markovian specification of the model (see [Moreni and Pallavicini, 2014]), the forward volatility in formula 3.10 should have the following form

$$\begin{aligned} \sigma(t,u;T,x) &= h(t)q(u;T,x)\,g(t,u) \\ g(t,u) &= \exp\left(-\int_t^u a(s)ds\right) \\ q(u;u,0) &= 1. \end{aligned}$$

We choose the following specification

$$\begin{aligned} h(t) &= h\left(e^{-\beta t}\beta_1 t + 1\right) \\ g(t,u) &= e^{-a\,(u-t)} \\ q(u;T,x) &= e^{-\gamma\,x}, \end{aligned} \tag{3.12}$$

where h, β, β_1, a and γ are all positive constant parameters.

3.3 Derivatives pricing

In this section, we present the pricing formula for interest rate options (cap/floor and swaptions) with time-changed Lévy process using the Fourier transform method of [Carr and Madan, 1999].

3.3.1 Caplets

Let us consider a caplet with strike K and maturity $T-x$ on the spot Libor rate on the period $[T-x,T]$, settled in arrears at time T. The risk neutral price is

$$\begin{aligned} C(0) &= P(0,T)\,\mathbb{E}^T\left[x\,(F^x(T-x,T,x)-K)^+\right] \\ &= P(0,T)\,\mathbb{E}^T\left[((1+x\,F^x(T-x,T,x))-(1+x\,K))^+\right] \end{aligned}$$

Once we know the characteristic function of the shifted log-FRA rate under the $\mathbb{P}^T$ measure,

$$\phi^T_{0,T-x}(u) := \mathbb{E}^T\left[\exp\left(iu\log\left(\frac{1+x\,F^x(T-x,T,x)}{1+x\,F^x(0,T,x)}\right)\right)\right],$$

then the caplet can be priced using the Fourier transform method (see [Carr and Madan, 1999])

$$C(0) = P(0,T)\,\frac{e^{-\delta k}}{\pi}\int_0^{+\infty} Re\left(e^{-i\gamma k}\frac{\phi^T_{0,T-x}(\gamma-i(\delta+1))}{(i\gamma+\delta)(i\gamma+\delta+1)}\right)d\gamma$$

where $\delta>0$ is such that the characteristic function in $\gamma-i(\delta+1)$ is well defined, and $k=\log\left(\frac{1+x\,K}{1+x\,F^x(0,T,x)}\right)$.

3.3.2 Characteristic function of the log-FRA rate

The characteristic function of the (shifted) log-FRA rate under $\mathbb{P}^T$ measure is transformed into an expectation under the risk neutral measure using the radon-Nikodym derivative in formula 3.9

$$\begin{aligned} \phi^T_{0,t}(u) &:= \mathbb{E}^T\left[\exp\left(iu\log\left(\frac{1+x\,F^x(t,T,x)}{1+x\,F^x(0,T,x)}\right)\right)\right] \\ &= \mathbb{E}\left[e^{-\int_0^t \Sigma(s,T)\,dY(s)-\int_0^t A(s,T)\,v(s_-)\,ds+iu\int_0^t \Sigma^x(s,T,x)\,dY(s)+iu\int_0^t A^x(s,T,x)\,v(s_-)\,ds}\right] \\ &= \mathbb{E}\left[e^{(iu-1)\int_0^t \psi(i\,\Sigma(s,T))\,v(s_-)ds-iu\int_0^t \psi(i\,\Sigma(s,T)-i\,\Sigma^x(s,T,x))\,v(s_-)ds}\right. \\ &\quad \left. e^{\int_0^t (iu\Sigma^x(s,T,x)-\Sigma(s,T))\,dY(s)}\right]. \end{aligned}$$

The characteristic function of the shifted log-FRA rate can be calculated as a Laplace transform of the time change intensity $v(t)$, $u\in\mathbb{C}$

$$\phi^T_{0,t}(u)=\tilde{\mathbb{E}}\left[e^{\int_0^t \tilde{\psi}(u,s)\,v(s_-)\,ds}\right], \tag{3.13}$$

where the expectation $\tilde{\mathbb{E}}[\,]$ is with respect to a new measure $\tilde{\mathbb{P}}\overset{\text{loc}}{\ll}\mathbb{P}$, defined by the density process

$$\varrho(t)=e^{\int_0^t (iu\,\Sigma^x(s,T,x)-\Sigma(s,T))\,dY(s)-\int_0^t \psi(u\,\Sigma^x(s,T,x)+i\,\Sigma(s,T))\,v(s)ds}, \tag{3.14}$$

the function $\tilde{\psi}(u,s)$ has form

$$\begin{aligned} \tilde{\psi}(u,s) &= \psi(u\,\Sigma^x(s,T,x)+i\,\Sigma(s,T))+(iu-1)\,\psi(i\,\Sigma(s,T)) \\ &- iu\,\psi(i\,\Sigma(s,T)-i\,\Sigma^x(s,T,x)), \end{aligned} \tag{3.15}$$

$\psi(u)$ is the characteristic exponent of the Lévy process X and $(\psi(u,t)\,v(t_-))_{t\geq 0}$ is the Fourier cumulant processes of Y.

The affine case

Here, we present an extension of the work of [Filipovic, 2001], in order to obtain a system of ordinary differential equations (ODEs) to calculate the characteristic function of the log-FRA rate in the affine case. We consider the case in which the activity rate process $v(t)$ is a Feller process with infinitesimal generator

$$\begin{aligned}\mathcal{A}f(v) &= (\alpha' - \beta\, v)\, f'(v) + \frac{1}{2}c^2\, v\, f''(v) \\ &+ \int_0^\infty \big(f(v+x) - f(v) - f'(v)\, h(x)\big)\, (m(dx) + v\, \mu(dx))\end{aligned}$$

where $\alpha' = \alpha + \int_{\mathbb{R}_0^+} h(x) m(dx)$, $h(x)$ is a truncation function, $\mu(dx)$ is a Lévy measure and $m(dx)$ is a Lévy measure of finite variation. Such process is quite general and it is known as (stochastically continuous) CBI process (continuous state branching process with immigration).
We assume that after the change of measure previously described, the dynamic of $v(t)$ is modified by the Girsanov theorem in the following way

$$\beta \to \tilde{\beta}(s) \text{ and } \mu(dy) \to \tilde{\mu}_s(dy).$$

The previous hypothesis is satisfied in all the examples presented in Section 3.4. Hence, the infinitesimal generator of v under the $\tilde{\mathbb{P}}$ measure is

$$\begin{aligned}\mathcal{A}_s f(s,v) &= (\alpha' - \tilde{\beta}(s)v)\, \partial_v f(s,v) + \frac{1}{2}\eta^2\, v\, \partial_v^2 f(s,v) \\ &+ \int_{\mathbb{R}_0^+} (f(s,v+y) - f(s,v) - \partial_v f(s,v)\, h(y))\, (m(dy) + v\, \tilde{\mu}_s(dy))\,.\end{aligned}$$

Let us define

$$\phi_{s,t}^T(u) = f(s,v) = \tilde{\mathbb{E}}\left[e^{\int_s^t \tilde{\psi}(u,t_1)\, v(t_{1-})\, dt_1} \mid \mathcal{F}(s),\ v(s) = v\right],$$

in virtue of the the Feynmann-Kac representation

$$\partial_s f + \mathcal{A}_s f + \tilde{\psi}(u,s)\, v\, f = 0 \text{ and } f(t,v) = 1.$$

We assume that the characteristic function is affine, i.e.

$$\phi_{s,t}^T(u) = f(s,v) = e^{-A(s,t) - B(s,t)\, v},$$

this implies that the Feynman-Kac differential equation can be decomposed in the following system of ODEs for the coefficients A and B

$$\begin{aligned}\partial_s A(s,t) &= -\alpha\, B(s,t) + \int_{\mathbb{R}_0^+} \left(e^{-B(s,t)y} - 1\right) m(dy), \\ \partial_s B(s,t) &= \tilde{\beta}(s)\, B(s,t) + \frac{1}{2}\eta^2\, B^2(s,t) + \int_{\mathbb{R}_0^+} \left(e^{-B(s,t)y} - 1 + B(s,t)h(y)\right) \tilde{\mu}_s(dy) \\ &+ \tilde{\psi}(u,s), \\ A(t,t) &= B(t,t) = 0.\end{aligned}$$

3.3.3 Swaptions

Due to lack of closed analytical formulas for the price of this product, in this section we develop an approximate valuation of an European swaption using the multiple-curve time-change Lévy model and the lower bound formula presented in Chapters 1 and 2.
Let us consider an European (payer) option on a Interest Rate Swap (IRS) with fixed interest rate K and payment dates $(T_1, \cdots T_N)$, the maturity of the option is T and it is the first fixing date of the IRS. The pricing formula under the risk neutral measure is

$$Swo(0) = P(0,T)\,\mathbb{E}^T\left[\left(\sum_{j=1}^{N} P(T,T_j)\,x\,(F^x(T,T_j,x)-K)\right)^+\right] \tag{3.16}$$

where $x = T_j - T_{j-1}$ for $j = 1, ..., N$, the zero coupon bond price $P(T,T_j)$ is defined in equation 3.5 and the FRA rate $F^x(T,T_j,x)$ is defined in equation 3.10.
We rewrite the swaption price as

$$Swo(0) = P(0,T)\,\mathbb{E}^T\left[\left(\sum_{j=1}^{N} w_{1,j}\,e^{Z_j(T)+U_j(T)} - w_{2,j}\,e^{Z_j(T)}\right)\mathrm{I}(\mathcal{A})\right],$$

where we define some useful quantities

$$\begin{aligned}
Z_j(T) &= \log\left(P(T,T_j)\right) - \log\left(\frac{P(0,T_j)}{P(0,T)}\right)\\
&= \int_0^T \left(\Sigma(s,T)-\Sigma(s,T_j)\right)\,dY(s) + \int_0^T \left(A(s,T)-A(s,T_j)\right)\,v(s_-)\,ds\\
U_j(T) &= \log\left(1+x\,F^x(T,T_j,x)\right) - \log\left(1+x\,F^x(0,T_j,x)\right)\\
&= \int_0^T \Sigma^x(s,T_j,x)\,dY(s) + \int_0^T A^x(s,T_j,x)\,v(s_-)\,ds\\
w_{1,j} &= \frac{P(0,T_j)}{P(0,T)}\,\left(1+x\,F^x(0,T_j,x)\right)\\
w_{2,j} &= (1+x\,K)\,\frac{P(0,T_j)}{P(0,T)}
\end{aligned}$$

and we point out the exercise region set

$$\mathcal{A} = \{\sum_{j=1}^{N} w_{1,j}\,e^{Z_j(T)+U_j(T)} \geq \sum_{j=1}^{N} w_{2,j}\,e^{Z_j(T)}\}. \tag{3.17}$$

Then, we perform an approximate evaluation by means of the lower bound proposed in Chapters 1 and 2

$$\begin{aligned}
Swo(0) &\geq \max_{k\in\mathbb{R}} LB_k(0)\\
LB_k(0) &= P(0,T)\,\mathbb{E}^T\left[\left(\sum_{j=1}^{N} w_{1,j}\,e^{Z_j(T)+U_j(T)} - w_{2,j}\,e^{Z_j(T)}\right)\,\mathrm{I}(\mathcal{G}_k)\right].
\end{aligned}$$

where $\mathcal{G}_k$ is the following approximate exercise region

$$\mathcal{G}_k = \{\sum_{j=1}^{N} U_j(T) \geq k\}. \tag{3.18}$$

In order to linearise the exercise region, we substitute the sum over the payment dates with a product (i.e we substitute an arithmetic average with a geometric one) and then we apply the logarithm. In Chapters 1 and 2, we describe a more sophisticate approximation of the exercise region based on the tangent hyperplane. However, in our case this approximation is not applicable, because it is too computational demanding to find the correct point of tangency (i.e. the point $\mathbf{X}^*$ on the true exercise boundary, where the density of the model factor is highest, see Section 1.2.2).
The lower bound is calculated using the Fourier transform method of [Carr and Madan, 1999]

$$LB_k(0) = P(0,T)\,\frac{e^{-\delta k}}{\pi}\int_0^{\infty} Re\left(e^{-ik\gamma}\,\widehat{LB}(\delta + i\gamma)\right)\,d\gamma. \tag{3.19}$$

$\widehat{LB}$ is the Fourier transform of the lower bound and it has the following form

$$\widehat{LB}(\omega) = \left(\sum_{j=1}^{N} w_{1,j}\,\phi_{Z,U}(-ib_j, -i(b_j + \omega b)) - w_{2,j}\,\phi_{Z,U}(-ib_j, -i\omega b)\right)\frac{1}{\omega},$$

b and b_j are N-dimensional vectors with, respectively, all the components equal to one and the jth component equal to one and the others equal to zero and $\phi_{Z,U}(z,u)$ is the joint characteristic function of the log-FRA rates and of the log-ZCB prices,

$$\phi_{Z,U}(z,u) = \mathbb{E}^T\left[e^{i\sum_{j=1}^{N} z_j Z_j(T) + u_j U_j(T)}\right].$$

3.3.4 The joint characteristic function

The calculus of the joint characteristic function the log-FRA rates and of the log-ZCB prices follows the same steps as in Section 3.3.2. Thus, let

$$\begin{aligned}
&\phi_{Z,U}(z,u) = \mathbb{E}^T\left[e^{i\sum_{j=1}^{N} z_j Z_j(T) + u_j U_j(T)}\right] \\
&= \mathbb{E}\left[\exp\left(\int_0^T (i\,\varsigma_N(s;z,u) - \Sigma(s,T))\,dY(s) + \int_0^T (i\varphi_N(s;z,u) - A(s,T))\,v(s_-)ds\right)\right],
\end{aligned}$$

where

$$\begin{aligned}
\varsigma_N(s;z,u) &= \sum_{j=1}^{N} z_j(\Sigma(s,T) - \Sigma(s,T_j)) + u_j\Sigma^x(s,T_j,x), \\
\varphi_N(s;z,u) &= \sum_{j=1}^{N} z_j(A(s,T) - A(s,T_j)) + u_j A^x(s,T_j,x).
\end{aligned}$$

Using the change of measure from $\mathbb{P}$ to $\tilde{\mathbb{P}}$ defined by the following density process

$$\varrho(t) = \exp\left(\int_0^T (i\,\varsigma_N(s;z,u) - \Sigma(s,T))\,dY(s) - \int_0^T \psi(\varsigma_N(s;z,u) + i\Sigma(s,T))\,v(s_-)ds\right),$$

the joint characteristic function of Z and U becomes a Laplace transform of the process $v(t)$,

$$\begin{aligned}\phi_{Z,U}(z,u) &= \tilde{\mathbb{E}}\left[e^{\int_0^T \tilde{\psi}(s;z,u)\,v(s_-)ds}\right],\\ \tilde{\psi}(s;z,u) &= \psi(\varsigma_N(s;z,u) + i\Sigma(s,T)) + i\varphi_N(s;z,u) - \psi(i\Sigma(s,T)).\end{aligned}$$

3.4 Some examples of driving processes

In this section we present different possible choices of the time-changed Lévy driving process and for each process we illustrate the specific calculus of characteristic function of the log-FRA rate.

3.4.1 Continuous diffusive case

We consider the case in which the driving Lévy process is a Brownian motion,

$$X(t) = W(t),$$

the intensity of the time-change is a CIR process,

$$\begin{aligned}\tau(t) &= \int_0^t v(s_-)ds,\\ dv(t) &= (\alpha - \beta v(t))dt + \eta\sqrt{v(t)}dZ(t),\end{aligned}$$

and the two Brownian motions, W and Z, are correlated

$$\mathbb{E}[dW(t)\,dZ(t)] = \rho dt.$$

Following the procedure described in Section 3.3.2, the characteristic function of the log-FRA rate is affine in v, hence

$$\phi(u;s,t) = e^{-A(s,t)-B(s,t)v(s)}$$

and the coefficients A and B are solutions of the following system of ordinary differential equations (ODEs)

$$\begin{aligned}\partial_s A(s,t) &= -\alpha B(s,t),\\ \partial_s B(s,t) &= \frac{1}{2}\eta^2 B^2(s,t) + (\beta - \eta\,\rho\,(iu\,\Sigma^x(s,T,x) - \Sigma(s,T)))\,B(s,t)\\ &- \frac{1}{2}(iu+u^2)\,(\Sigma^x(s,T,x))^2,\\ A(t,t) &= 0 \text{ and } B(t,t) = 0.\end{aligned}$$

3.4.2 Pure jump case

The dynamic of the time-changed Lévy process is inspired by [Carr and Wu, 2015]

$$X(t) = \int_0^t \int_{\mathbb{R}} x(\mu^X(ds, dx) - \pi(x)\, dx\, ds),$$

$$v(t) - v_0 = \int_0^t (\alpha - \beta\, v(s_-))\, ds + \eta \int_0^t \int_{\mathbb{R}^+} x(\mu^v(ds, dx) - \pi(x)\, dx\, v(s_-)\, ds),$$

$$Y(t) = X(\tau(t)) = \int_0^t \int_{\mathbb{R}} y(\mu^Y(ds, dy) - \pi(y)\, dy\, v(s_-)\, ds).$$

where $\mu^i(ds, dx)$, with $i \in \{X, v, Y\}$ is the counting measure of the jumps of the respective process, and $\pi(x)$ is the Lévy density.
The function $\pi(x)v(s_-)$ represents the activity rate of the jumps. The model includes a self-exciting behaviour: an upside-jumps of the Libor FRA rate increases the intensity of future upside-jump event. This is typical of crisis periods, in which the spread between the Libor rate and the the risk free rate, represented by the OIS rate, increases. Instead downside-jumps have no effect on the activity rate.
In this case, the density process defined in formula 3.14 can be simplified to

$$\varrho(t) = e^{\int_0^t \int_{\mathbb{R}} (iu\, \Sigma^x(s,T,x) - \Sigma(s,T))\, y\, \mu^Y(ds,dy) - \int_0^t \int_{\mathbb{R}} \left(e^{(iu\, \Sigma^x(s,T,x) - \Sigma(s,T))\, y} - 1\right) \pi(y)\, dy\, v(s_-)\, ds} \tag{3.20}$$

By the Girsanov theorem for semimartingale, extended for complex measures, we obtain the dynamic of $v(t)$ under the measure $\tilde{\mathbb{P}}$:

$$\begin{aligned}
v(t) - v_0 &= \int_0^t (\alpha - \tilde{\beta}(s)\, v(s))\, ds + \eta \int_0^t \int_0^\infty y(\mu^v(ds, dy) - \tilde{\pi}(y, s)\, v(s_-)\, dy\, ds), \\
\tilde{\beta}(t) &= \beta - \int_0^\infty \eta\, h(y)(e^{(iu\, \Sigma^x(s,T,x) - \Sigma(s,T))\, y} - 1)\pi(y)\, dy, \\
\tilde{\pi}(y, t) &= e^{(iu\, \Sigma^x(s,T,x) - \Sigma(s,T))\, y}\, \pi(y) \mathrm{I}(y > 0),
\end{aligned}$$

where $h(y) = y$ is the truncation function (see Assumption 3.2).
From results in Section 3.3.2, the characteristic function of the log-FRA rate is affine in v and consequently

$$\phi(u; s, t) = \mathbb{E}\left[e^{iu \log F(t,T,S)} \mid \mathcal{F}_s\right] = F(s, T, S)^{iu}\, e^{-A(s,t) - B(s,t)v(s)}$$

for A and B solutions of the following ODE system

$$\begin{aligned}
\partial_s A(s, t) &= -\alpha B(s, t), \\
\partial_s B(s, t) &= \tilde{\beta}(s)\, B(s, t) + \int_0^\infty \left(e^{-B(s,t)\eta\, y} - 1 + B(s, t)\eta\, h(y)\right) \tilde{\pi}(y, s)\, dy \\
&+ \tilde{\psi}(u, s), \\
A(t, t) &= 0 \text{ and } B(t, t) = 0,
\end{aligned}$$

where $h(y) = y$ is the truncation function and the expression of $\tilde{\psi}(u, s)$ is reported in formula 3.15.

Now, we exemplify the case of a Variance Gamma process, which is a pure Lévy process with infinite activity and finite variation (see [Madan et al., 1998] for further details). The Variance Gamma Lévy density has form

$$\begin{aligned}\pi(x) &= \frac{e^{-\frac{x}{\nu^+}}}{x}\mathrm{I}(x>0) + \frac{e^{-\frac{|x|}{\nu^-}}}{\mid x \mid}\mathrm{I}(x<0) \\ &= e^{-\frac{x}{\nu^+}}x^{-1}\mathrm{I}(x>0) - e^{\frac{x}{\nu^-}}x^{-1}\mathrm{I}(x<0).\end{aligned}$$

Then, substituting the Lévy density specification in the characteristic function ODE system we obtain.

$$\begin{aligned}\partial_s A(s,t) &= -\alpha B(s,t), \\ \partial_s B(s,t) &= (\beta + \eta\nu^+)\, B(s,t) - \log(1+\eta\tilde{\nu}^+(s)B(s,t)) + \tilde{\psi}(u,s) \\ A(t,t) &= 0 \text{ and } B(t,t) = 0,\end{aligned}$$

where

$$\begin{aligned}\tilde{\nu}^+(s) &= \frac{\nu^+}{1-(iu\Sigma^x(s,T,x)-\Sigma(s,T))\,\nu^+}, \\ \tilde{\psi}(u,s) &= -\log\left(1-iu\Sigma^x(s,T,x)\nu^{+,T}\right) - \log\left(1+iu\Sigma^x(s,T,x)\nu^{-,T}\right) \\ &+ iu\,\left[\log\left(1-\Sigma^x(s,T,x)\,\nu^{+,T}\right) + \log\left(1+\Sigma^x(s,T,x)\,\nu^{-,T}\right)\right], \\ \nu^{\pm,T} &= \frac{\nu^\pm}{1\pm\Sigma(s,T)\nu^\pm}.\end{aligned}$$

The choice of the VG density induces a restriction in the domain of the (extended) characteristic function (see Assumption 3.1.1). In fact the moment generating function of a VG process is well defined only if $Re(u) \in \left[-\frac{1}{\nu^+}, \frac{1}{\nu^-}\right] \subset \mathbb{R}$. This condition impose an upper limit to the volatility function, as required in Assumption 3.2.4.

3.5 Example of cap volatility calibration

For the construction of the initial term structure of the Eonia, Euribor 3M and Euribor 6M curves, we follow a consolidated procedure, described for example in [Crépey et al., 2015]. Zero coupon bonds curves are taken from Bloomberg (ICVS function). Figure 3.1 shows the Nelson-Siegel-Svensson fitting of the zero coupon rates for the Eonia, Euribor 3M and 6M curves on January 4^{th} 2011 .
We calibrate the models parameters to cap implied volatility surfaces on Euribor of the 4^{th} January 2011 (BBIR Bloomberg data). Bloomberg provides the cap implied volatility surface for 3 months tenor until a maturity of two years and then for 6 months tenor; the surface is constructed in an arbitrage free manner, with Eonia as discounting curve. Implied volatilities are obtained from quoted prices using the Black model. We note an humped shape of the volatility surface for short maturities. Maturities are from 1 year to 10 years, to fit the volatility smile at each maturities, we use the at the money forward (ATMF) strike plus three out of the money forward (OTMF) fixed strikes quoted in Bloomberg.

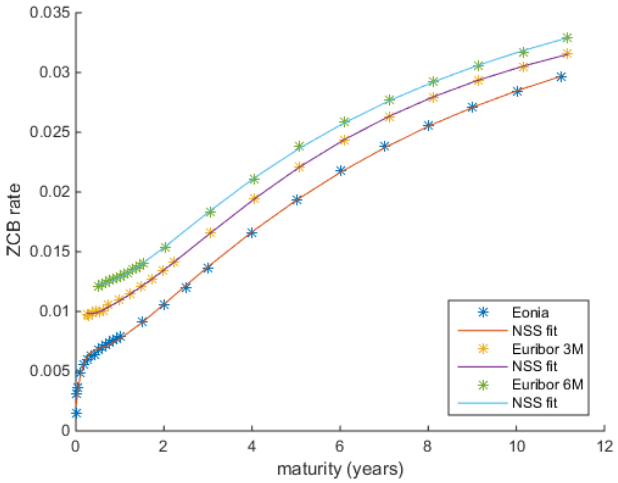

Figure 3.1: Nelson-Siegel-Svensson fit of the market zero coupon rates for the Euribor 3M/6M and the Eonia curves at the 4^{th} January 2011.

The calibration is performed in two step, first through the minimization of the quadratic difference between model and market prices with a differential evolution algorithm, and then through the minimization of the quadratic distance between the implied and the market volatilities with an interior-point method (Matlab function *fmincon*). The accuracy of the calibration is quantified through different error indicators: the root mean square error (RMSE) of model prices (or volatilities) with respect to market data, the mean absolute percentage error (MAPE) and the maximum absolute error (MAE). Definitions the error indicators are reported in Table 3.1.

RMSE	$\frac{1}{\sqrt{N}}\sqrt{\sum_{i=1}^{N}(X_i - X_i^{mkt})^2}$
MAPE	$\frac{1}{N}\sum_{i=1}^{N} \mid \frac{X_i}{X_i^{mkt}} - 1 \mid$
MAE	$\max_{i=1,\dots,N} \mid X_i - X_i^{mkt} \mid$

Table 3.1: Error indicators formulas: N is the number of market quotes, X_i and X_i^{Mkt} are the model and the market quantities, respectively.

The calibrated parameters are reported in Tables 3.2 and 3.3, while the calibration errors are shown in Table 3.4 and 3.5. Figures 3.2 and 3.3 illustrate the calibration results.

v_0	α	β	η	ρ	a	h	β_1	γ
0.0017437	3.2275	0.23993	0.0015698	-0.1845	1.6524	0.0024864	4.8203	0.002952

Table 3.2: Time-changed diffusive model. Calibrated parameters on the Euribor cap volatility surface at 04 January 2011.

v_0	α	β	η	ν^+	ν^-	a	h	β_1	γ
2.8166	1.7873	0.3155	1.3108	0.41102	0.61621	0.4047	0.0122	1.6305	1.3653

Table 3.3: Time-changed variance gamma model. Calibrated parameters on the Euribor cap volatility surface at 04 January 2011.

Volatility	
RMSE (%)	1.89
MAPE (%)	5.53
Max Absolute error (%)	4.69
Price	
RMSE (bps)	17.93
MAPE (%)	9.29
Max Absolute error (bps)	70.23

Table 3.4: Time-changed diffusive model. Calibration results on the Euribor cap volatility surface at 04 January 2011.

Volatility	
RMSE (%)	2.66
MAPE (%)	6.85
Max absolute error (%)	7.52
Price	
RMSE (bps)	16.50
MAPE (%)	15.46
Max absolute error (bps)	49.54

Table 3.5: Time-changed variance gamma model. Calibration results on the Euribor cap volatility surface at 04 January 2011.

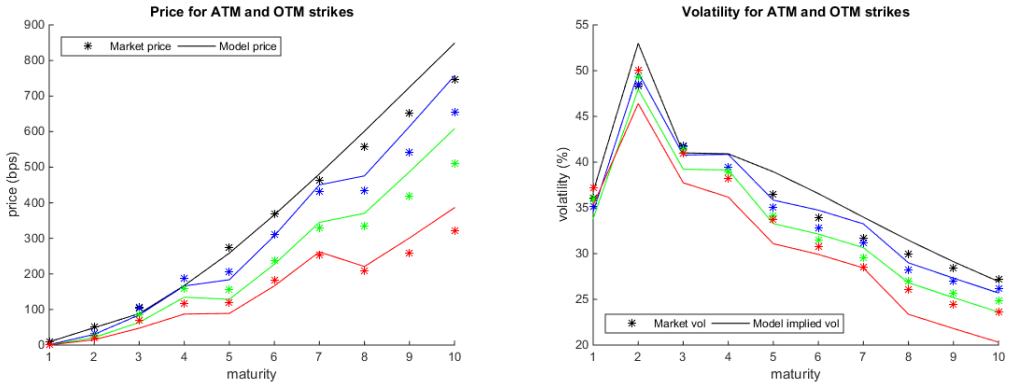

(a) Price (b) Volatility

Figure 3.2: Time-changed diffusive model. Calibration results on the Euribor cap volatility surface at 04 January 2011.

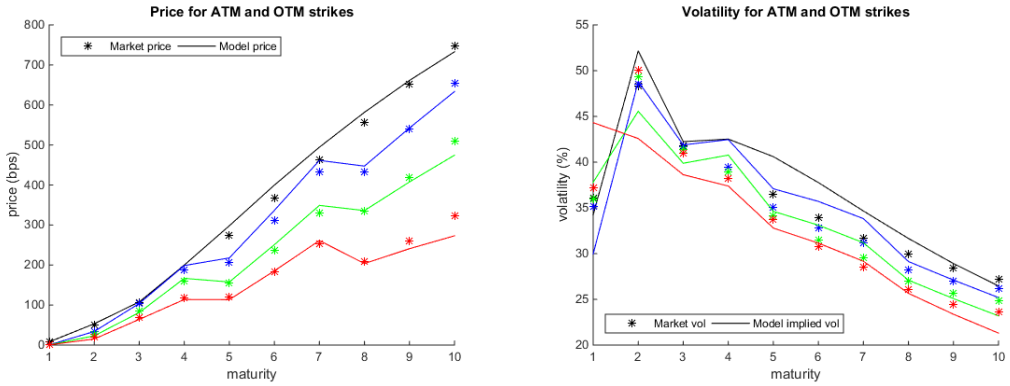

(a) Price (b) Volatility

Figure 3.3: Time-changed variance gamma model. Calibration results on the Euribor cap volatility surface at 04 January 2011.

3.6 In-sample and out-of-sample numerical tests

In order to obtain a deeper analysis of the models accuracy, we perform an in-sample and out-of-sample numerical test. First, we calibrate the parameter of the models to the sample, composed by the third Wednesday cap quotes of each month of 2015; in particular we use ICAP[1] quotations obtained through the provider Bloomberg. Calibration is performed each day as described in the previous section, the only difference is that the 2015 cap (implied) volatility surfaces are obtained from quoted prices with the normal model, instead of the Black model. This difference is due to the fact that the Black model does not accept negative rates. Indeed, for instance, the zero coupon rates for the Eonia curve of the 21^{th} January 2015 are negative for short maturities (figure 3.4), which implies discount factors greater than one. However

[1]ICAP is a brokerage company, specialised in interest rate derivatives market.

the Nelson-Siegel-Svensson parametrization is flexible enough to fit the curve. The calibration accuracy is quantified via the error indicators defined in Table 3.1 and used in previous section. Then we perform the out-of-sample test, i.e. we price cap market quotes of the next day (i.e. the third Thursday of each month), using the parameters previously calibrated and the market data for the discounting and forwarding curves, of the next day. This test is important because it verifies if the model is stable. Moreover, in practice, calibration are performed by practitioner each day using the parameters obtained the previous day as starting point. As shown in Tables 3.7 and 3.9, error are similar in the in-sample and in the out-of-sample case, this means that both models are stable.

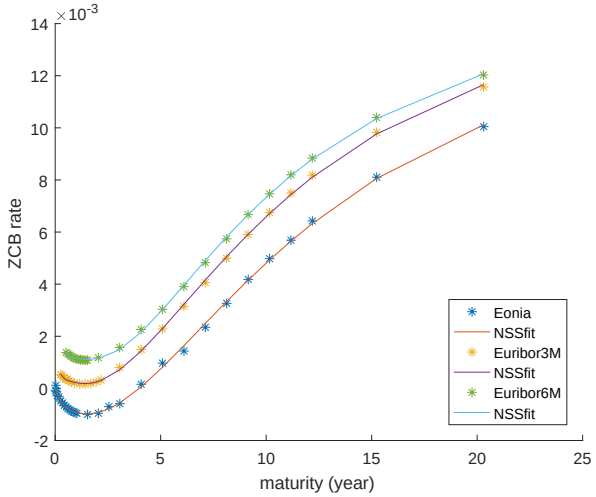

Figure 3.4: Figure shows the Nelson-Siegel-Svensson fit of the market zero coupon rates for the Euribor 3M/6M and the Eonia curves at the 21^{th} January 2015.

Calibrated parameters	v_0	α	β	η	ρ	a	h	β_1	γ
January	0.9933	3.7117	0.0409	2.5548	-0.0250	0.9283	0.0016	1.3670	1.0294
February	1.2192	3.3328	0.0398	2.4739	-0.0330	2.0064	0.0019	2.0544	0.8417
March	1.2145	3.2735	0.0626	2.4218	-0.0633	2.1138	0.0021	2.2922	0.8575
April	0.3463	3.1051	0.0939	2.4283	-0.0361	2.2614	0.0034	1.4669	0.3770
May	0.7323	3.3695	0.1085	1.9588	-0.0785	1.4992	0.0017	2.3645	0.1728
June	0.8874	3.4051	0.1261	2.2839	-0.0579	0.8739	0.0012	2.8807	0.3146
July	0.8813	3.4453	0.1154	2.2899	-0.0596	0.7279	0.0009	2.9882	0.3411
August	0.0958	3.3936	0.1160	1.9553	-0.0381	1.2217	0.0014	2.5465	0.1627
September	0.8837	3.6121	0.0869	1.5278	-0.0478	1.3727	0.0011	2.6369	0.0760
October	0.8974	3.8108	0.1260	1.5585	-0.0482	0.4715	0.0007	3.3682	0.3756
November	1.1164	3.7450	0.1153	1.5498	-0.0966	0.8952	0.0011	3.1726	0.6590
December	0.9374	3.5602	0.1164	2.0606	-0.0650	0.9103	0.0012	2.9134	0.5725

Table 3.6: Time-changed diffusive model. Calibrated parameters on the Euribor cap volatility surface at third Wednesday of each month of 2015.

Volatility	In sample			Out of sample		
	RMSE (%)	MAPE (%)	MAE (%)	RMSE (%)	MAPE (%)	MAE (%)
January	0.05	9.27	0.11	0.04	8.32	0.10
February	0.05	9.85	0.13	0.06	10.49	0.15
March	0.06	8.07	0.27	0.06	8.42	0.30
April	0.04	6.84	0.10	0.04	6.83	0.09
May	0.04	5.83	0.17	0.04	5.59	0.19
June	0.05	6.45	0.15	0.05	6.74	0.17
July	0.03	4.41	0.13	0.04	4.67	0.12
August	0.05	8.81	0.13	0.05	8.98	0.11
September	0.05	7.50	0.14	0.05	8.04	0.14
October	0.04	5.98	0.09	0.05	7.26	0.18
November	0.05	5.81	0.19	0.05	5.83	0.19
December	0.03	5.11	0.11	0.03	5.55	0.11
Price	**In sample**			**Out of sample**		
	RMSE (bps)	**MAPE (%)**	**MAE (bps)**	**RMSE (bps)**	**MAPE (%)**	**MAE (bps)**
January	14.51	22.24	42.70	14.94	16.38	49.50
February	14.78	40.80	42.41	15.33	55.10	42.04
March	12.33	15.22	40.49	13.02	15.59	37.46
April	11.70	13.34	29.77	11.71	13.53	31.89
May	5.22	12.16	12.87	4.49	11.37	12.69
June	7.06	31.08	21.26	8.84	22.80	26.47
July	6.57	9.21	15.25	7.04	9.68	17.95
August	9.60	19.59	23.95	11.18	19.34	27.76
September	11.50	16.19	29.93	12.24	17.91	36.69
October	8.36	12.39	23.65	8.41	12.72	23.95
November	4.58	10.46	11.34	5.24	10.35	15.29
December	6.96	10.12	24.63	7.29	10.55	20.94

Table 3.7: Time-changed diffusive model. Calibration results on the Euribor cap volatility surface at third Wednesday of each month of 2015 and the out-of-sample results on the Euribor cap volatility surface at third Thursday of each month of 2015.

Calibrated parameters	v_0	α	β	η	ν^+	ν^-	a	h	β_1	γ
January	1.2525	3.3092	0.0375	3.0871	0.8134	0.7382	1.0311	0.0018	1.3544	1.2851
February	1.4558	3.2182	0.0409	3.3349	0.7355	0.6598	1.1091	0.0018	1.4596	1.0392
March	2.0232	3.0133	0.0591	3.4167	0.5236	0.5189	1.1926	0.0027	1.3100	0.7759
April	1.7837	2.8636	0.1026	3.5637	0.5043	0.4253	1.0650	0.0030	1.5001	0.4902
May	1.7245	2.9874	0.1223	3.5088	0.3469	0.5487	0.6330	0.0022	1.8751	0.4009
June	1.7326	2.9901	0.1212	3.5123	0.3964	0.5485	0.6230	0.0022	1.8999	0.3988
July	1.6511	3.0326	0.1216	3.4944	0.3760	0.5500	0.4746	0.0017	2.1414	0.4183
August	0.0985	2.3946	0.1401	2.7756	0.4745	0.4673	0.6235	0.0020	2.8716	0.4562
September	0.7980	2.6267	0.0928	2.5904	0.4114	0.2311	1.2103	0.0025	2.8637	0.1067
October	0.9980	2.7811	0.0920	2.5453	0.3512	0.3795	1.5952	0.0033	3.1251	0.7377
November	1.0543	2.7723	0.1025	2.5456	0.3450	0.4149	1.5874	0.0034	3.1053	0.7197
December	1.0358	2.8563	0.1099	2.5441	0.3706	0.3965	1.2851	0.0026	3.2397	0.5301

Table 3.8: Time-changed variance gamma model. Calibrated parameters on the Euribor cap volatility surface at third Wednesday of each month of 2015.

Volatility	In sample			Out of sample		
	RMSE (%)	MAPE (%)	MAE (%)	RMSE (%)	MAPE (%)	MAE (%)
January	0.06	12.66	0.19	0.04	9.01	0.11
February	0.06	11.18	0.16	0.06	11.65	0.17
March	0.05	8.62	0.13	0.05	8.65	0.14
April	0.04	6.98	0.11	0.04	7.60	0.12
May	0.04	6.23	0.12	0.04	6.22	0.13
June	0.05	6.99	0.12	0.05	7.03	0.14
July	0.03	6.16	0.11	0.04	6.30	0.11
August	0.04	8.16	0.14	0.04	8.43	0.14
September	0.05	8.31	0.15	0.05	9.41	0.15
October	0.05	9.34	0.18	0.04	8.30	0.10
November	0.03	5.19	0.12	0.04	5.51	0.12
December	0.03	5.71	0.09	0.03	5.97	0.09
Price	**In sample**			**Out of sample**		
	RMSE (bps)	**MAPE (%)**	**MAE (bps)**	**RMSE (bps)**	**MAPE (%)**	**MAE (bps)**
January	7.19	52.38	20.87	7.68	19.59	22.73
February	9.00	33.23	27.19	9.38	38.48	26.46
March	11.40	17.98	34.94	10.94	17.75	32.01
April	9.52	14.97	28.26	10.40	17.20	28.58
May	4.79	12.50	12.86	5.01	12.11	15.22
June	5.83	22.49	17.33	6.64	20.59	17.08
July	5.75	15.99	14.70	5.96	16.37	13.92
August	6.27	20.52	20.49	7.11	19.95	25.13
September	5.27	25.51	12.76	11.16	25.02	36.86
October	8.19	32.55	21.93	7.92	15.97	22.79
November	3.13	9.54	7.93	4.18	10.07	14.74
December	5.77	11.04	17.76	6.71	11.15	20.73

Table 3.9: Time-changed variance gamma model. Calibration results on the Euribor cap volatility surface at third Wednesday of each month of 2015 and the out-of-sample results on the Euribor cap volatility surface at third Thursday of each month of 2015.

3.7 Preliminary numerical tests of swaption lower bound

For each model we fix the set of parameters calibrated on cap volatility surface (Tables 3.2 and 3.3) and we calculate ATM swaption prices with different maturities and swap lengths. Monte Carlo is used as a benchmark for the computation of the true swaption price. The 97.5% mean-centred Monte Carlo confidence interval is used as measure of the accuracy. Furthermore, we compare the ATM swaption prices obtained with the parameters calibrated on caps with market quotations.

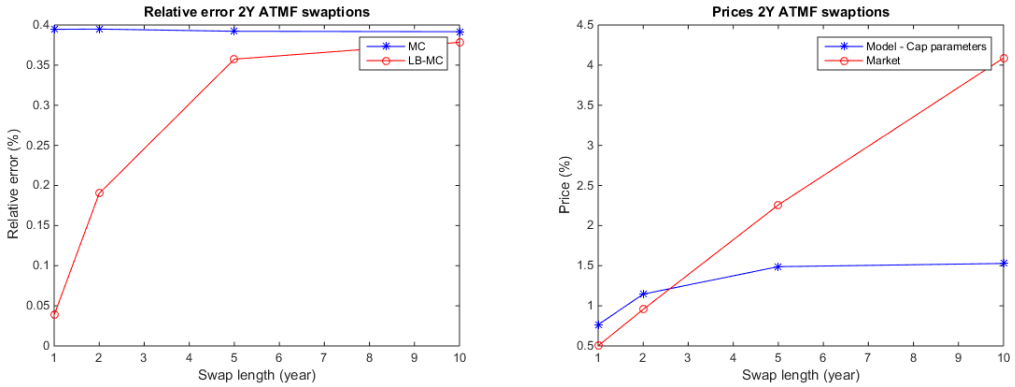

(a) (b)

Figure 3.5: Time-changed diffusive model. Figure (a) shows the relative error of the lower bound respect to the Monte Carlo method. Monte Carlo error is the ratio between the confidence interval and the price. Figure(b) compares model prices and the market swaption prices. Prices are obtained using parameters in Table 3.2.

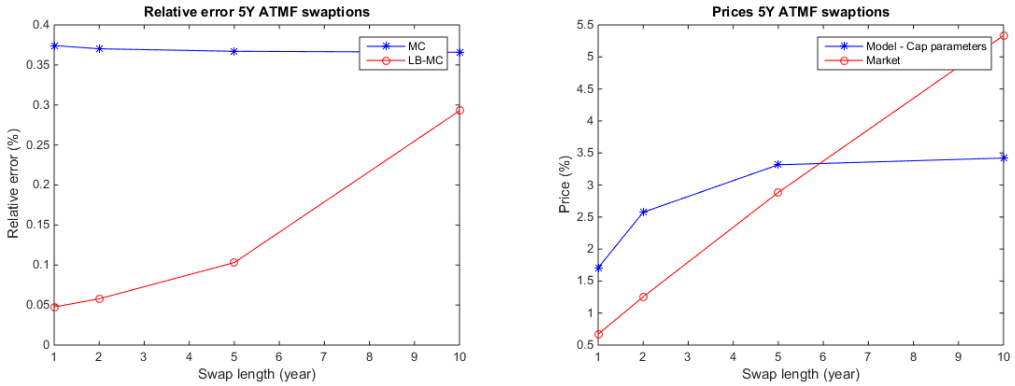

Figure 3.6: Time-changed variance gamma model Figure (a) shows the relative error of the lower bound respect to the Monte Carlo method. Monte Carlo error is the ratio between the confidence interval and the price. Figure(b) compares model prices and the market swaption prices. Prices are obtained using parameters in Table 3.3.

Conclusion

In this chapter we introduce a novel multi-curve model with time-changed Lévy process. The choice of time-changed Lévy as driving process is motivated by their flexibility in reproducing the smile and the term structure of the implied volatility of quoted interest rate derivatives. In particular our model is capable to reproduce the market volatility across maturities and strikes without using time dependent parameters and hence, preserving the parsimony of the model.
We build a coherent and arbitrage free term structure for zero coupon bonds and Libor Forward Rate Agreement (FRA) rates and we study the pricing of interest rate derivatives in a semi-analytical way and we derive the ordinary differential equation to obtain the characteristic function of the log-FRA rate. Then, we calibrate two different driving processes on real market data and we compare the precision of the calibration results. We can not conclude that a pure Lévy driving process is more flexible than a time-changed diffusion process. However, in order to have a complete answer, others Lévy specifications should be tested. Furthermore, we present an in-sample/out-of-sample test that confirms the stability of the two models. Finally, we perform preliminary numerical results, that verifies the precision of the swaption lower bound formula.

Chapter 4

Quantitative assessment of common practice procedures in the fair evaluation of embedded options in insurance contracts

The most recent and widely adopted European Embedded Value (EEV) and Solvency II principles and standards require a market consistent approach for determining the fair value of asset and liabilities of insurance funds (see [CFO-Forum, 2016a] and [CFO-Forum, 2016b]).
According to the standard formula approved by the European Insurance and Occupational Pension Authority (EIOPA) and local regulators, government bonds issued by countries belonging to European Union all have the same risk[1], i.e. the credit and liquidity risk that they carry is not accounted in the valuation of insurance products. In order to cope with this assumption, it is a common practice by insurance companies to introduce a deterministic adjustment on assets cash flows, so that their present value, calculated discounting over the risk-free curve, and their market value, are equal. This approach in the context of market consistent evaluation, is called certainty equivalent [CFO-Forum, 2016a, principle 13].
Hence, in the common model, credit and liquidity risk factors do not affect the volatility of the assets portfolio and the correlation between credit and liquidity spreads of different issuers is not considered at all. This has the further consequence that the tools generally adopted by insurance companies for Solvency II related valuations are not adequate for risk management. Instead, in this chapter we propose a model for credit and liquidity risks, which allows for a stochastic behaviour of these factors and for correlated movements across different issuers. Therefore, it is more suitable for risk management than the approach suggested by regulators.
In addition, we also disentangle the two sources of risk, credit and liquidity, in order to assess their relative importance. In fact, some econometric literature suggests

[1]For a more precise definition of bonds that are treated like government bonds under Solvency II standards see `https://eiopa.europa.eu/regulation-supervision/insurance/solvency-ii/solvency-ii-technical-specifications`

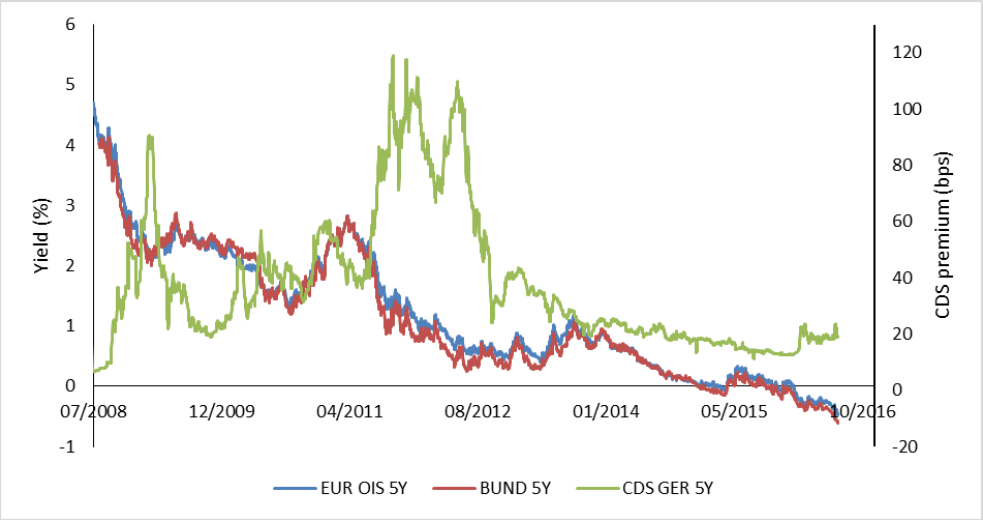

Figure 4.1: The figure shows the historical series of the 5 year German Bund BVAL yields (red line), the Eur OIS 5Y rate (blue line) and the 5 year German CDS premium (green line).

that the liquidity effect is quite important in crisis period (see for instance [Beber et al., 2009]). An example of liquidity spread is reported qualitatively in Figure 4.1 for the German sovereign case. The historical series show that in several periods the Bund yield becomes smaller than the overnight rates in spite of a positive CDS premium. This behaviour can be interpreted as a *fly-to-liquidity* effect as explained in [Beber et al., 2009], i.e. there is a liquidity component in the bond spread and it turns out to be negative. This behaviour is also consistent when explained in terms of the re-denomination risk as suggested in a working paper of the European Central Bank ([Santis, 2015]). In order to separate the effects of the two sources of risk, we consider firstly a model where the stochastic spread is driven by only one factor and we calibrate it on the Credit Default Swap (CDS) quotations; then we add a second stochastic factor to the spread and we calibrate it on the bonds yields. Assuming that CDS quotations are not affected by liquidity risk[2], we can isolate the contribution of the two stochastic components in the valuation of the portfolio.
The chapter is organized as follows. Section 2 describes a with-profit Italian segregated fund and explains the generally adopted (in market consistent evaluations) certainty equivalent approach used to evaluate the minimum guaranteed option. In Section 3 we describe our jointly stochastic model for interest rate, credit and liquidity risks and we perform the calibration of this model on market data. Section 4 presents the numerical evaluation of the embedded options. Results obtained with the common procedure are compared to the results obtained with our model, inclusive of credit and liquidity risk. Conclusive remarks are presented in last Section.

[2]This assumption is widely used in literature, see for instance [Duffie and Singleton, 2003] and [F. Longstaff and Neis, 2005].

4.1 Quantitative assessment of the common practice

Fundamental aspects in the evaluation of insurance products and in particular of segregated funds are the statutory accounting rules which drive the profit sharing mechanism (between policyholder and shareholder) and ultimately, the shareholder obligations toward policyholders.
The common practice for the implementation of a market consistent framework consists in using a certainty equivalent approach (CEQ) to evaluate assets, which for risky securities boils down to applying a risk adjustment to their cash flows. Then, in practical valuations, it becomes critical to determine which assets are considered risk free (and therefore risk adjusted according to CEQ), or risky. In the latter case, the certainty equivalent approach may not be applied, depending on the sophistication of the calculators implemented. Unfortunately, according to Solvency II standard formula, all government bonds issued by sovereign countries belonging to the European Monetary Union are risk free [3] .
This is also in contrast with the view of capital markets, which quote very different government bonds spreads (e.g. over the Euro overnight interest rate swap) on EMU sovereign issuers.The consequence is that insurance companies, in order to treat homogeneously government bonds under the certainty equivalent approach, heavily risk-adjust bonds cash flows. They have to do so in order to recover a present value, discounting cash flows using the risk free curve provided by EIOPA, equal to the assets market price. Unfortunately, the value of financial options embedded in insurance contracts (minimum guaranteed options) is not invariant to risk adjustment on cash flows because their pay-off is determined by statutory accounting rules, as explained in the next section.

4.1.1 Description of segregated fund characteristics

A segregated fund is a type of investment fund administered by insurance companies in the form of life insurance contracts offering certain guarantees to the policyholder, as a minimum rate of return (minimum guaranteed). Segregated funds are owned by the life insurance company, not the individual investors, and must be kept separate from the company's other assets.
These funds consist of a pool of investments in securities such as bonds and stocks but their value does not fluctuate according to the market value of the underlying securities. In fact, for the purpose of determining the rate of return of the fund, assets are evaluated at their amortized (average) cost, and income is computed according to the dividends, coupons and amortization payments accrued over the year, plus any realized gain or loss derived from the sales of assets with respect to their amortized cost. Segregated funds accounting rules are explained further in the Appendix F.1. Every year at a specific date not necessarily coincident with the end of the fiscal year, this rate is published and shared with the policyholder for the part exceeding the minimum guaranteed, according to predefined contractual rules. The amount

[3] `https://eiopa.europa.eu/regulation-supervision/insurance/solvency-ii/solvency-ii-technical-specifications`.

passed as a bonus to the policyholder is accrued in the statutory reserve representing the insurance company obligations to policyholders.
To make the matter even more complicated, the determination of the return of the segregated fund (AKA credited or bonus rate) is subject to discretionary rules applied by the insurance company or management actions. These can be: the investment policy, investment limits and crediting (or gains and losses) realization strategy.
Let $p(t)$ be the payoff of the annual profit earned by an insurer holding a minimum guaranteed investment fund, $N(t)$ be the notional amount, $R(t)$ be the rate of return of the segregated fund, $\bar{r}$ be the minimum guaranteed rate, β be the policyholder participation coefficient and f be the fee charged by the insurer to the policyholder. The payoff $p(t)$ is given by

$$\begin{aligned} p(t) &= N(t)\left(R(t) - \max(\beta\left(R(t) - f\right), \bar{r})\right) \\ &= N(t)\left[(1-\beta)\, R(t) + \beta\, f - \left(\bar{r} - \beta\left(R(t) - f\right)\right)^{+}\right]. \end{aligned} \tag{4.1}$$

Hence, a guaranteed investment fund contains an embedded option which is similar to a set of floorlet sold by the insurance company to the policyholder. However, the embedded option can not be evaluated as a "classical" strip of put options written on the segregated fund. In fact, the underlying of the option is a return determined according to accounting rules, which depends on both accounting and market value of assets, and the discretionary management actions applied to the fund. Moreover, the notional amount of the floorlet depends on the history of accrued rates. This makes the option path dependent. In fact, if the rate of return is greater than the minimum guaranteed, then next year the notional amount which is the value of the statutory reserve is increased by a corresponding percentage.
For these reasons, in order to estimate the value of financial options embedded in a generic insurance product backed by a segregated fund (value of guarantees or VOG), we have to proceed simulating the fund applying a Monte Carlo approach which includes an appropriate asset and liabilities management (ALM) model.

4.1.2 Description of the simulation apparatus

In order to evaluate the options embedded in insurance contracts linked to segregated funds, we have developed a full ALM model. The first step is assets calibration. By this term, we mean a procedure apt to make the value of securities, calculated as a present value of contractual cash flows, exactly identical to their observed market value. This procedure should not be confused with the calibration described in Section 4.2.1 of the interest, credit and liquidity risk models. In fact, while the purpose of the latter is to determine the values of a set of parameters so that the mathematical model describing the dynamic of some stochastic processes is in agreement with observed data, the former is used to correct any discrepancy in securities pricing which is not explained by the modelled risk factors. These discrepancies can arise for different reasons. Generally speaking, the more complete the pricing model, the closer the price of a security should be to its observed market value. Since we want to compare results calculated simulating alternative models, we need to be sure that the asset portfolio has the same initial value regardless the

discounting factor's specification that is used to recover the present value of the securities. This means that all the residual value in assets pricing, not explained by the model, is captured by the (constant) calibration factors introduced from time to time.
This assets calibration is performed basically in two ways: adjusting the cash flows (this is used under the CEQ approach) or adjusting the discount rate using a flat z-spread.
In our analysis both approaches have been utilised. The first one has been applied to test the standard, common, approach where the discount rate must be the risk free rate alone. In this case the assets calibration consists in applying a constant positive probability of default to cash flows of risky securities which are priced above their market value using the risk free curve for discounting. In formula, the price at valuation date (time zero) of the i-th security $P_{0,i}$ is

$$P_{0,i} = \sum_{t=0}^{T} \frac{C_{t,i}(1-p_i)^t}{(1+r_t)^t} \quad with \quad 0 < p_i < 1,$$

where p_i is the calibration parameter specific for the i-th security, representing the i-th security's default rate, r_t is the risk free rate, $C_{t,i}$ is the cash flow paid by the i-th security at time t, and T is the i-th security's maturity.
The second approach has been used to test our model against the standard procedure. The z-spread is calibrated initially for each security, added to the market curve, and then kept constant during the simulation. In mathematical terms, we can express it similarly to the previous one

$$P_{0,i} = \sum_{t=0}^{T} \frac{C_{t,i}}{(1+\tilde{r}_t + z_i)^t}$$

where $\tilde{r}_t$ is the market (risky) rate including, for example, credit and liquidity spread, and z_i is the z-spread specific fo the i-th security.
There are some remarkable differences between the two approaches. Using the z-spread approach, cash flows are not affected by assets calibration, in fact the z-spread affects only the discounting curve. The z-spread is greatly reduced by modelling appropriately a security's market discounting curve. That is the case of our sovereign bond model, which includes interest, credit and liquidity risk. Furthermore, the CEQ calibration factor (default probability) depends arbitrarily on the choice of the risk free curve, which is the only possible discounting curve in the CEQ model. Finally, whenever the choice of the discounting curve is not appropriate the probability of default of the CEQ approach may not be constrained between 0 and 1.
After having calibrated the assets portfolio the simulation is run. The simulation consists in performing algorithmically all the calculation steps that a real insurance company would perform over the year. Firstly, the assets portfolio is evaluated. Then, assets cash flows and payment of contractual obligations which are matured are collected. In case available cash is not enough to pay the contractual obligations, assets are sold and gains or losses are accounted.
Thereafter, crediting strategy is performed, i.e. assets are sold to meet the level of income targeted by the insurance company; usually the target is the minimum guaranteed plus a fixed management fee. Then, assets and liabilities are aligned and

capital is injected or withdrawn depending on whether assets book value[4] is lower or higher, respectively, than liabilities statutory value[5]. Finally, the portfolio is rebalanced according to investment limits.
Management actions occur during the process just described. Because the purpose of our analysis is to evaluate the impact of introducing a more sophisticated evaluation framework, which includes the stochastic credit and liquidity risk component of sovereign bonds, all the parameters affecting the ALM policy and the management actions are set flat and constant during the projection and across scenarios. In particular, investment limits are set fixed and they do not depend on the economic scenario or on time. Same applies to the targeted credited rate.
Reinvestment strategy deserves a particular comment, since in our model new investments occur on constant maturity strategy[6]. This gives mainly two advantages: the exposure on key rate maturities can be controlled easily during the simulation, and no accounting option emerges to bias the results. In fact, modelling on an accounting base new bonds would introduce another option in the evaluation since bonds can be booked in more than one way, e.g. immobilized or available for sales.
Another important assumption is relative to the actuarial factors which are assumed constant across the scenarios. For instance, the death rate of policyholders is deterministic and estimated from life tables. In the context of this study, hypothesising constant actuarial factors over time serve the purpose of having a greater focus on financial aspect. However, our model can be easily extended adding an affine stochastic mortality rate process (see for instance [Schrager, 2006] and [Vigna and Luciano, 2008]).
Finally, VOG is calculated under the hypothesis that the insurance company is always solvent, i.e. it can not default, and it is always able to provide enough capital to cover statutory liabilities.
Without these assumptions, comparability of results would be greatly impaired.

4.2 The model

The model for sovereign bonds discussed in this section allows for three different sources of risk: interest rates, credit and liquidity. Credit and liquidity risks are modelled considering a specific term structure of spreads for each issuer.
At first, we model the risk free interest rate curve using the classical Vasicek model (see [Vasicek, 1977]). The dynamics of the short rate is described by the following stochastic differential equation

$$\begin{aligned} dr(t) &= a(\bar{r} - r(t))dt + \sigma dW(t), \\ r(0) &= r_0, \end{aligned} \tag{4.2}$$

[4]The assets book value is calculated under the local generally adopeted accounting principles (GAAP).

[5],This is the old, Solvency I, coverage ratio; under Solvency II there are more stringent coverage conditions but they are less easy to model in a computational efficient way

[6]A constant maturity strategy is an investment strategy where every year a bond with a specific maturity is purchased to be sold the following year. The proceeds are then used to finance the purchase of a new bond with the same maturity of the bond initially purchased

where $\bar{r}$ and a are the so called long run mean and speed of reversion coefficient (larger a faster r will move towards its mean and converge to $\bar{r}$), σ is the volatility parameter and $W(t)$ is a standard Brownian motion. The adoption of a Gaussian interest rate model is consistent with the recent experience of negative rates. Without loss of generality, the above dynamic is assumed to hold under the risk-neutral measure.
The time t price of a risk free Zero Coupon Bond (ZCB) with maturity T is obtained by computing the following expectation under the risk-neutral measure

$$P(t,T) = E\left[e^{-\int_t^T r(s)\,ds}\right],$$

and it can be easily shown (see [Brigo and Mercurio, 2006] page 59) that this expectation can be written as

$$P(t,T) = A(t,T)e^{-B(t,T)\,r(t)}, \tag{4.3}$$

where

$$\begin{aligned} B(t,T) &= \frac{1-e^{-a(T-t)}}{a}, \\ A(t,T) &= \exp\left[\left(\bar{r}-\frac{\sigma^2}{2a^2}\right)(B(t,T)-T+t) - \frac{\sigma^2}{4a}B(t,T)^2\right]. \end{aligned}$$

In order to model the price of a bond issued by a defaultable issuer, we adopt an intensity model with zero recovery. This is equivalent, see for example [Jarrow and Turnbull, 1995], to sum a spread to the short rate. The spread is related to the creditworthness of the issuer I. Therefore, the price of a defaultable ZCB is obtained as

$$P^I(t,T) = E\left[e^{-\int_t^T (r(u)+s^I(u))\,du}\right]. \tag{4.4}$$

Assuming independence between spread and risk free short rate model[7], the price of the ZCB can be split into the product of two components, the risk free ZCB and an adjustment factor

$$P^I(t,T) = P(t,T)\,Adj_c^I(t,T),$$

where

$$Adj_c^I(t,T) = E\left[e^{-\int_t^T s^I(u)\,du}\right], \tag{4.5}$$

the adjustment factor can be interpreted as a survival probability, i.e. a no-default probability of the bond issuer.
The credit spread $s^I(t)$ is modelled as a positive stochastic process, for instance the square-root Cox-Ingersoll-Ross (CIR, see [Cox et al., 1985]) process. Therefore, we write

$$\begin{aligned} ds^I(t) &= b_I\left(\bar{s}_I - s^I(t)\right)dt + \eta_I\sqrt{s^I(t)}dZ_I(t), \\ s^I(0) &= s_0^I, \end{aligned} \tag{4.6}$$

[7] A common assumption in literature, see for instance [Brigo and Masetti, 2005a] and [Brigo and Morini, 2005].

where Z_I is a standard Brownian motion, assumed to be independent from the Brownian motion driving the dynamics of the risk-free rate.
If the spread follows the dynamic in equation (4.6), then the adjustment factor can be expressed in closed form (see [Brigo and Mercurio, 2006] page 66)

$$\begin{aligned} Adj_c^I(t,T) &= A_c^I(t,T)\, e^{-B_c^I(t,T)\, s^I(t)}, \\ A_c^I(t,T) &= \left[\frac{2h\, e^{(b+h)(T-t)/2}}{2h + (b+h)\left(e^{(T-t)\,h} - 1\right)}\right]^{2b\bar{s}/\eta^2}, \\ B_c^I(t,T) &= \frac{2\left(e^{(T-t)\,h} - 1\right)}{2h + (b+h)\left(e^{(T-t)\,h} - 1\right)}, \\ h &= \sqrt{b^2 + 2\eta^2}. \end{aligned} \tag{4.7}$$

A similar financial model is proposed in [Grbac and Runggaldier, 2015] in the so called multiple-curve Libor market, i.e. a Libor rates model with different tenors.
If we consider in our model also the liquidity risks then we add a liquidity spread, $l^I(t)$, to the rate in the ZCB formula

$$P^I(t,T) = E\left[e^{-\int_t^T (r(u) + s^I(u) - l^I(u))\, du}\right]. \tag{4.8}$$

In this case we do not require $l^I(t)$ to take only positive values and we can use again the Vasicek model

$$\begin{aligned} dl^I(t) &= k_I(\bar{l}_I - l^I(t))dt + \phi_I dY^I(t), \\ l^I(0) &= l_0^I, \end{aligned} \tag{4.9}$$

where Y^I is a standard Brownian motion, assumed to be independent from the Brownian motions driving the dynamics of the risk-free rate and the credit spread.
The possibility of having negative liquidity spread is relevant for example in the German sovereign case as previously shown. In practice, a negative liquidity spread allows us to capture the so called fly-to-liquidity effects; in other words a negative liquidity spread is an implicit convenience yield that arises to the owner of a liquid bond. If we assume that the liquidity spread is independent from both the risk free rate and the credit spread, then, simply, the ZCB formula contains a second multiplicative adjustment factor that has the following closed form

$$Adj_l^I(t,T) = A_l^I(t,T) e^{+B_l^I(t,T)\, l^I(t)}, \tag{4.10}$$

where

$$\begin{aligned} B_l^I(t,T) &= \frac{1 - e^{-k(T-t)}}{k}, \\ A_l^I(t,T) &= \exp\left[\left(-\bar{l} - \frac{\phi^2}{2k^2}\right)(B(t,T) - T + t) - \frac{\phi^2}{4k} B(t,T)^2\right]. \end{aligned}$$

The assumption of independence is necessary for the analytical tractability of the model. The liquidity spread is calibrated using the bond yields quoted in the market.

Finally, credit and liquidity spreads of different issuers can be correlated through the Brownian motions of the CIR or Vasicek processes, i.e. for $I \neq J$

$$dZ_I(t)\, dZ_J(t) = \rho_c^{IJ}\, dt,$$
$$dY_I(t)\, dY_J(t) = \rho_l^{IJ}\, dt.$$

4.2.1 Model calibration

In this section we describe a possible calibration procedure of the model.
The implementation of the model requires firstly to identify the risk-free curve. EIOPA proposes a risk-free discounting curve based on Euribor 6 months par Interest Rate Swap (IRS) rates[8]. However, as highlighted in several papers, [Ametrano and Bianchetti, 2009], [Henrard, 2009], [Mercurio, 2009] and [Morini, 2009] among others, the Euribor par swap rate is affected by credit and liquidity risk of the interbank market, which is not negligible. To fix this problem the EIOPA curve contains a Credit Risk Adjustment (CRA). Finally, a Volatility Adjustment (VA) is applied to the curve (see [EIOPA, 2016]). These adjustments lead to a market consistency issue of the curve as highlighted in [Karoui et al., 2015]. Therefore, according to the recent financial literature (for instance [Z.Kenyon, 2010], [Morini, 2009] and [Moreni and Pallavicini, 2014]), we identify the overnight rate (in particular the Eonia rate for Euro currency) to be the best proxy for the risk free interest rate. In particular, given that there are no liquid options written on the Eonia rate, we calibrate the parameters of the stochastic model of $r(t)$ to the Euro overnight indexed swap (OIS) curve.
In the model previously presented in Section 4.2 ZCB price can be written as

$$\begin{aligned} P^I(t,T) &= P(t,T)\, Adj_c^I(t,T)\, Adj_l^I(t,T) \\ &= e^{(-R(t,T)-S^I(t,T)+L^I(t,T))\,(T-t)} \end{aligned}$$

where $R(t,T)$ is the zero risk free rate, $S^I(t,T)$ and $L^I(t,T)$ are the credit spread and the liquidity spread, respectively, calculated between t and T for the issuer I. In order to estimate from the market the credit component, we bootstrap the term structure of survival probabilities (i.e. the no-default probabilities of the issuer) from the quotations of credit default swap (CDS) spreads for each specific issuer. However, there are no liquid quotations of CDS for maturities longer than 10 years. Hence, we extract the long term issuer survival probabilities from sovereign ZCB curves under the hypothesis that the long term liquidity spread remains constant and equal to the 10 years spread. We fix $t = 0$ and $T^* = 10$ years and we assume that for maturities T longer than T^* the liquidity spread remains constant, i.e.

$$L^I(0,T) = L^I(0,T^*).$$

Without this assumption, we observe too large values of long maturity liquidity

[8] More details about the construction of the EIOPA curve are given in Appendix F.2.

spread[9]. Hence, we obtain the following formula for the issuer survival probabilities

$$PS^I(0,T) \quad = \quad \frac{P^I(0,T)}{P(0,T)} \left(\frac{P(0,T^*)\, PS^I(0,T^*)}{P^I(0,T^*)} \right)^{\frac{T}{T^*}}, \text{ if } T \geq T^*.$$

By the previous formula the issuer survive probabilities $PS^I(0,T)$ for $T > T^*$ are extracted using (a) CDS quotations up to time T^*, i.e. $PS^I(0,T^*)$, (b) using the ZCB prices of the issuer I, $P^I(0,T)$ and $P^I(0,T^*)$, obtained from quoted sovereign spot curves and (c) using the risk free ZCB prices, $P(0,T)$ and $P(0,T^*)$, bootstrapped from the OIS curve.
By this procedure, we have now a market implied term structures of $P(0,T)$, $PS^I(0,T)$ and $P^I(0,T)$ up to 30 years and we use them to calibrate the parameters of the processes $r(t)$, $s^I(t)$ and $l^I(t)$, i.e. the risk free short rate and the stochastic credit and liquidity spreads of the issuers. Calibration results on market quotations at March 30, 2016 of the Vasicek model for $r(t)$, of the CIR model for $s^I(t)$ and of the Vasicek model for $l^I(t)$ are given in Table 4.1, 4.2 and 4.3 and Figure 4.2, 4.3 and 4.4, respectively. The calibrations are performed through the minimization of Root Mean Square Deviation (RMSD) between market data (ZCB prices and probabilities of default) and the corresponding model quantity. In Tables 4.1-4.3, we report the RMSD and the maximum relative error (MRE), i.e. the maximum of the relative error between market and model quantities. More details about the calibration procedure are given in Appendix F.3. Market data are reported in Appendix F.4.
Finally, we estimate the historical correlations between the credit spreads of the two issuers and we do the same for the liquidity spreads of the two issuers. The data set covers the period from March, 30^th 2015 to March, 30^th 2016 and it is composed by Euro OIS rates with maturity from 1 months to 10 years, CDS spread quotations of the two issuers with maturity from 6 months to 10 years and bond yield curves of the two issuers with maturity from 3 months to 10 years. For each date in the sample, we bootstrap the ZCB prices from OIS rates, then we choose the most liquid maturity and we invert formula (4.3) to extract $r(t)$. In this way, we obtain the historical time series of the risk free short rate $r(t)$. In order to extract the historical series of the stochastic credit spreads for each issuer, $s^I(t)$, we bootstrap in each date the issuer survival probability curve from CDS quotations, using OIS as discounting curve, and then we choose the most liquid maturity and we invert formula (4.7) to compute $s^I(t)$. The correlation calculated between the series of daily returns of the two credit spreads is assumed to be a proxy of the correlation between the two Brownian motions driving the CIR processes. Finally, we subtract the risk free and the credit components from the bond yields and the remaining part can be identified with the natural logarithm of formula (4.10), so that we obtain also the series of the liquidity spreads $l^I(t)$. The correlation calculated between the series of daily returns is assumed to be a proxy of the correlation between the two Brownian motions driving the Vasicek processes of the two liquidity spreads. More details are given in

[9] This quantity is given by the following form (as in [Vasicek, 1977])

$$L^I(0,\infty) = -\bar{l}^I - \frac{1}{2}\frac{\phi_I^2}{k_I^2}.$$

Appendix F.3. The historical values of the correlation between Italian and German credit and liquidity spreads are equal to $\rho_c = 0.2463$ and $\rho_l = 0.3341$, respectively. From a risk management point of view, it is very important to assess the impact of the correlation on the volatility of portfolio. For this reason, we simulate the portfolio using not only the historical based estimates od correlations but also considering extreme correlation scenarios, i.e. $\rho_c = \rho_l = \pm 1$, as well as the zero correlation case.

r_0	a	$\bar{r}$	σ	RMSD	MRE (%)
-0.0107	0.1993	0.0135	0.0006	4.9×10^{-3}	1.5

Table 4.1: Vasicek model: calibrated parameters on the Eonia curve on March 30 2016. The result of the calibration is shown in Figures 4.2. The root mean square deviation (RMSD) and the maximum relative error (MRE) of the calibration are also reported.

Country	s_0	b	$\bar{s}$	η	RMSD	MRE (%)
GER	0.0001	0.3659	0.0075	0.0742	4.1×10^{-3}	1.1
ITA	0.0001	0.4761	0.0389	0.1925	1.1×10^{-2}	4.8

Table 4.2: CIR model: calibrated parameters on CDS and sovereign ZCB curves on March 30 2016. The results of the calibrations are shown in Figure 4.3. The root mean square deviation (RMSD) and the maximum relative error (MRE) of the calibrations are also reported.

Country	l_0	k	$\bar{l}$	ϕ	RMSD	MRE (%)
GER	-0.0078	0.9990	0.0090	0.0021	3.8×10^{-3}	1.0
ITA	-0.0001	0.4806	0.0261	0.0011	8.0×10^{-3}	3.4

Table 4.3: Vasicek model: calibrated parameters on the sovereign ZCB curves on March 30 2016. The results of the calibrations are shown in Figure 4.4.

4.2.2 Risk neutral evaluation and martingale test

In order to prove that the Economic Scenario Generator (ESG) built upon the model presented in previous section is risk neutral and market consistent, as required by the regulator under Solvency II directive, martingale tests on sovereign coupon bonds with different maturities are performed. The martingale process is built by dividing the total return performance of an asset by a the total return performance of the cash account, i.e. the numeraire of the risk neutral measure. The results are shown in Figures 4.5-4.7, using the calibrated parameters presented in Tables 4.1-4.3.

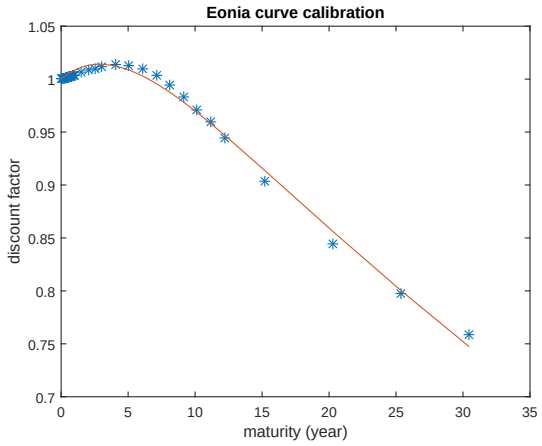

Figure 4.2: Calibration of the Eonia curve on March 30, 2016 with the Vasicek model. Blue markers are the market quotations.

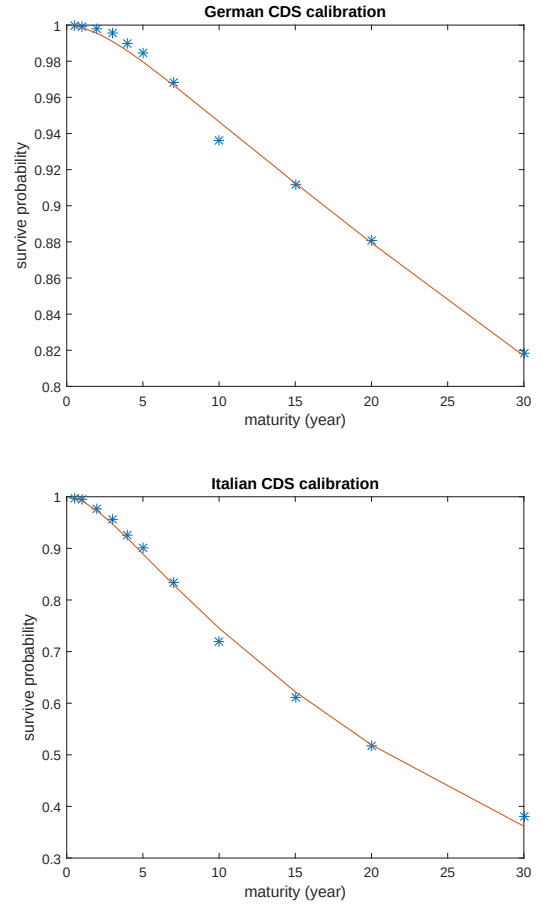

Figure 4.3: Calibration of the CDS and ZCB sovereign curves on March 30, 2016 with the CIR model. Blue markers are the market quotations. The last four market quotations (15, 20, 25 and 30 years) are extracted from ZCB sovereign curves with the assumption of long term constant liquidity spread as explained in Section 4.2.1.

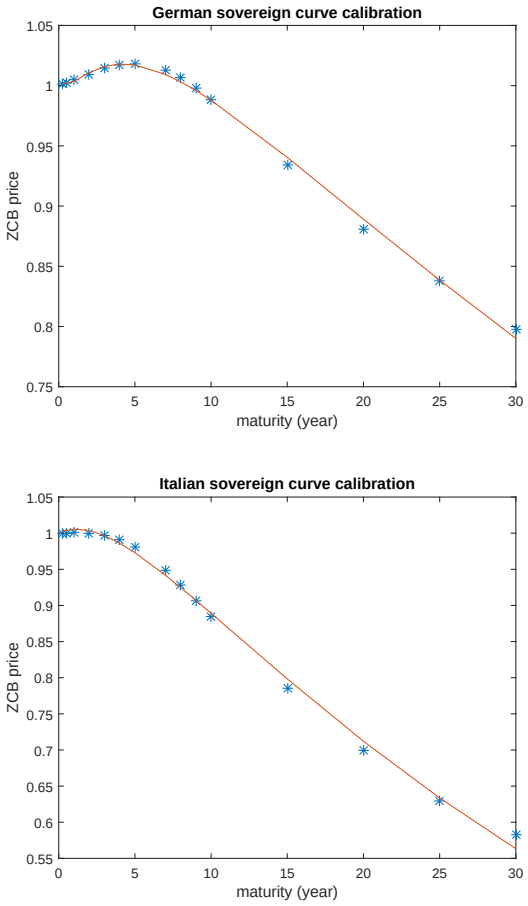

Figure 4.4: Calibration of the sovereign BVAL curves on March 30, 2016 with Vasicek model for the risk free and the liquidity component and a CIR model for the credit factor. Blue markers are the market quotations.

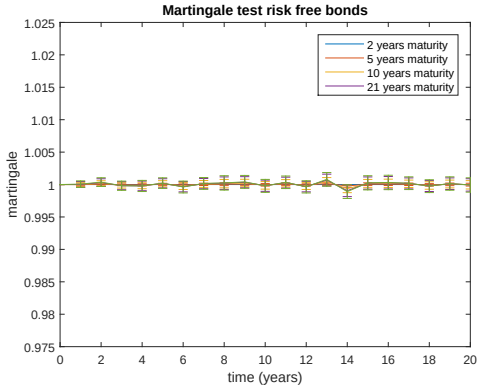

Figure 4.5: Martingale test performed on risk free coupon bonds with 100 Monte Carlo simulations and parameter reported in Table 4.1. The error bars are the 97.5% confidence intervals.

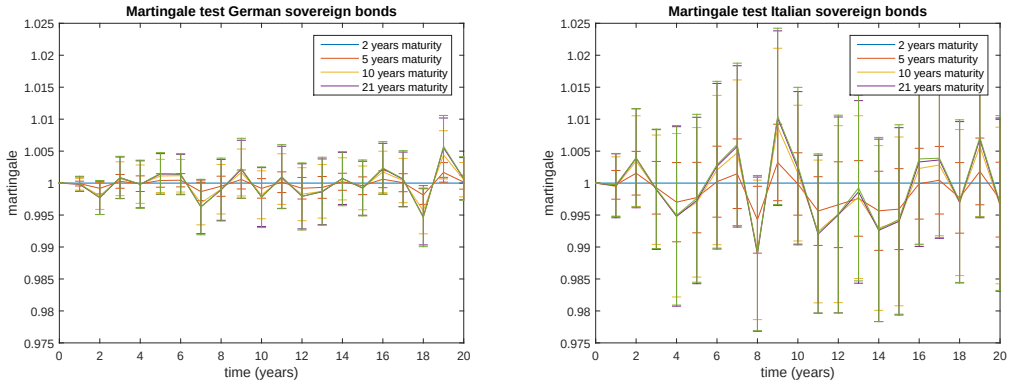

Figure 4.6: Martingale tests performed on sovereign German and Italian coupon bonds with 100 Monte Carlo simulations and parameter reported in Tables 4.1 and 4.2. The error bars are the 97.5% confidence intervals.

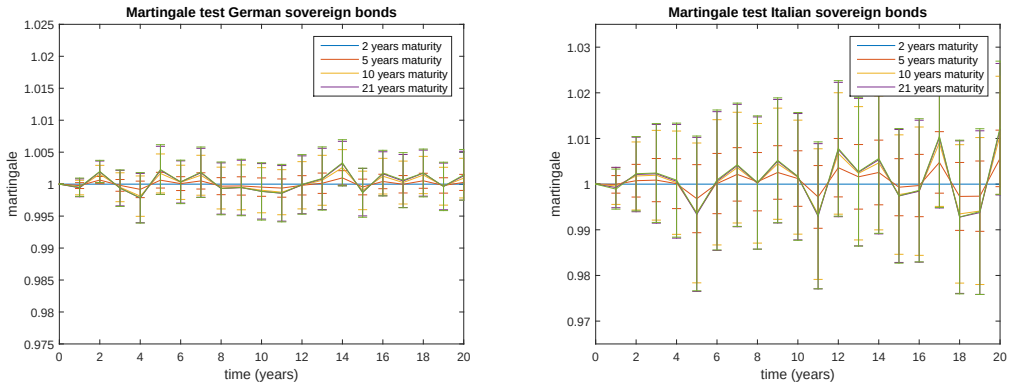

Figure 4.7: Martingale tests performed on sovereign German and Italian coupon bonds with 100 Monte Carlo simulations and parameter reported in Tables 4.1, 4.2 and 4.3. The error bars are the 97.5% confidence intervals.

4.3 Numerical results

In this section, we compare the value of contractual options embedded in Italian insurance (with-profit) traditional products, assuming that all government bonds are risk free, with the value provided by the more complete model described in previous sections. Overcoming the need of adopting a CEQ approach makes the evaluations more sensible and robust, and ultimately, more consistent with a risk management framework. In particular for the credit and liquidity model we study the role of the correlation among issuers. The possibility to stress parameters such as correlation is of paramount importance for a model to be of use as a risk management tool [10]. This opportunity is not achievable under the commonly adopted framework. In order to test the consistency of our approach, we compare the full model including credit and liquidity spreads with a (less complete) model that includes only credit spread and with one (incomplete) including only the risk free interest rate as stochastic factor. In the latter case, we evaluate the embedded option using the (standard) CEQ approach and a z-spread adjustment calibrated at valuation date. Significantly, all the results agree with theory. In particular, results show that adjusting cash flows for risk undesirably affects the value of the option through the statutory accounting rules of the segregated fund.

4.3.1 Description of the tested portfolio

The ALM set-up described in the previous section is used to simulate, over a 20 years time-horizon a portfolio of endowments, i.e. life liabilities with death, surrender and maturity benefit (no annuities), which has a total duration (modified) of about nine years and which runs-off in approximately 20 years. Liabilities have an average minimum guaranteed of 3% ($\bar{r}$), a total value (mathematical reserve) of one billion and a vintage year of 4 years. The average policyholder participation coefficient β is near to one and fixed fees are set very low at 25 basis points.
The life liabilities are written on a portfolio of government bonds with fixed or floating rate, issued by Italy or Germany (90% Italian and 10% German) with a total duration (modified) of about nine years. The asset portfolio has an operating (current) accounting return higher than 3% for the next 5 years.

4.3.2 Evaluation of the embedded option

We perform a Monte Carlo simulation using the apparatus described above and a set of stochastic scenarios consisting of the risk free rate, the Italian and German credit spreads and the Italian and German liquidity spreads. The stochastic model adopted is described in Section 4.2 and the calibration parameters are reported in Tables 4.1, 4.2 and 4.3 in Section 4.2.1.
The embedded option is evaluated under alternative set-ups. In Table 4.4 the stochastic scenarios used to evaluated the VOG are generated using all available risk factors (set-up 1), which are interest rate, credit and liquidity, while in the set-up 2 only interest rate and credit risk are used.

[10] The approach presented in this work is also in agreement with the prudent person principle. For more details please check [AIFIRM, 2016, Paragraph 6]

The asset calibration is carried out using a z-spread, which is very few basis points when the complete model is used.
In the first two set-ups different dependence scenarios between the two issuers are generated and tested. Historical correlations for credit and liquidity spreads of the two issuers are estimated in calibration Section 4.2.1. Extreme values (-1 and 1) of the correlation between Brownian motions of credit and liquidity spreads are tested. Moreover, the portfolio is simulated also in the hypothesis of independent issuers.
Table 4.4 shows clearly that correlation affects sensibly the results and that adding the liquidity risk to the model increases the value of the option. This is consistent with the diversification effect which is expected when correlation turns negative. In fact, increasing the correlation increases the variance of the portfolio and makes the options more expensive. Although the standard error is still material with only 500 simulations, also in the set-up 2 it is evident that a diversification effect is operating.
In Table 4.5, only interest rate is used to generate stochastic scenarios. In this case the evaluation is done, in the first case performing the assets calibration with the z-spread, and in the second case applying a risk adjustment to securities cash flows, according to the CEQ approach. The difference in results of Table 4.5 is striking.
The explanation is that the option is written on an underlying that depends on accounting rules that are not invariant to arbitrary risk adjustments of cash flows.
Compared to the model used to generate the results reported in Table 4.5, the results in Table 4.4, Set-Up 1, are obtained using five risk factors (encompassing all the assets classes in position which are German and Italian government bonds), instead of just one. Therefore, we would have expected a result of the CEQ model close to the one we have got using Set-Up 1 and perfect correlation. Because the magnitude of the discrepancy observed between these models cannot be explained by some missing risk factor or by a smaller volatility of the richer model compared to the CEQ, the only explanation must be the appropriateness of the constant and arbitrary adjustment derived from the application of the CEQ approach. From Appendix F.1, it will be clear that any risk adjustment applied to a security's cash flows would change the assessment of the statutory income through the gains or losses at maturity of bonds available for sales, the coupons received, the difference between accrued interest, and finally, the calculation of average book value, and that all these changes do not necessarily compensate. To confirm our interpretation of the numerical results, we have calculated the VOG evaluating the segregated fund return (which is the option's underlying) at market value, i.e. we have evaluated the fund applying the same principles as for the assets classified in the Fair Value Through Profit and Loss (FVTPL) category as defined by International Financial Reporting Standards (IFRS). In line with our expectation, the choice of the accounting rules has a great impact on the value of the embedded option. The most relevant aspect is that the results obtained with a CEQ approach and whit our model in case of perfect correlation, are quite close if the fund is evaluated "mark to market" (see Table 4.6). These results have also an interesting implication, with respect to a topic quite controversial in economic literature which is whether or not accounting rules have an impact on the economic value of assets. In case of options embedded into the traditional insurance life contracts, they do because of the smoothing effect of the volatility of the option's underlying they provide (e.g. immobilized assets don't show return volatility by

definition if they can be hold to maturity; see also Section 4.1.2).

Correlation (Spread corr.)	VOG - Set-Up 1 (Std error)	VOG - Set-Up 2 (Std error)
-1	10,582,957	8,753,313
(-60.2%)	(635,986)	(626,633)
0	11,476,256	10,126,767
(-0.8%)	(835,419)	(780,436)
Hist	11,524,598	10,613,700
(19.1%)	(837,614)	(848,216)
1	12,210,034	9,995,398
(99.0%)	(876,037)	(856,718)

Table 4.4: The table reports the Value of Options and Guarantees (VOG) calculated running 500 stochastic simulations; in parenthesis is reported in the first column the average correlation observed on simulated spread and in the second and third columns the standard error of VOG.

VOG - Set-Up 3 (z-spread)	VOG - Set-Up 3 (CEQ)
1,987,941	36,754,113
(36,397)	(337,158)

Table 4.5: The table reports the value of VOG calculated using the z-spread and using the CEQ approach. Both methods use only interest rate as a stochastic risk factor.

VOG - Set-Up 3 (z-spread)	VOG - Set-Up 3 (CEQ)	VOG - Set-Up 1 (corr=1)
104,977,985	187,379,809	180,569,933
(1,941,351)	(1,738,295)	(8,756,981)

Table 4.6: The table reports the value of VOG calculated using the z-spread and the CEQ approach with only the interest rate as stochastic risk factor and our full model with correlation equal to 1. In all cases, the segregated fund which is the option underlying is evaluated using the FVTPL accounting rule of IFRS.

The reasons for the CEQ approach is not appropriate for the evaluation of this type of options may be summarised as follows:

- the return of the funds and hence the value of the option depends on accounting conventions;
- the value of the option also depends on the interaction of assets and liabilities which is not completely under control of the insurance company and which depends on unobservable (in the capital market) variables such as mortality and surrender rates;
- the value of the option depends on discretionary actions (management actions) defined by the company such as the commercial targets on segregated fund statutory

return, the investment rules including the guidelines to classify newly purchased assets on the segregated fund balance sheet, the criteria to sell assets to pay for contractual obligations or for realize gains or losses.

Conclusion

The European directive also known as Solvency II has driven more focus on the need of sounder risk management practice by insurance companies. At the same time, it has introduced standards in the evaluation of assets and liabilities in the attempt of creating a fairer playing field in the insurance sector. Although the European regulator has succeeded in its attempt, this success is not without critics. One of most debated issues is the assumption that all European government bonds has to be evaluated using a risk free discounting curve. This assumption together with the adoption, mandatory in the Solvency II framework, of market consistent evaluations, has pushed insurance companies to adopt the certainty equivalent approach to cope with the complexity of simulation apparatus needed to carry out all the necessary calculations, while being consistent with the assumptions of the (Solvency II) Standard Formula. In this chapter we have analysed the consequences of oversimplified risk models, in particular where risk adjustment is applied to options whose underlying depends on accounting rules. Moreover, we have introduced a new model for European government bonds that is more consistent with prices observed in capital markets and at the same time, more flexible to be used for day-to-day risk management.

Bibliography

[Ahn et al., 2002] Ahn, D., Dittmar, R., and Gallant, A. (2002). Quadratic term structure models: Theory and evidence. *Rev. Financ. Stud.*, 15(1):243–288.

[AIFIRM, 2016] AIFIRM, M. R. C. (2016). Prudent Valuation guidelines and sound practices. *availabe at http://www.aifirm.it/wp-content/uploads/2016/06/Documento-AIFIRM-Mar2016-Prudent-Valuation-Guidelines-and-Sound-Practices.pdf*.

[Ametrano and Bianchetti, 2009] Ametrano, F. M. and Bianchetti, M. (2009). *Bootstrapping the illiquidity: Multiple yield curves construction for market coherent forward rates estimation*. Risk Books, Incisive Media.

[Barndorff-Nielsen and Shiryaev, 2015] Barndorff-Nielsen, O. and Shiryaev, A. (2015). *Change of Time and Change of Measure.*, volume 21. World Scientific Publishing Co Inc.

[Beber et al., 2009] Beber, A., Brandt, M., and Kavajecz, K. (2009). Flight-to-Quality or Flight-to-Liquidity? Evidence from the Euro-Area Bond Market. *Rev. Financ. Stud.*, 22(3):925–957.

[Brigo and Masetti, 2005a] Brigo, D. and Masetti, M. (2005a). A Formula for Interest Rate Swaps Valuation under Counterparty Risk in presence of Netting Agreements. *availabe at https://papers.ssrn.com/sol3/papers.cfm?abstract_id=717344*.

[Brigo and Masetti, 2005b] Brigo, D. and Masetti, M. (2005b). Risk Neutral Pricing of Counterparty Risk. In Counterparty Credit Risk Modelling, Risk Management, Pricing and Regulation. *Risk Books, Pykhtin*.

[Brigo and Mercurio, 2006] Brigo, D. and Mercurio, F. (2006). *Interest Rate Models: Theory and Practice.* Springer, 2nd edition.

[Brigo and Morini, 2005] Brigo, D. and Morini, M. (2005). CDS Market Formulas and Models. *availabe at http://wwwf.imperial.ac.uk/ dbrigo/cdsmktfor.pdf*.

[Carr and Madan, 1999] Carr, P. and Madan, D. (1999). Option valuation using the fast fourier transform. *Journal of computational finance*, 2(4):61–73.

[Carr and Wu, 2004] Carr, P. and Wu, L. (2004). Time-changed lévy processes and option pricing. *Journal of Financial economics*, 71(1):113–141.

[Carr and Wu, 2015] Carr, P. and Wu, L. (2015). Leverage Effect, Volatility Feedback, and Self-Exciting Market Disruptions. *JFQA - forthcoming*.

[CFO-Forum, 2016a] CFO-Forum (April 2016a). Market Consistent Embedded Value Basis for Conclusions. *availabe at http://www.cfoforum.nl/downloads/CFO-Forum_MCEV_Basis_for_Conclusions_April_2016.pdf*.

[CFO-Forum, 2016b] CFO-Forum (April 2016b). Market Consistent Embedded Value Principles-Giudance. *availabe at http://www.cfoforum.nl/downloads/CFO-Forum_MCEV_Principles_and_Guidance_April_2016.pdf*.

[Cheng and Scaillet, 2007] Cheng, P. and Scaillet, O. (2007). Linear-Quadratic Jump-Diffusion Modeling. *Math. Finance*, 17:575–598.

[Collin-Dufresne and Goldstein, 2002] Collin-Dufresne, P. and Goldstein, R. (2002). Pricing Swaptions Within an Affine Framework. *J. Derivatives*, 10(1):1–18.

[Corvino, 2003] Corvino, G. (2003). *I prodotti assicurativi vita rivalutabili. Caratteristiche, regolamentazione e gestione*. EGEA.

[Cox et al., 1985] Cox, J., Ingersoll, J., and Ross, S. (1985). A Theory of the Term Structure of Interest Rates. *Econometrica*, (53):385–407.

[Criens et al., 2015] Criens, D., Glau, K., and Grbac, Z. (June 2015). Martingale property of exponential semimartingales: a note on explicit conditions and applications to asset price and Libor models. *http://arxiv.org/abs/1506.08127#*.

[Crépey et al., 2015] Crépey, S., Grbac, Z., Ngor, N., and Scovmand, D. (2015). A Lévy HJM multiple-curve model with application to CVA computation. *Quantitative Finance*, 15(3):401–419.

[Duffie and Kan, 1996] Duffie, D. and Kan, R. (1996). A yield-factor model of interest rates. *Math. Finance*, 6:379–406.

[Duffie et al., 2000] Duffie, D., Pan, P., and Singleton, K. (2000). Transform Analysis and Asset Pricing for Affine Jump-Diffusions. *Econometrica*, 68:1343–1376.

[Duffie and Singleton, 1997] Duffie, D. and Singleton, K. (1997). An Econometric Model of the Term Structure of Interest-Rate Swap Yields. *J. Finance*, 52:1287–1321.

[Duffie and Singleton, 2003] Duffie, D. and Singleton, K. (2003). *Credit Risk.* Princeton University Press.

[Eberlein and Kluge, 2006] Eberlein, E. and Kluge, W. (2006). Exact pricing formulae for caps and swaptions in a Lévy term structure model. *Journal of Computational Finance*, 9(2):99–125.

[Eberlein and Raible, 1999] Eberlein, E. and Raible, S. (1999). Term Structure models driven by General Lévy processes. *Mathematical Finance*, 9(1):31–53.

[EIOPA, 2016] EIOPA (May 2016). Technical documentation of the methodology to derive EIOPA's risk-free interest rate term structures. *https://eiopa.europa.eu/regulation-supervision/insurance/solvency-ii-technical-information/risk-free-interest-rate-term-structures*.

[F. Longstaff and Neis, 2005] F. Longstaff, S. M. and Neis, E. (2005). Corporate yield spreads: Default risk or liquidity? new evidence from the credit default swap market. *Journal of Finance*, 60:2213–2253.

[Fanelli, 2016] Fanelli, V. (2016). A Defaultable HJM Modelling of the Libor Rate for Pricing Basis Swaps after the Credit Crunch. *EJOR*, 249(1):238–244.

[Filipovic, 2001] Filipovic, D. (2001). A general characterization of one factor affine term structure models. *Finance and Stochastics*, 5:389–412.

[Gambaro et al., 2016a] Gambaro, A., Ballotta, L., and Fusai, G. (2016a). HJM multiple-curve model with time-changed Lévy processes. *working paper*.

[Gambaro et al., 2015] Gambaro, A., Caldana, R., and Fusai, G. (2015). Accurate pricing of swaptions via Lower Bound. *Recent advances in Commodity and Financial Modeling, Springer*.

[Gambaro et al., 2017] Gambaro, A., Caldana, R., and Fusai, G. (2017). Approximate pricing of swaptions in affine and quadratic models. *Quantitative finance - forthcoming*.

[Gambaro et al., 2016b] Gambaro, A., Casalini, R., Fusai, G., and Ghilarducci, A. (2016b). Quantitative Assessment of Common Practice Procedures in the Fair Evaluation of Embedded Options in Insurance Contracts. *Available at SSRN: https://ssrn.com/abstract=2872184*.

[Grbac and Runggaldier, 2015] Grbac, Z. and Runggaldier, J. (2015). *Post-Crisis challenges and Approaches.* Springer, 1st edition.

[Henrard, 2009] Henrard, M. (2009). The irony in the derivatives discounting part II: the crisis. *SSRN eLibrary*.

[Hubalek et al., 2006] Hubalek, F., Kallsen, J., and Krawczyk, L. (2006). Variance-optimal hedging for processes with stationary independent increments. *Ann. Appl. Probab.*, 16(2):853–885.

[Jacod, 1979] Jacod, J. (1979). *Calcul Stochastique et Problémes de Martingales.* Number 714 in Lecture Notes in Mathematics. Springer.

[Jacod and Shiryaev, 2002] Jacod, J. and Shiryaev, A. (2002). *Limit Theorems for Stochastic Processes*, volume 288 of *Grundlehren der Mathematischen Wissenschaften.* Springer, second edition.

[Jamshidian, 1989] Jamshidian, F. (1989). An exact bond option pricing formula. *J. Finance*, 44:205–209.

[Jarrow and Turnbull, 1995] Jarrow, R. and Turnbull, S. (1995). Pricing Derivatives on Financial Securities Subject to Credit Risk. *The Journal of Finance*, L(1).

[Kallsen and Shiryaev., 2002a] Kallsen, J. and Shiryaev., A. (2002a). The cumulant process and Esscher's change of measure. *Finance Stochastics*, 6(4):397–428.

[Kallsen and Shiryaev., 2002b] Kallsen, J. and Shiryaev., A. (2002b). Time change representation of stochastic integrals. *Theory of Probability & Its Applications*, 46(3):522–528.

[Karoui et al., 2015] Karoui, N. E., Loisel, S., Prigent, J., and Vedani, J. (2015). Market inconsistencies of the market-consistent European life insurance econimin valuation: pitfalls and practical solutions. *working paper, https://hal.archives-ouvertes.fr/hal-01242023*.

[Kim, 2007] Kim, D. (2007). Spanned Stochastic Volatility in Bond markets: A Reexamination of the Relative Pricing between Bonds and Bond Options. *BIS working paper*.

[Kim, 2014] Kim, D. (2014). Swaption Pricing in Affine and other models. *Mathematical Finance*, 24(4):790–820.

[Leippold and Strømberg, 2014] Leippold, M. and Strømberg, J. (2014). Time-changed Lévy LIBOR market model: Pricing and joint estimation of the cap surface and swaption cube. *Journal of Financial Economics*, 111:224–250.

[Leippold and Wu, 2002] Leippold, M. and Wu, L. (2002). Asset Pricing under the Quadratic Class. *J. Finan. Quant. Anal.*, 2:271–295.

[Madan et al., 1998] Madan, D., Carr, P., and Chang, E. (1998). The Variance Gamma Process and Option Pricing. *Rev. Finance*, 2(1):79–105.

[Margrabe,] Margrabe, W. The Value of an Option to Exchange One Asset for Another. *J. Finance*, 33.

[Mercurio, 2009] Mercurio, F. (2009). Interest Rates and The Credit Crunch:New Formulas and Market Models. *Bloomberg Portfolio Research Paper No. 2010-01-FRONTIERS. Available at SSRN: http://ssrn.com/abstract=1332205*.

[Mercurio, 2010] Mercurio, F. (2010). A LIBOR market model with stochastic basis. *Risk. Mag.*, pages 84–89.

[Moreni and Pallavicini, 2014] Moreni, N. and Pallavicini, A. (2014). Parsimonious HJM modelling for multiple yield-curve dynamics. *Quant. Finance*, 14(2):199–210.

[Morini, 2009] Morini, M. (2009). Solving the puzzle in the interest rate market. *SSRN eLibrary*.

[Munk, 1999] Munk, C. (1999). Stochastic Duration and Fast Coupon Bond Option Pricing in Multi-Factor Models. *Rev. Derivat.*, 3:157–181.

[Nunes and Prazeres, 2014] Nunes, J. and Prazeres, P. (2014). Pricing Swaptions under Multifactor Gaussian HJM Models. *Math. Finance*, 24:762–789.

[PWC, 2010] PWC (2010). IFRS versus German GAAP. Summary of similarities and differences.

[Raible, 2000] Raible, S. (2000). Lévy Processes in Finance: Theory, Numerics, and Empirical Facts. *Doctoral thesis, available at https://www.freidok.uni-freiburg.de/data/51/.*

[Revuz and Yor, 1998] Revuz, D. and Yor, M. (1998). *Continuous martingales and Brownian motion.* Springer, Berlin, third edition.

[Santis, 2015] Santis, R. D. (April 2015). A measure of redenomination risk. *European Central Bank working paper series*.

[Schrager, 2006] Schrager, D. (2006). Affine stochastic mortality. *Insurance: mathematics and economics*, 38(1):81–97.

[Schrager and Pelsser, 2006] Schrager, D. and Pelsser, A. (2006). Pricing Swaptions and Coupon Bond Options in Affine Term Structure Models. *Math. Finance*, 16:673–694.

[Singleton and Umantsev, 2002] Singleton, K. and Umantsev, L. (2002). Pricing Coupon-Bond Options and Swaptions in Affine Term Structure Models. *Math. Finance*, 12:427–446.

[Therond, 2008] Therond, P. (2008). Provisions techniques relatives aux actifs, financiers des assureurs. *Resource Actuarielles*.

[Titchmarsh, 1986] Titchmarsh, E. (1986). *Introduction to the Theory of Fourier Integrals.* Chelsea Publishing Co.: New York, third edition.

[Vasicek, 1977] Vasicek, O. (1977). An equilibrium characterization of the term structure. *Journal of Financial Economics*, (5):177–188.

[Vigna and Luciano, 2008] Vigna, E. and Luciano, E. (2008). Mortality risk via affine stochastic intensities: calibration and empirical relevance. *Belgian Actuarial Bulletin*, (8):5–16.

[Zheng, 2013] Zheng, C. (2013). Method for Swaption Pricing Under Affine Term Structure Models and Measure of Errors. *Available at SSRN: http://ssrn.com/abstract=2351162*.

[Z.Kenyon, 2010] Z.Kenyon (2010). Short-rate pricing after the liquidity and credit shocks: Including the basis. *Risk Mag.*, pages 83–87.

Appendix A

Proofs of Chapter 1

A.1 Proof Proposition 1.1.1

We consider the lower bound to the swaption price as in formula (1.4) for quadratic models:

$$LB_{\boldsymbol{\beta},\Gamma}(k;t) = P(t,T)\,\mathbb{E}_t^T\left[\left(\sum_{h=1}^{n} w_h\, e^{\mathbf{X}(T)^\top C_h \mathbf{X}(T)+\mathbf{b}_h^\top \mathbf{X}(T)+a_h} - 1\right) I(\mathcal{G})\right]$$

where the set $\mathcal{G} = \{\omega \in \Omega : \mathbf{X}(T)^\top \Gamma\, \mathbf{X}(T) + \boldsymbol{\beta}^\top \mathbf{X}(T) \geq k\}$.
We apply the extended Fourier transform (refer to [Titchmarsh, 1986] for a comprehensive treatment and to [Hubalek et al., 2006] for examples of financial applications) with respect to the variable k to the T-forward expected value,

$$\psi(z) \;=\; \int_{-\infty}^{+\infty} e^{zk}\mathbb{E}_t^T\left[\left(\sum_{h=1}^{n} w_h\, e^{\mathbf{X}(T)^\top C_h \mathbf{X}(T)+\mathbf{b}_h^\top \mathbf{X}(T)+a_h} - 1\right) I(\mathbf{X}(T)^\top \Gamma\, \mathbf{X}(T) + \boldsymbol{\beta}^\top \mathbf{X}(T) \geq k)\right] dk.$$

Assuming that we can apply Fubini's Theorem, which is verified in concrete cases, we have

$$\begin{aligned}\psi(z) \;=\; & \mathbb{E}_t^T\left[\left(\sum_{h=1}^{n} w_h\, e^{\mathbf{X}(T)^\top C_h \mathbf{X}(T)+\mathbf{b}_h^\top \mathbf{X}(T)+a_h} - 1\right)\right. \\ & \left.\int_{-\infty}^{+\infty} e^{zk} I(\mathbf{X}(T)^\top \Gamma\, \mathbf{X}(T) + \boldsymbol{\beta}^\top \mathbf{X}(T) \geq k)\, dk\right].\end{aligned}$$

The function $\psi(z)$ is defined for $k \to -\infty$ if $Re(z) > 0$ and

$$\psi(z) \;=\; \mathbb{E}_t^T\left[\left(\sum_{h=1}^{n} w_h e^{\mathbf{X}(T)^\top C_h \mathbf{X}(T)+\mathbf{b}_h^\top \mathbf{X}(T)+a_h} - 1\right) e^{z(\mathbf{X}(T)^\top \Gamma\, \mathbf{X}(T)+\boldsymbol{\beta}^\top \mathbf{X}(T))}\right] \frac{1}{z}.$$

Using the (quadratic) characteristic function of $\mathbf{X}$, Φ, calculated under the T-forward measure, the function $\psi(z)$ can be written as

$$\psi(z) = \left(\sum_{h=1}^{n} w_h e^{a_h}\Phi\left(\mathbf{b}_h + z\boldsymbol{\beta}, C_h + z\Gamma\right) - \Phi\left(z\boldsymbol{\beta}, z\Gamma\right)\right)\frac{1}{z}. \tag{A.1}$$

Finally, the lower bound is the inverse transform of $\psi(z)$ in the sense of the Chauchy principal value integral,

$$LB_{\boldsymbol{\beta},\Gamma}(k;t) \;=\; P(t,T)\,\frac{1}{i2\pi}\lim_{\xi\to\infty}\int_{\delta-i\xi}^{\delta+i\xi} e^{-kz}\psi(z)dz,$$

where δ is a positive constant. The function $\psi(\delta+i\gamma)$ is the Fourier transform of the real function $e^{-\delta k}LB_{\boldsymbol{\beta},\Gamma}(k;t)$, then $\psi(\delta+i\gamma)$ has an even real part and an odd imaginary part. This is useful to simplify the expression above to

$$LB_{\boldsymbol{\beta},\Gamma}(k;t) \;=\; P(t,T)\,\frac{e^{-\delta k}}{\pi}\int_0^{+\infty} Re\left(e^{-i\gamma k}\psi(\delta+i\gamma)\right)\,d\gamma.$$

The proof for a payer swaption follows the same reasoning.

A.2 Proof of Proposition 1.3.1

Here, we show the calculation of the quantity ϵ_1, defined in equation (1.13). The computation of the quantity ϵ_2 follows the same reasoning. Hence, we have to calculate a sum of terms that have the following form:

$$\mathbb{E}_t^T[(w_h P(T,T_h)-K_h)^+\,I(\mathcal{G}^c)].$$

Substituting into the previous expression the definition of the zero-coupon bond price $P(T,T_h)$ as in formula (1.5), the strike K_h as in formula (1.16) and the complement of the approximate exercise region $\mathcal{G}$ as defined in section 1.1.1, we obtain the following formulation:

$$\mathbb{E}_t^T[(w_h P(T,T_h)-K_h)^+\,I(\mathcal{G}^c)] = w_h e^{a_h}\,f(k,k_h),$$

where

$$f(k,k_h)=\mathbb{E}_t^T[(e^{\mathbf{X}(T)^\top C_h\mathbf{X}(T)+\mathbf{b}_h^\top\mathbf{X}(T)}-e^{k_h})^+\,I(\mathbf{X}(T)^\top\Gamma\,\mathbf{X}(T)+\boldsymbol{\beta}^\top\mathbf{X}(T)<k)],$$

and $k_h=\log(K_h)-\log(w_h)-a_h$. We apply the extended Fourier transform with respect to the variable k to the function $f(k,k_h)$ and by Fubini's theorem we obtain

$$\int_{-\infty}^{+\infty} e^{zk}\,f(k,k_h)\,dk = -\mathbb{E}_t^T\left[(e^{\mathbf{X}(T)^\top C_h\mathbf{X}(T)+\mathbf{b}_h^\top\mathbf{X}(T)}-e^{k_h})^+\,\frac{e^{z\,(\mathbf{X}(T)^\top\Gamma\,\mathbf{X}(T)+\boldsymbol{\beta}^\top\mathbf{X}(T))}}{z}\right].$$

The integral converges for $k\to+\infty$ if $Re(z)<0$, then we apply a second extended Fourier transform with respect to the variable k_h,

$$\begin{aligned}
&-\int_{-\infty}^{+\infty} e^{y\,k_h}\,\frac{1}{z}\,\mathbb{E}_t^T\left[(e^{\mathbf{X}(T)^\top C_h\mathbf{X}(T)+\mathbf{b}_h^\top\mathbf{X}(T)}-e^{k_h})^+\,e^{z\,(\mathbf{X}(T)^\top\Gamma\,\mathbf{X}(T)+\boldsymbol{\beta}^\top\mathbf{X}(T))}\right]\,dk_h\\
&=-\frac{1}{z}\,\mathbb{E}_t^T\left[\left(\int_{-\infty}^{+\infty} e^{y\,k_h}\,\left(e^{\mathbf{X}(T)^\top C_h\mathbf{X}(T)+\mathbf{b}_h^\top\mathbf{X}(T)}-e^{k_h}\right)\right.\right.\\
&\qquad\left.\left.I(\mathbf{X}(T)^\top C_h\mathbf{X}(T)+\mathbf{b}_h^\top\mathbf{X}(T)>k_h)\,dk_h\right)\,e^{z\,(\mathbf{X}(T)^\top\Gamma\,\mathbf{X}(T)+\boldsymbol{\beta}^\top\mathbf{X}(T))}\right].
\end{aligned}$$

The integral converges for $k_h \to -\infty$ if $Re(y) > 0$. Then the function $\psi(z, y)$ is in the form

$$\begin{aligned}\psi(z,y) &= \int_{-\infty}^{+\infty} dk \int_{-\infty}^{+\infty} dk_h \, e^{zk} e^{yk_h} \, f(k,k_h) \\ &= -\frac{\Phi(z\boldsymbol{\beta} + (y+1)\mathbf{b}_h, z\,\Gamma + (y+1)C_h)}{zy(y+1)}\end{aligned}$$

and it is defined for $Re(z) < 0$ and $Re(y) > 0$.
Finally, $f(k, k_h)$ is the inverse transform of $\psi(z, y)$ in the sense of a Cauchy principal value integral,

$$f(k,k_h) = \frac{1}{(i2\pi)^2} \lim_{\xi\to\infty} \lim_{\varsigma\to\infty} \int_{\delta-i\xi}^{\delta+i\xi} dz \, e^{-zk} \int_{\eta-i\varsigma}^{\eta+i\varsigma} dy \, e^{-yk_h} \psi(z,y),$$

where $\delta < 0$ and $\eta > 0$ are constants. Noting that $\psi(\delta + i\gamma, \eta + i\omega)$ is the double Fourier transform of the function $e^{\delta k} e^{\eta k_h} f(k, k_h)$, we obtain

$$f(k,k_h) = \frac{e^{-\delta k} e^{-\eta k_h}}{4\pi^2} \lim_{\xi\to\infty} \lim_{\varsigma\to\infty} \int_{-\xi}^{+\xi} d\gamma \, e^{-i\gamma k} \int_{-\varsigma}^{+\varsigma} d\omega \, e^{-i\omega k_h} \psi(\delta + i\gamma, \eta + i\omega),$$

where $\delta < 0$ and $\eta > 0$ are constants. The inner integral of the above formula is the Fourier transform of a real function, and so we can use the same symmetry properties explained in Appendix A.1 and we obtain

$$f(k,k_h) = \frac{e^{-\delta k} e^{-\eta k_h}}{2\pi^2} \lim_{\xi\to\infty} \int_0^{+\xi} d\gamma \, Re\left(e^{-i\gamma k} \lim_{\varsigma\to\infty} \int_{-\varsigma}^{+\varsigma} d\omega \, e^{-i\omega k_h} \psi(\delta + i\gamma, \eta + i\omega) \right).$$

A.3 Proof of the analytical lower bound for Gaussian affine models

Since $\mathbf{X}(T) \sim N(\boldsymbol{\mu}, V)$ in T-forward measure, then the approximate exercise region $\mathcal{G}$ becomes

$$\mathcal{G} = \{\omega \in \Omega : \boldsymbol{\beta}^\top \mathbf{X}(T) > k\} = \{\omega \in \Omega : z > d\},$$

where z is a standard normal random variable and $d = \frac{k - \boldsymbol{\beta}^\top \boldsymbol{\mu}}{\sqrt{\boldsymbol{\beta}^\top V \boldsymbol{\beta}}}$.
The lower bound expression can be written using the law of iterative expectation,

$$LB_{\boldsymbol{\beta}}(k;t) = P(t,T)\, \mathbb{E}_t^T \left[\mathbb{E}_t^T \left[\left(\sum_{h=1}^{n} w_h e^{\mathbf{b}_h{}^\top \mathbf{X}(T) + a_h} - 1 \right) | z \right] I(z > d) \right].$$

Conditionally to the random variable z, the variable $\mathbf{X}$ is distributed as a multivariate normal with mean and variance

$$\mathbb{E}_t^T[\mathbf{X}|z] = \boldsymbol{\mu} + z\,\mathbf{v} \text{ and } Var(\mathbf{X}|z) = V - \mathbf{v}\mathbf{v}^\top, \text{ with } \mathbf{v} = \frac{V\boldsymbol{\beta}}{\sqrt{\boldsymbol{\beta}^\top V \boldsymbol{\beta}}}.$$

We can now compute the inner expectation,

$$\begin{aligned} LB_{\boldsymbol{\beta}}(k;t) &= P(t,T)\left(\sum_{h=1}^{n} w_h\, \mathbb{E}_t^T\left[e^{a_h+\mathbf{b}_h^\top\boldsymbol{\mu}+z\mathbf{b}_h^\top\mathbf{v}+\frac{1}{2}V_h} I(z>d)\right] - \mathbb{E}_t^T\left[I(z>d)\right]\right) \\ &= P(t,T)\left(\sum_{h=1}^{n} w_h\, e^{a_h+\mathbf{b}_h^\top\boldsymbol{\mu}+\frac{1}{2}V_h+\frac{1}{2}d_h^2} N(d_h-d) - N(-d)\right). \end{aligned}$$

where $V_h = \mathbf{b}_h^\top(V-\mathbf{v}\mathbf{v}^\top)\mathbf{b}_h$, $d_h = \mathbf{b}_h^\top\mathbf{v}$ and $N(x)$ is the cumulative distribution function of standard normal variable. The proof for a payer swaption follows the same reasoning.

A.4 Proof of the upper bound formula for Gaussian affine models

Since $\mathbf{X}\sim\mathcal{N}(\boldsymbol{\mu},V)$ in T-forward measure and using the law of iterative expectations, then

$$\begin{aligned} & \mathbb{E}_t^T[(w_h e^{a_h+b_h^\top\mathbf{X}(T)}-K_h)^+ I(\beta^\top X<k)] \\ = \;& \mathbb{E}_t^T[\mathbb{E}_t^T[(w_h e^{a_h+b_h^\top\mathbf{X}(T)}-K_h)^+|Z]I(Z<d)], \\ & = \int_{-\infty}^{d} dz\,\frac{1}{\sqrt{2\pi}} e^{-\frac{z^2}{2}}\,\mathbb{E}_t^T[(w_h e^{a_h+\mathbf{b}_h^\top\mathbf{X}(T)}-K_h)^+|Z=z]. \end{aligned}$$

where $Z\sim\mathcal{N}(0,1)$ and $d=\frac{k-\beta^\top\mu}{\sqrt{\beta^\top V\beta}}$.
Since $\mathbf{b}_h^\top\mathbf{X}$ conditioned to the variable Z is a normal random variable with mean and variance,

$$\begin{aligned} &M_h = \mathbb{E}_t^T[\mathbf{b}_h^\top\mathbf{X}|Z=z] = \mathbf{b}_h^\top\boldsymbol{\mu}+z\mathbf{b}_h^\top\mathbf{v}, \\ &V_h = Var_t[\mathbf{b}_h^\top\mathbf{X}|Z=z] = \mathbf{b}_h^\top(V-\mathbf{v}\mathbf{v}^\top)\mathbf{b}_h \\ &\mathbf{v} = \frac{V\boldsymbol{\beta}}{\sqrt{\boldsymbol{\beta}^\top V\boldsymbol{\beta}}}, \end{aligned}$$

then the conditioned expectation can be evaluated with a Black formula,

$$\begin{aligned} &\mathbb{E}_t^T[(w_h e^{a_h+b_h^\top\mathbf{X}(T)}-K_h)^+|Z=z] \\ &= w_h e^{a_h}\left(e^{M_h+\frac{V_h}{2}} N\left(\frac{M_h-\log Y_h+V_h}{\sqrt{V_h}}\right) - Y_h N\left(\frac{M_h-\log Y_h}{\sqrt{V_h}}\right)\right), \end{aligned}$$

where $Y_h=\frac{K_h}{w_h e^{a_h}}$ and $N(x)$ is the cumulative distribution function of a standard normal variable.

Appendix B

Models description of Chapter 1

B.1 Affine Gaussian models

Affine Gaussian models assign the following stochastic differential equation (SDE) to the state variable $\mathbf{X}$,

$$d\mathbf{X}(t) = K(\boldsymbol{\theta} - \mathbf{X}(t))\, dt + \Sigma\, d\mathbf{W}(t) \quad \text{and} \quad \mathbf{X}(0) = \mathbf{x}_0$$

where $\mathbf{W}_t$ is a standard d-dimensional Brownian motion, K is a $d \times d$ diagonal matrix and Σ is a $d \times d$ triangular matrix. The short rate is obtained as a linear combination of the state vector $\mathbf{X}$; it is always possible to rescale the components $X_i(t)$ and assume that $r(t) = \phi + \sum_{i=1}^{d} X_i(t)$, $\phi \in \mathbb{R}$ without loss of generality.
The ZCB formula (1.5) and T-forward characteristic function (1.6) of $\mathbf{X}$ can be obtained in closed form using the moment-generating function of a multivariate normal variable or solving the ODE system in [Duffie et al., 2000], and the solution is given, for example, in [Collin-Dufresne and Goldstein, 2002].

B.2 Multi-factor CIR model

In this model, the risk-neutral dynamics of the state variates are

$$dX_i(t) \;=\; a_i(\,\theta_i - X_i(t))dt + \sigma_i \sqrt{X_i(t)} dW^i(t) \quad \text{and} \quad \mathbf{X}(0) = \mathbf{x}_0,$$

where $i = 1, ..., d$, $W^i(t)$ are independent standard Brownian motions, and a_i, θ_i and σ_i are positive constants. The short rate is obtained as $r(t) = \phi + \sum_{i=1}^{d} X_i(t)$, where $\phi \in \mathbb{R}$.
In multi-factor CIR models, the bond price (1.5) and the characteristic function (1.6) have closed-form expressions, which are given, for example, in [Collin-Dufresne and Goldstein, 2002].

B.3 Gaussian model with double exponential jumps

In this model, the risk-neutral dynamics of the state variates are

$$d\mathbf{X}(t) = K(\boldsymbol{\theta} - \mathbf{X}(t))\, dt + \Sigma\, d\mathbf{W}(t) + d\mathbf{Z}^{+}(t) - d\mathbf{Z}^{-}(t) \quad \text{and} \quad \mathbf{X}(0) = \mathbf{x}_0,$$

where $\mathbf{W}_t$ is a standard d-dimensional Brownian motion, K is a $d \times d$ diagonal matrix, Σ is a $d \times d$ triangular matrix and $\mathbf{Z}^{\pm}$ are pure jump processes whose jumps have fixed probability distribution ν on $\mathbb{R}^d$ and constant intensity $\mu^{\pm}$. The short rate is obtained as a linear combination of the state vector $\mathbf{X}$. In particular, $\mathbf{Z}^{\pm}$ are compounded Poisson processes with jump sizes that are exponentially distributed, i.e.

$$Z_l^{\pm} = \sum_{j=1}^{N^{\pm}(t)} Y_{j,l}^{\pm}$$

where $l = 1, ..., d$ is the factor index, $N^{\pm}(t)$ are Poisson processes with intensity $\frac{\mu^{\pm}}{d}$ and $Y_{j,l}^{\pm}$, for a fixed l, are independent identically distributed exponential random variables of mean parameters $m_l^{\pm}$.
Since $\mu^{\pm}$ do not depend on $\mathbf{X}$, we know that

$$\Phi(\boldsymbol{\lambda}) = \mathbb{E}_t^T \left[e^{\boldsymbol{\lambda}^\top \mathbf{X}(T)} \right] = \Phi^D(\boldsymbol{\lambda})\, e^{\tilde{A}^J(T-t,\boldsymbol{\lambda}) - A^J(T-t)} \tag{B.1}$$

where $\Phi^D(\boldsymbol{\lambda})$ is the T-forward characteristic function of the affine Gaussian model and the function $\tilde{A}^J(\tau, \boldsymbol{\lambda})$ is available in closed form (see [Duffie et al., 2000] for further details).

B.4 Gaussian quadratic model

In this model, the risk-neutral dynamics of the state variates are

$$d\mathbf{X}(t) = K(\boldsymbol{\theta} - \mathbf{X}(t))\, dt + \Sigma\, d\mathbf{W}_t \quad \text{and} \mathbf{X}(0) = \mathbf{x}_0,$$

where $\mathbf{W}_t$ is a standard d-dimensional Brownian motion, $\boldsymbol{\theta}$ is a d-dimensional constant vector, K and Σ are $d \times d$ matrix. The short rate is a quadratic function of the state variates, $r(t) = a_r + b_r^\top \mathbf{X}(t) + \mathbf{X}(t)^\top C_r \mathbf{X}(t)$, $a_r \in \mathbb{R}$, $b_r \in \mathbb{R}^d$ and C_r is a $d \times d$ symmetric matrix.
We solve the system of ordinary differential equation for the functions $\tilde{A}(\tau, \boldsymbol{\lambda}, \Lambda)$, $\tilde{\mathbf{B}}(\tau, \boldsymbol{\lambda}, \Lambda)$, $\tilde{C}(\tau, \boldsymbol{\lambda}, \Lambda)$ in formula (1.6), using the method proposed in [Cheng and Scaillet, 2007]. The closed-form evaluation of these functions proposed in [Cheng and Scaillet, 2007] requires the calculus of a matrix exponentiation and a numerical integration. However, numerical tests show that this method is much faster than numerically solving the ODE system using the Runge-Kutta or Dormand-Prince schemes.

Appendix C

Proofs of Chapter 2

C.1 Proof of Proposition 2.2.1

The proof is similar to the single-curve affine Gaussian case. As in that case, $\mathbf{X}(T) \sim N(\boldsymbol{\mu}, V)$ in T-forward measure and the approximate exercise region $\mathcal{G}$ becomes

$$\mathcal{G} = \{\omega \in \Omega : \boldsymbol{\beta}^\top \mathbf{X}(T) > k\} = \{\omega \in \Omega : z > d\},$$

where z is a standard normal random variable and $d = \frac{k - \boldsymbol{\beta}^\top \boldsymbol{\mu}}{\sqrt{\boldsymbol{\beta}^\top V \boldsymbol{\beta}}}$.
The lower bound expression can be written using the law of iterative expectation,

$$LB_{\boldsymbol{\beta}}(k;t) = P(t,T)\, \mathbb{E}_t^T \left[\mathbb{E}_t^T \left[\left(\sum_{j=1}^n w_{1j} e^{\mathbf{G}_{1j}{}^\top \mathbf{X}(T) + a_{1j}} - w_{2j} e^{\mathbf{G}_{2j}{}^\top \mathbf{X}(T) + a_{2j}} \right) |z \right] I(z > d) \right].$$

Conditionally to the random variable z, the variable $\mathbf{X}$ is distributed as a multivariate normal with mean and variance

$$\mathbb{E}_t^T[\mathbf{X}|z] = \boldsymbol{\mu} + z\,\mathbf{v} \text{ and } Var(\mathbf{X}|z) = V - \mathbf{v}\mathbf{v}^\top, \text{ with } \mathbf{v} = \frac{V\boldsymbol{\beta}}{\sqrt{\boldsymbol{\beta}^\top V \boldsymbol{\beta}}}.$$

We can now compute the inner expectation,

$$\begin{aligned} LB_{\boldsymbol{\beta}}(k;t) &= P(t,T) \left(\sum_{j=1}^n w_{1j}\, \mathbb{E}_t^T \left[e^{a_{1j} + \mathbf{G}_{1j}^\top \boldsymbol{\mu} + z \mathbf{G}_{1j}^\top \mathbf{v} + \frac{1}{2} V_{1j}^G} I(z > d) \right] \right. \\ &- \left. \sum_{j=1}^n w_{2j} \mathbb{E}_t^T \left[e^{a_{2j} + \mathbf{G}_{2j}^\top \boldsymbol{\mu} + z \mathbf{G}_{2j}^\top \mathbf{v} + \frac{1}{2} V_{2j}^G} I(z > d) \right] \right) \\ &= \sum_{j=1}^n w_{1j}\, e^{a_{1j} + \mathbf{G}_{1j}^\top \boldsymbol{\mu} + \frac{1}{2} V_{1j}^G + \frac{1}{2} d_{1j}^2} N(d_{1j} - d) - w_{2j}\, e^{a_{2j} + \mathbf{G}_{2j}^\top \boldsymbol{\mu} + \frac{1}{2} V_{2j}^G + \frac{1}{2} d_{2j}^2} N(d_{2j} - d). \end{aligned}$$

where $V_{ij}^G = \mathbf{G}_{ij}^\top (V - \mathbf{v}\mathbf{v}^\top) \mathbf{G}_{ij}$, $d_{ij} = \mathbf{G}_{ij}^\top \mathbf{v}$ and $N(x)$ is the cumulative distribution function of the standard normal variable. The proof for a receiver swaptions follows the same reasoning.

C.2 Proof of Proposition 2.3.1

The proof is similar to the single-curve affine Gaussian case except that instead of the Black formula, we apply Margrabe's formula ([Margrabe,]) for exchange options. Here, we show the computation of the quantity ϵ_1 defined in proposition (2.3.1). The evaluation of ϵ_2 follows the same steps. Since $\mathbf{X} \sim \mathcal{N}(\boldsymbol{\mu}, V)$ in T-forward measure and using the law of iterative expectations, then

$$\begin{aligned}
& \mathbb{E}_t^T[(w_{1j}\, e^{a_{1j}+G_{1j}^\top \mathbf{X}(T)} - \tilde{w}_{2j}\, e^{a_{2j}+G_{2j}^\top \mathbf{X}(T)})^+ I(\beta^\top X < k)] \\
= \;& \mathbb{E}_t^T[\mathbb{E}_t^T[(w_{1j}\, e^{a_{1j}+G_{1j}^\top \mathbf{X}(T)} - \tilde{w}_{2j}\, e^{a_{2j}+G_{2j}^\top \mathbf{X}(T)})^+ | Z] I(Z < d)], \\
& = \int_{-\infty}^{d} dz\, \frac{1}{\sqrt{2\pi}} e^{-\frac{z^2}{2}}\, \mathbb{E}_t^T[(w_{1j}\, e^{a_{1j}+G_{1j}^\top \mathbf{X}(T)} - \tilde{w}_{2j}\, e^{a_{2j}+G_{2j}^\top \mathbf{X}(T)})^+ | Z = z].
\end{aligned}$$

where $Z \sim \mathcal{N}(0,1)$ and $d = \frac{k-\beta^\top \mu}{\sqrt{\beta^\top V \beta}}$.
$\mathbf{G}_{ij}^\top \mathbf{X}$ conditioned to the variable Z is a normal random variable with mean and variance

$$\begin{aligned}
M_{ij} &= \mathbb{E}_t^T[\mathbf{G}_{ij}^\top \mathbf{X} | Z = z] = \mathbf{G}_{ij}^\top \boldsymbol{\mu} + z \mathbf{G}_{ij}^\top \mathbf{v}, \\
V_{ij}^G &= Var_t[G_{ij}^\top \mathbf{X} | Z = z] = G_{ij}^\top (V - \mathbf{v}\mathbf{v}^\top) G_{ij} \\
\mathbf{v} &= \frac{V\boldsymbol{\beta}}{\sqrt{\boldsymbol{\beta}^\top V \boldsymbol{\beta}}}.
\end{aligned}$$

Hence, considering for each fixed j the following two underlying variables

$$\begin{aligned}
S_{1j} &= w_{1j}\, e^{a_{1j}+G_{1j}^\top \mathbf{X}(T)}, \\
S_{2j} &= \tilde{w}_{2j}\, e^{a_{2j}+G_{2j}^\top \mathbf{X}(T)},
\end{aligned}$$

the conditional expectation can be evaluated with the Margrabe formula

$$\begin{aligned}
& \mathbb{E}_t^T[(w_{1j}\, e^{a_{1j}+G_{1j}^\top \mathbf{X}(T)} - \tilde{w}_{2j}\, e^{a_{2j}+G_{2j}^\top \mathbf{X}(T)})^+ | Z = z] \\
= \;& w_{1j}\, e^{a_{1j}+M_{1j}+\frac{1}{2}V_{1j}^G}\, N(d_{1j}) - \tilde{w}_{2j}\, e^{a_{2j}+M_{2j}+\frac{1}{2}V_{2j}^G}\, N(d_{2j}), \\
d_{1j} &= \frac{\log\left(\frac{w_{1j}}{\tilde{w}_{2j}}\right) + M_{1j} + a_{1j} - M_{2j} - a_{2j} + V_{1j}^G - Cov_j}{\sqrt{V_{1j}^G + V_{2j}^G - 2Cov_j}}, \\
d_{2j} &= d_{1j} - \sqrt{V_{1j}^G + V_{2j}^G - 2Cov_j},
\end{aligned}$$

where $Cov_j = G_{1j}^\top (V - vv^\top) G_{2j}$ for $i = 1, 2$ and $j = 1, ..., d$ and $N(x)$ is the standard Gaussian cumulative distribution function.

Appendix D

Parameters values - Chapter 1 and 2

Three-factors Gaussian model and Cox–Ingersoll–Ross model
We verify the accuracy of our bounds using models and parameter values that have already been examined in the literature[1]

- Three-factor Gaussian model: $K = \begin{bmatrix} 1.0 & 0 & 0 \\ 0 & 0.2 & 0 \\ 0 & 0 & 0.5 \end{bmatrix}$, $\theta = [0, 0, 0]^\top$, $\boldsymbol{\sigma} = [0.01, 0.005, 0.002]^\top$, $\rho = \begin{bmatrix} 1 & -0.2 & -0.1 \\ -0.2 & 1 & 0.3 \\ -0.1 & 0.3 & 1 \end{bmatrix}$, Σ = diag($\boldsymbol{\sigma}$) chol(ρ)[2], $x_0 = [0.01,\ 0.005,\ -0.02]^\top$ and ϕ = 0.06;
- Two-factor Cox-Ingersoll–Ross model: $\mathbf{a} = [0.5080, -0.0010]^\top$, $\boldsymbol{\theta} = [0.4005, -0.7740]^\top$, $\boldsymbol{\sigma} = [0.023,\ 0.019]^\top$, $x_0 = [0.374,\ 0.258]^\top$ and ϕ = -0.58.

Numerical results for this model are shown in Tables 1.1 and 1.6.
Moreover, we specify the interval of parameters of the two-factor CIR model from which we extract the 100 parameters sets for the RMSD calculation: $x_0 \in [0.001, 0.5] \times [0.001, 0.5]$, $\phi \in [0.001, 1]$, $\mathbf{a} \in [0.001, 1] \times [0.001, 1]$, $\boldsymbol{\theta} \in [0.001, 1] \times [0.001, 1]$, $\boldsymbol{\sigma} \in [0.001, \sqrt{2a(1)\theta(1)}] \times [0.001, \sqrt{2a(2)\theta(2)}]$.

Two-factor Gaussian model with double exponential jumps
We test the affine Gaussian model with exponentially distributed jumps using parameter values obtained by minimization of the least square distance between the model and the market discount curve implied by bootstrapping the Euribor six-month swap curve up to 30 years. The calibration is performed on January 4^{th}, 2015, to obtain the parameters set reported below.
Parameters:

[1] [Schrager and Pelsser, 2006] and [Duffie and Singleton, 1997] for the two-factor CIR model.
[2] diag($\boldsymbol{\sigma}$) means the diagonalization of the vector $\boldsymbol{\sigma}$ and chol(ρ) means the Cholesky decomposition of the correlation matrix ρ, where $\boldsymbol{\sigma}$ and ρ are the volatility vector and the correlation matrix, respectively, of the original paper.

- Gaussian parameters: $K = \begin{bmatrix} 0.050926 & 0 \\ 0 & 1.3687 \end{bmatrix}$, $\theta = [0, 0]^\top$, $\boldsymbol{\sigma} = [0.0048887, 0.24025]^\top$, $\rho = \begin{bmatrix} 1 & -0.1482 \\ -0.1482 & 1 \end{bmatrix}$, Σ = diag($\boldsymbol{\sigma}$) chol(ρ), $x_0 = [0.00035256,\ 0.00035497]^\top$ and ϕ = 4.332 $\times 10^{-5}$;
- Jump parameters: $\boldsymbol{\mu}^+$ = 0.4372, $\mathbf{m}^+ = [0.027372, 0.045667]^\top$, $\boldsymbol{\mu}^-$ = 0.1101, $\mathbf{m}^- = [0.027043, 0.012339]^\top$.

Figure 3 shows fitting of the calibration. Numerical results for this model are shown in Tables 1.7-1.9.

[Figure 3 approximately here]

Two-factor quadratic Gaussian model

Beyond the affine framework, we test the two-factor quadratic Gaussian model using the following parameter values as proposed by [Kim, 2007]:
$K = \begin{bmatrix} -0.0541 & 0.0361 \\ -1.2113 & 0.4376 \end{bmatrix}$,
$\theta = [0.1932,\ 0.1421]^\top$, $\Sigma = \begin{bmatrix} 0.0145 & 0 \\ 0 & 0.0236 \end{bmatrix}$, $x_0 = [0.1690,\ -0.0501]^\top$,
a_r = 0.0444, $b_r = [0,\ 0]^\top$ and $C_r = \begin{bmatrix} 1 & 0.4412 \\ 0.4412 & 1 \end{bmatrix}$; Numerical results for this model are shown in Tables 1.10-1.12.

Multiple-curve two-factor Gaussian model

We verify the accuracy of our bounds using the following fixed parameters:
$\lambda = [0.0073, 4.7344]$, $\eta = [0.1581, 0.8894]$, $h = [0.0059, 0.0411]$, $\rho_{12} = -0.8577$, $\beta_0 = 1.3160$, $\beta_1 = 1.3327$ and $\beta_2 = 0.5900$. Numerical results for this model are shown in Tables 2.2-2.4.

Appendix E

Appendices - Chapter 3

E.1 Martingales: change of time and change of measure

In most of the practical cases, it is true that the time change does not affect the martingale property. However this is not a trivial consequence of the optional stopping theorem. This is why the optional stopping theorem requires the boundedness of the stopping time or the uniform integrability of the initial martingale. As we see in the previous section the random time change is a family of almost surely finite, but not bounded, stopping times. Moreover the uniform integrability is a strong requirement that is not easy to ensure (See [Kallsen and Shiryaev., 2002a] or [Criens et al., 2015]). In this section we investigate the sufficient conditions to guaranteed that a time-changed martingale is again a martingale without the two previously mentioned hypothesis.
First it is useful to connect the martingale property with the change of measure toolkit.
Consider a filtered space $(\Omega, \mathcal{F})$ and two measures, $\mathbb{P}$ and $\mathbb{Q}$, defined on it. $\mathbb{P}$ is a probability measure, instead $\mathbb{Q}$ can be a probability measure or a complex measure.

Definition E.1.1. The measure $\mathbb{Q}$ is said to be locally absolutely continuous with respect to $\mathbb{P}$ and we write $\mathbb{Q} \overset{\text{loc}}{\ll} \mathbb{P}$, if $\mathbb{Q}_t \ll \mathbb{P}_t \ \forall t \in \mathbb{R}^+$, where $\mathbb{P}_t$ and $\mathbb{Q}_t$ are the restriction of the measures on $\mathcal{F}_t$.[1]

Definition E.1.2. If $\mathbb{Q} \overset{\text{loc}}{\ll} \mathbb{P}$, we define the Radon-Nikodyn derivative as the random variable

$$Z = \frac{d\mathbb{Q}}{d\mathbb{P}}$$

and the density process is defined as

$$Z(t) = \left.\frac{d\mathbb{Q}}{d\mathbb{P}}\right|_{\mathcal{F}(t)}.$$

The link between change of measures and martingales is given by the following proposition.

[1] If $\mathbb{Q} \overset{\text{loc}}{\ll} \mathbb{P}$ and $\mathbb{Q}_\infty \ll \mathbb{P}_\infty$, then $\mathbb{Q} \ll \mathbb{P}$.

Proposition E.1.3 ([Jacod, 1979] Proposition 7.14)**.** *The following statements are equivalent:*

(i) $\mathbb{Q} \overset{loc}{\ll} \mathbb{P}$,

(ii) Z *is a* $\mathbb{P}$*-martingale and* $\mathbb{E}[Z(0)] = 1$.

Now we are interested in the behaviour of the process $Z(t)$, when we introduce a stopping time. A relatively well known result concerning the relationship between change of measures and stopping time, is the following.

Proposition E.1.4. *If* $\mathbb{Q} \overset{loc}{\ll} \mathbb{P}$ *and* T *is a* $\mathcal{F}$*-stopping time then*

$$\mathbb{Q}(A \cap \{T < \infty\}) = \int_{A \cap \{T < \infty\}} Z(T)\, d\mathbb{P} \tag{E.1}$$

for each $A \in \mathcal{F}$*, i.e. with restriction to the set* $\{T < \infty\}$, $\mathbb{Q}_T \ll \mathbb{P}_T$ *and*

$$Z(T) = \left.\frac{d\mathbb{Q}}{d\mathbb{P}}\right|_{\mathcal{F}(T)}.$$

The previous proposition is presented in different books, we cite some of them for interested readers: [Revuz and Yor, 1998] (Proposition VIII.1.3) and [Jacod and Shiryaev, 2002] (Theorem III.3.4).
Now we derive a straightforward, but important, application of the results previously presented.

Corollary E.1.5. *Let* $\tau(t)$ *be a time change as defined in section 3.1 and* $\mathbb{Q} \overset{loc}{\ll} \mathbb{P}$ *with respect to the filtration* $\mathcal{F}$*.*
If $\forall t \in \mathbb{R}^+\ \mathbb{Q}(\tau(t) = \infty) = 0$*, then the process*

$$M(t) := Z(\tau(t)) = \left.\frac{d\mathbb{Q}}{d\mathbb{P}}\right|_{\mathcal{G}(t)}, \tag{E.2}$$

is a $\mathbb{P}$*-martingale respect to the time-changed filtration* $\mathcal{G} = (\mathcal{F}_{\tau(t)})_{t \geq 0}$.

Proof
For each fixed $t \in \mathbb{R}^+$, $\mathbb{Q}_{\tau(t)} \ll \mathbb{P}_{\tau(t)}$, by proposition E.1.4, and the restriction to the set $\{\tau(t) < \infty\}$ is negligible since $\tau(t)$ is finite $\mathbb{P}$-almost surely and $\mathbb{Q}$-almost surely. Hence $\mathbb{Q} \overset{\text{loc}}{\ll} \mathbb{P}$ on the time-changed filtration $\mathcal{G} = (\mathcal{F}_{\tau(t)})_{t \geq 0}$, by definition. Finally due to the equivalence in proposition E.1.3, the density process $Z(\tau(t))$ is a martingale on $(\Omega, \mathcal{G}, \mathbb{P})$. □

Now, for clarity, we resume the results and we explained what happens in practice.

- We start with a $\mathbb{P}$-martingale Z such that $\mathbb{E}[Z(0)] = 1$,
- then Z "induces" a new measure $\mathbb{Q}$ that is locally absolutely continuous respect to $\mathbb{P}$,

- if the time change $\tau(t)$ is finite $\mathbb{Q}$-almost surely then we known that the time-changed process, $M(t) = Z(\tau(t))$, is again a martingale.

Remark E.1.6. It is useful to note that the starting measure $\mathbb{P}$ is always a a probability measure (a real positive finite measure), instead $\mathbb{Q}$ is a measure that can be complex. $\mathbb{Q}$ can be (locally) absolutely continuous respect to $\mathbb{P}$, but if it is complex then the vice-versa does not make sense. This means that, if $\mathbb{Q}$ is complex, $\mathbb{P}$ and $\mathbb{Q}$ can not be (locally) equivalent and the change of measure makes sense only in one way, from $\mathbb{P}$ to $\mathbb{Q}$. Instead if $\mathbb{Q}$ is a probability measure and $\mathbb{Q} \overset{\text{loc}}{\sim} \mathbb{P}$ (i.e.$\mathbb{Q} \overset{\text{loc}}{\ll} \mathbb{P}$ and $\mathbb{P} \overset{\text{loc}}{\ll} \mathbb{Q}$), then Z and $\frac{1}{Z}$ are real strictly positive martingales and $\frac{1}{Z}$ is the Radon-Nikodyn derivative of $\mathbb{P}$ respect to $\mathbb{Q}$.

Remark E.1.7. In practical cases $\tau(t)$ is modelled as a $\mathbb{P}$-semimartingale. The Girsanov theorem for semimartingales asserts that, if $\mathbb{Q} \overset{\text{loc}}{\ll} \mathbb{P}$ with Radon-Nikodyn derivative Z, then $\tau(t)$ is a $\mathbb{Q}$-semimartingale and more important the new semimartingale characteristic is $\mathbb{Q}$-almost surely finite valued, as observed in [Jacod and Shiryaev, 2002] (theorem 3.24, pages 172-173).

E.2 Integrated time-changed Lévy processes

We are interested in studying the behaviour of the process

$$M_\theta(t) = e^{i\theta \int_0^t f(s)\, dY(s) - \int_0^t \psi(\theta f(s))\, v(s_-)\, ds}, \tag{E.3}$$

where $\theta \in \mathbb{C}$, $Y = X(\tau)$ is a time changed Lévy process, $\tau(t) = \int_0^t v(s_-)ds$, $\psi()$ is the characteristic exponent of X analytically extended to $\mathbb{C}$ and $f : \mathbb{R} \to \mathbb{R}$ is a continuous deterministic function. For instance, the density process in equation 3.9 is modelled as $M_i(t)$, where $f(s) = \Sigma(s, T)$ represents the volatility function.
Our aim is to prove that M_θ is a $\mathbb{P}$-martingale. In Appendix E.1, we prove that a time-changed martingale is again a martingale. In the following, we summarize the main results concerning time-changed martingale:

- If a process, Z, is a $\mathbb{P}$-martingale such that $\mathbb{E}[Z(0)] = 1$, then it "induces" a new measure $\mathbb{Q}$ that is locally absolutely continuous respect to $\mathbb{P}$.

- If the time change $\tau(t)$ is finite $\mathbb{Q}$-almost surely, i.e. $\mathbb{Q}(\tau(t) = \infty) = 0$, then we know that the time-changed process, $M(t) = Z(\tau(t))$, is again a $\mathbb{P}$-martingale.

- Moreover, if $\tau(t)$ is modelled as a $\mathbb{P}$-semimartingale, the technical condition $\mathbb{Q}(\tau(t) = \infty) = 0$ is not a real constraint. In fact the Girsanov theorem for semimartingales guarantees the finiteness of τ (see Remark E.1.7).

In order to show that M_θ is a time-changed martingale, we require the existence of a process Z_θ such that $M_\theta = Z_\theta(\tau)$ and Z_θ is a martingale.
Hence, we need the following result about the change of variable for stochastic integrals.

Proposition E.2.1. *Let X be a $\mathcal{F}$-semimartingale. Let τ be a continuous and strictly positive $\mathcal{F}$-time change. $\widehat{\tau}$ is the right inverse of τ. If $H \in L(\mathcal{G}, X(\tau))$, where $\mathcal{G}_t = \mathcal{F}_{\tau(t)}$, then $H(\widehat{\tau}-) \in L(\mathcal{F}, X)$. Moreover, for all $t \geq 0$*

$$\int_0^t H(s)\, dX(\tau(s)) = \int_0^{\tau(t)} H(\widehat{\tau}(s_-))\, dX(s), \tag{E.4}$$

with probability one.

Now we have to give a rigorous definition of the right-inverse of a time change, we refer the interested reader to [Barndorff-Nielsen and Shiryaev, 2015].

Definition E.2.2. Given a random time change $\tau(t)$, its right-inverse is the process defined by

$$\widehat{\tau}(s) = \inf\{t \geq 0 : \tau(t) > s\}.$$

Lemma E.2.3 ([Barndorff-Nielsen and Shiryaev, 2015]). *Let $A = (A(t))_{t\geq 0}$ be a $\mathcal{F}$-adapted right-continuous random process with $A(0) = 0$ and*

$$\widehat{\tau}(s) = \inf\{t \geq 0 : A(t) > s\}.$$

The family of random variable $\widehat{\tau} = (\widehat{\tau}(s))_{s\geq 0}$ constitutes a time-change.

Since $\tau(t)$ is a RCLL increasing process then the family of random variables $(\widehat{\tau}(s))_{s\geq 0}$ is a random time change with respect to the time-changed filtration $\mathcal{G}$. Moreover, if τ is continuous and strictly increasing, we have the following result.

Lemma E.2.4 ([Barndorff-Nielsen and Shiryaev, 2015]). *If $\tau(t)$ is continuous and strictly positive then*

- *$\widehat{\tau}(\tau(t)) = t$ and $\tau(\widehat{\tau}(s)) = s$,*

- *$\widehat{\tau}(s) = \tau^{-1}(s)$ and $\tau(t) = \widehat{\tau}^{-1}(t)$.*

Further, if T is a $\mathcal{F}$-stopping time then $\mathcal{F}_T = \mathcal{G}_{\widehat{\tau}(T)} = \mathcal{F}_{\tau(\widehat{\tau}(T))}$.

Now we have all the elements to prove the proposition E.2.1.
Proof of Proposition E.2.1
By Lemma E.3.1, $Y := X(\tau)$ is a $\mathcal{G}$-semimartingale. $\widehat{\tau}$ is a $\mathcal{G}$-time change. Since τ is continuous ($\tau(t) = \tau(t_-)$), for any $s > 0$

$$Y(\widehat{\tau}(s)) = X(\tau(\widehat{\tau}(s))) = X(\tau(\widehat{\tau}(s)_-)) = X(\tau(\widehat{\tau}(s_-))) = Y(\widehat{\tau}(s_-)).$$

Thus, Y is $\widehat{\tau}$-adapted. Let $H \in L(\mathcal{G}, X(\tau))$, from proposition E.3.2 $H(\widehat{\tau}-) \in L(\widehat{\mathcal{G}}, X)$, where $\widehat{\mathcal{G}}_t = \mathcal{G}_{\widehat{\tau}(t)}$. Since τ is continuous and strictly positive, then by Lemma E.2.4 $\widehat{\mathcal{G}} = \mathcal{F}$. Thus, $H(\widehat{\tau}-) \in L(\mathcal{F}, X)$. By proposition E.3.2, with probability one

$$\begin{aligned}
&\int_0^{\widehat{\tau}(t)} H(s)\, dY(s) = \int_0^t H(\widehat{\tau}(s_-))\, dY(\widehat{\tau}(s)) \\
&= \int_0^t H(\widehat{\tau}(s_-))\, dX(\tau(\widehat{\tau}(s))) = \int_0^t H(\widehat{\tau}(s_-))\, dX(s)
\end{aligned}$$

for all $t \geq 0$. The last passage derives from the fact that τ is continuous and therefore $\tau(\widehat{\tau}(t)) = t$ almost surely
Hence, with probability one,

$$\int_0^{\widehat{\tau}(\tau(t))} H(s)\, dY(s) = \int_0^{\tau(t)} H(\widehat{\tau}(s_-))\, dX(s).$$

Since Y is $\widehat{\tau}$-adapted, i.e. Y is constant in $[\widehat{\tau}(t_-), \widehat{\tau}(t)]$, then $\int_0^{\cdot} H(s)dY(s)$ is $\widehat{\tau}$-adapted.
By Lemma E.2.4 $\widehat{\tau}(\tau(t)) = t$, consequently

$$\int_0^{\widehat{\tau}(\tau(t))} H(s)\, dY(s) = \int_0^{t} H(s)\, dY(s).$$

Hence the thesis is proved. □

If τ is continuous and strictly increasing (i.e. v strictly positive), we apply Proposition E.2.1 to the exponent of M_θ (formula E.3) to obtain

$$M_\theta(t) = Z_\theta(\tau(t)) \quad \text{and} \quad Z_\theta(t) = e^{i\theta \int_0^t f(\widehat{\tau}(s_-))\, dX(s) - \int_0^t \psi(\theta f(\widehat{\tau}(s_-)))\, ds}. \tag{E.5}$$

As $f(\widehat{\tau}-)$ is a $\mathcal{F}$-predictable process with continuous paths, we can apply the following proposition, deduced from [Raible, 2000].

Proposition E.2.5. *Let X be a Lévy process satisfying Assumption 3.1.1. Let H be an adapted process with left continuous paths such that it takes value in $[-M_1, M_2] \subset \mathbb{R}$. Define the set*

$$\Theta := \{\theta \in \mathbb{C} : -(1+\epsilon)\min\left(\frac{M_1}{M_2}, \frac{M_2}{M_1}\right) < -Im(\theta) < 1+\epsilon\}.$$

If $\theta \in \Theta$, then the process

$$Z_\theta(t) = e^{i\theta \int_0^t H(s)dX(s) - \int_0^t \psi(\theta H(s))ds}$$

is a martingale, where ψ is the characteristic exponent of X.

Remark E.2.6. Since $\theta = -i$ always belongs to Θ, then

$$Z_{-i}(t) = e^{\int_0^t H(s)dX(s) - \int_0^t \psi(-iH(s))ds} = e^{\int_0^t H(s)dX(s) - \int_0^t \kappa(H(s))ds}$$

is a martingale.

Identifying $f(\widehat{\tau}-)$ with the process H of Proposition E.2.5, we can conclude that if f is bounded and $\bar{f} = \sup_{t\geq 0} \mid f(t) \mid \leq \min(M_1, M_2)$, then Z_θ is a martingale on the probability space $(\Omega, \mathcal{F}, \mathbb{P})$.
So Z_θ induces a new measure $\mathbb{Q}^\theta \overset{\text{loc}}{\ll} \mathbb{P}$ and by Corollary E.1.5, we know that if $\mathbb{Q}^\theta(\tau = \infty) = 0$, then M_θ is a martingale respect to $(\Omega, \mathcal{G}, \mathbb{P})$.
As previously mentioned, the finiteness of τ under $\mathbb{Q}^\theta$ is guaranteed by the Girsanov theorem for semimartingales.

E.3 Useful literature results

We report useful literature results for the reader's convenience.

Proposition E.3.1 ([Kallsen and Shiryaev., 2002b], Lemma. 2.7)**.** *Let τ be a time change. Let Z be a $\mathcal{F}$-semimartingale and τ-adapted*[2]*, i.e. for any $t \geq 0$, Z is constant on $[\tau(t_-), \tau(t)]$. If (B, C, ν) is the characteristic of Z, then $Y = Z(\tau)$ is a martingale respect to the filtration $\mathcal{G}$, where $(\mathcal{G}_t)_{t\geq 0} = (\mathcal{F}_{\tau(t)})_{t\geq 0}$, with characteristic (B^Y, C^Y, ν^Y) defined as*

$$B^Y(t) = B(\tau(t)),\ \ C^Y(t) = C(\tau(t)) \text{ and } \mathbb{I}_{\mathbf{E}} * \nu^Y_t = \mathbb{I}_{\mathbf{E}} * \nu_{\tau(t)}$$

where $t \in \mathbb{R}_+$, $\mathbf{E} \in \mathcal{B}^d$. [3]

Proposition E.3.2 ([Jacod, 1979], Prop. 10.21)**.** *Let τ be a time change. Let Z be a $\mathcal{F}$-semimartingale and τ-adapted. If $H \in L(Z, \mathcal{F})$ (i.e. H is a $\mathcal{F}$-predictable process integrable respect to the semimartingale Z), then $H(\tau-) \in L(Z(\tau), \mathcal{G})$. Moreover with probability one, for all $t \geq 0$:*

$$\int_0^{\tau(t)} H(s)\, dZ(s) = \int_0^t H(\tau(s_-))\, dZ(\tau(s)). \tag{E.6}$$

Remark E.3.3. An important observation is that every stochastic process is τ-adapted, if τ belongs to the class of *absolutely continuous time changes*. If τ is defined through the path-wise integral of an intensity as in equation (3.3), then it is absolutely continuous.

Proposition E.3.4. *([Raible, 2000] Prop. 7.8) Let H be a predictable bounded process and let X be a Lévy process. For each $u \in \mathbb{R}$, the process*

$$Z_u(t) = e^{iu\int_0^t H(s)dX(s) - \int_0^t \psi(uH(s))ds}$$

is a martingale, where ψ is the characteristic exponent of X.

[2] In literature are common also the expressions τ-continuous or τ-synchronized.

[3] $\mathcal{B}^d$ is the Borel sigma algebra of $\mathbb{R}^d$.

Appendix F

Appendices - Chapter 4

F.1 Segregated fund accounting rules

In this section we describe briefly how the performance of fixed income securities (coupon bonds) is calculated in case of Italian segregated funds. More information can be found in the book [Corvino, 2003]. Similar rules are applied to traditional saving and pension products also by other countries in continental Europe (e.g. France, Germany; see [Therond, 2008] or [PWC, 2010]).
The components of the accounting performance are the determination of the bond current (periodical) income and the average book value.
A bond's current income is made of the following elements:

- coupons paid during the year or calculation period,
- difference between initial and final accrued interests, during the calculation period,
- amortisation,
- any realized gain or loss due to sales of part or all the quantity in position,
- any realized gain or loss at a bond's maturity date.

The amortisation depends on the classification the bond receives when it is purchased. The same asset can have more than one classification in the same segregated fund. Admissible classifications are of two types: Immobilised, or Available for Sales. When a bond is classified as immobilised it cannot be sold before maturity and the difference between price paid when the asset was purchased and its value at maturity (reimbursement) can be amortised linearly every year. If instead a bond is classified as available for sales, the bond can be sold at any time, but only the difference between issue price and reimbursement price can be amortized. Therefore, a remarkable characteristic of assets classified as available for sale within a segregated fund, is that in case they are purchased above par, the difference between the face value and the price is accounted as a loss (negative income or a cost) when the bond matures. Obviously, the same applies with opposite sign when assets are purchased below par.

In order to calculate the statutory accounting return or performance, the income assessed during the calculation period has to be divided by the average book value. The average book value is the time weighted average of the book values of the assets in position during the calculation period. A numerical example may help understanding. Let us assume the calculation period is one year, that a bond with a notional of 1000 Euro is purchased at a price of 100 at the beginning of the year and then another bond of the same type with a notional of 1000 Euro is bought at a price of 110 after 6 months and hold until year's end. Then the average book value is $1000\,0.5 + 2100\,0.5 = 1550$.
For those that have some knowledge of financial assets performance measurement, this is a way to compute a money weighted performance.

F.2 EIOPA curve construction

In this Appendix, for aim of completness, we describe the procedure to obtain the regulatory-specific risk free curve. Our presentation is based on the EIOPA official technical documentation as of May, 30 2016 ([EIOPA, 2016]).
EIOPA curve is based on the bootsrapping of the 6 months Euro swap rates from 1 year maturity onwards.
The credit risk adjustment (CRA) is applied trough a parallel downward shift of the observed par swap rates. For the Euro curve, the CRA is the difference between the 3 months OIS rate and the 3 months Euro swap rate, in spite of the fact that in the technical documentation is said "*The maturity of the OIS rate used to derive the CRA is consistent with the tenor of the floating legs of the swap instruments used to derive the term structure.*"
After the CRA, a Smith-Wilson method (described in details in EIOPA technical documentation) is used to extrapolate forward rates between a maturity of 20 years (the "last liquid point") and a maturity of 60 years (the "convergence point"). The one-year zero-coupon forward rate is assumed to converge towards a Ultimate Forward Rate (UFR), that for the Euro zone is settled equal to 4.2%. As specified in the documentation: "*The control input parameters for the interpolation and extrapolation are the last liquid point, ultimate forward rate (UFR), the convergence point and the convergence tolerance.*"
Finally, a Volatility Adjustment (VA) treatment is applied on the ZCB curve. The VA is published by EIOPA at least on a quarterly basis for each relevant currency. The technical documentation defines the VA in the following way: "*The volatility adjustment (VA) is an adjustment to the relevant risk-free interest rate term structure. The VA is based on 65% of the risk-corrected spread between the interest rate that could be earned from bonds, loans and securitisations included in a reference portfolio and the basic risk-free interest rates.*"
As highlighted in [Karoui et al., 2015], the two adjustments, CRA and VA, create a market consistency issue of the curve. In particular, it is not clear why the CRA for the Euro currency is based on a different tenor with respect to the swap curve. In addition, after the VA correction the curve is no more risk free, since this adjustment contains the credit and liquidity risk of bonds loans and securization.

F.3 Calibration procedure

The calibrations are performed through the minimization of the sum of squared differences between model and market data as follows:

$$\min_{\Theta} \frac{\sum_{n=1}^{N}(Market_n - Model_n(\Theta))^2}{N},$$

where N is the number of available market quotations, $Market_n$ and $Model_n$ are the market and the model quantities, respectively, and Θ is the vector of the model parameters.
Once we have calibrated the model, for each curve, we report the root mean square deviation (RMSD) and the maximum relative error (MRE), defined as follows

$$\begin{aligned} RMSD &= \frac{1}{\sqrt{N}}\sqrt{\sum_{n=1}^{N}(Market_n - Model_n^*)^2} \\ MRE &= \max_{n=1,\dots,N} \frac{\mid Market_n - Model_n^* \mid}{Market_n} \end{aligned}$$

where $Model_n^*$ is the model quantity calculated in correspondence of the optimal parameters vector, Θ^*.
The market quantities used for calibration purpose are ZCB prices for the Eonia and sovereign bonds curves, and CDS quotes.
The calibration is performed in three steps; firstly a Vasicek model is calibrated on the Eonia ZCB curve, secondly a CIR model is calibrated on the survival probability curve, finally the liquidity parameters (Vasicek) are calibrated on the sovereign or corporate ZCB curve, fixing the other parameters previously obtained.
We report the explicit form of the historical correlation estimated between the liquidity spreads through the procedure described in section 4.2.1:

$$\rho_l^H = Corr(dl^1(t), dl^2(t)) = \rho_l \frac{1 - e^{-(k_1+k_2)dt}}{\sqrt{(1 - e^{-2k_1 dt})(1 - e^{-2k_2 dt})}} \frac{2\sqrt{k_1 k_2}}{k1 + k2} \tag{F.1}$$

where ρ_l is the correlation between the two Brownian motions. Hence, the estimated correlation is not exactly equal to the model correlation. However, for small dt the difference between the two correlations goes to zero, for this reason we choose historical series of daily returns.
We do not have an explicit formula for the correlation between credit spreads, but the procedure of the estimation follows similar reasoning.

F.4 Market data

We report market data on March 30, 2016 used for calibrating the model. Market data are taken from the provider Bloomberg.

Maturity	Mid swap rate (%)	Maturity	Mid swap rate (%)
04-Apr-16	-0.3470	03-Apr-18	-0.4106
08-Apr-16	-0.3574	01-Oct-18	-0.3908
15-Apr-16	-0.3555	01-Apr-19	-0.3813
02-May-16	-0.3482	01-Apr-20	-0.3315
01-Jun-16	-0.3503	01-Apr-21	-0.2548
01-Jul-16	-0.3507	01-Apr-22	-0.1547
01-Aug-16	-0.3645	03-Apr-23	-0.0437
01-Sep-16	-0.3690	02-Apr-24	0.0724
03-Oct-16	-0.3696	01-Apr-25	0.1819
01-Nov-16	-0.3724	01-Apr-26	0.2855
01-Dec-16	-0.3760	01-Apr-27	0.3655
02-Jan-17	-0.3816	03-Apr-28	0.4624
01-Feb-17	-0.3860	01-Apr-31	0.6499
01-Mar-17	-0.3936	01-Apr-36	0.8062
03-Apr-17	-0.3982	01-Apr-41	0.8659
02-Oct-17	-0.4067	02-Apr-46	0.8818

Table F.1: Term Structure of zero rates from EONIA swap market quotes on March 30, 2016.

CDS Germany		CDS Italy	
tenor (year)	spread (bps)	tenor (year)	spread (bps)
0.5	5.29	0.5	28.45
1.0	5.44	1	36.00
2.0	6.71	2	67.06
3.0	8.94	3	86.62
4.0	14.86	4	114.10
5.0	18.38	5	122.36
7.0	27.01	7	150.81
10.0	38.54	10	186.00

Table F.2: Term Structure of German and Italian CDS spreads on March 30, 2016.

German sovereign curve		Italian sovereign curve	
tenor	yield(%)	tenor	yield (%)
0.25	-0.504	0.25	-0.166
0.5	-0.422	0.5	-0.053
1	-0.460	1	-0.058
2	-0.481	2	-0.002
3	-0.469	3	0.093
4	-0.426	4	0.230
5	-0.361	5	0.396
7	-0.183	7	0.772
8	-0.079	8	0.965
9	0.024	9	1.143
10	0.117	10	1.300
15	0.467	15	1.827
20	0.679	20	2.145
25	0.776	25	2.360
30	0.844	30	2.382

Table F.3: Term Structure of zero rate of German and Italian BVAL sovereign curves on March 30, 2016.